GEMS & GEMOLOGY

WINTER 2014
VOLUME L

THE QUARTERLY JOURNAL OF THE GEMOLOGICAL INSTITUTE OF AMERICA

Rough Diamond Auctions and Their Market Impact

Thirty Years of Argyle Pink Diamond Tenders

Study of the Blue Moon Diamond

GEMS & GEMOLOGY
Winter 2014
VOLUME 50, No. 4


pg. 253


pg. 273

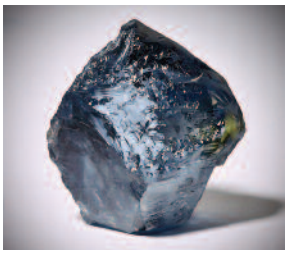
pg. 281


pg. 296

Editorial

Feature Articles

Notes and New Techniques

Regular Features

GEMS & GEMOLOGY®

gia.edu/gems-gemology

Subscriptions
Copies of the current issue may be purchased for $29.95 plus shipping. Subscriptions are $79.99 for one year (4 issues) in the U.S. and $99.99 elsewhere. Canadian subscribers should add GST. Discounts are available for group subscriptions, GIA alumni, and current GIA students. To purchase print subscriptions, visit store.gia.edu or contact Customer Service. For institutional rates, contact Customer Service.

Database Coverage
Gems & Gemology's impact factor is 0.778, according to the 2013 Thomson Reuters Journal Citation Reports (issued July 2014). *G&G* is abstracted in Thomson Reuters products (Current Contents: Physical, Chemical & Earth Sciences and Science Citation Index—Expanded, including the Web of Knowledge) and other databases. For a complete list of sources abstracting *G&G*, go to gia.edu/gems-gemology, and click on "Publication Information."

Manuscript Submissions
Gems & Gemology, a peer-reviewed journal, welcomes the submission of articles on all aspects of the field. Please see the Guidelines for Authors at gia.edu/gandg or contact the Managing Editor. Letters on articles published in *G&G* are also welcome. Please note that Field Reports, Lab Notes, and Gem News International entries are not peer-reviewed sections but do undergo technical and editorial review.

Gems & Gemology is published quarterly by the Gemological Institute of America, a nonprofit educational organization for the gem and jewelry industry.

Postmaster: Return undeliverable copies of *Gems & Gemology* to GIA, The Robert Mouawad Campus, 5345 Armada Drive, Carlsbad, CA 92008.

Our Canadian goods and service registration number is 126142892RT.

About the Cover

As rough diamond production and sales have transitioned from one company to a host of players in recent years, auction sales have become increasingly prevalent. The lead article in this issue examines the effect of these rough diamond auctions on the global market. The photo on the cover shows diamonds from the Kao mine in Lesotho being prepared for tender. The 17.88 ct yellow diamond in tweezers is set against a background of colorless octahedra totaling 34.11 carats. Courtesy of Fusion Alternatives, Antwerp. Photo by Robert Weldon/GIA.

Printing is by L+L Printers, Carlsbad, CA.
GIA World Headquarters The Robert Mouawad Campus 5345 Armada Drive Carlsbad, CA 92008 USA

ISSN 0016-626X

A Fitting Conclusion to **Our 80th Anniversary**

Welcome to the final issue of *G&G*'s 80th anniversary! Topics we've covered thus far include the Chinese and Sri Lankan gem and jewelry industries, beneficiation through Botswana's diamond industry, three-phase inclusions in emerald, HPHT synthetic diamonds, Myanmar's remarkable "Jedi" spinel, and pleochroism in colored gems.

In this Winter 2014 issue, three of our four articles focus on aspects of diamond. I was privileged to see the subject of one these papers up close: the Blue Moon diamond, prior to its exhibition at the Natural History Museum of Los Angeles County. This spectacular gem was recovered from the Cullinan mine—formerly a De Beers operation—in early 2014. As such, it's a piece of the story told in our first two articles, which respectively survey recent changes in rough diamond distribution with the growth of the auction system and review the Argyle mine's exclusive pink diamond tenders, held annually since 1985.

"Our lead article discusses the sweeping changes brought to rough diamond pricing and supply through the adoption of tenders and live auctions."

Our lead article, by GIA senior industry analyst Russell Shor, discusses the sweeping changes brought to rough diamond pricing and supply through the adoption of tenders and live auctions by leading producers. He explains that current opinion is divided: Some advocate auctions as a more accurate reflection of rough diamond market values, while others fear they encourage volatility of prices and speculation.

Our second paper, by the GIA laboratory's John King, Dr. Jim Shigley, and Claudia Jannucci, is a very timely one. The fall of 2014 marked the 30th edition of Argyle's pink diamond tenders, the invitation-only auctions of the mine's most prized gems. This paper offers an insightful review of each auction to date. Over the years, GIA has been in the fortunate position to grade these premium pink to red diamonds, and this article also presents a concise survey of the color, carat weight, and cutting style of the gems offered.

Next, Dr. Eloïse Gaillou of the Paris School of Mines, Dr. Jeffrey Post of the Smithsonian Institution, and their coauthors present a rare gemological study of the 12.03 ct Blue Moon diamond. Prior to its fashioning, this Fancy Vivid blue, internally flawless diamond set a record price for a rough gem, bringing US$25.6 million in early 2014.

In our final article, Dr. Le Thi-Thu Huong from the Hanoi University of Science and her coauthors deliver a preliminary study—contrasting FTIR and Raman spectrometry—on the topic of separating natural and synthetic emeralds using vibrational spectroscopy.

In addition to these four feature articles, you'll find our regular Lab Notes and Gem News International sections. We've gathered a variety of GNI contributions in the winter issue, including entries on the first non-nacreous beaded cultured pearl described so far, a new Ethiopian black opal deposit, a beryl and topaz doublet set in fine jewelry, and demantoid garnet from a new deposit in Pakistan's Baluchistan province. This last entry is coauthored by one of GIA's new postdoctoral research associates, Dr. Aaron Palke. We're also delighted to publish a letter from distinguished gemologist Dr. Karl Schmetzer offering comment on the summer edition's emerald inclusion article.

As another year begins, we hope you find this issue a fitting conclusion to our 80th anniversary!

Duncan Pay | Editor-in-Chief | dpay@gia.edu

Rough Diamond Auctions: Sweeping Changes in Pricing and Distribution

Russell Shor

Since 2007, rough diamond prices have become extremely volatile. One reason is the growing percentage of rough diamonds now sold by tender and live auctions rather than the century-old system of marketing rough diamonds at set prices to a pre-approved clientele. This report explains the tender and live auction processes and discusses their effect on the rough diamond market, including pricing and the opening of a market that was once difficult to enter.

For more than a century, the vast majority of rough diamonds (figure 1) were mined by a single company, De Beers, and marketed through its sales subsidiary at preset prices in a series of periodic sales called sights. Recently, diamonds have been mined by a growing number of smaller companies, many of which have put their production up for bids at tender sales and auctions. De Beers and other major producers have also integrated tenders and live auctions into their sales processes to gauge market prices for their sight goods. A tender is a silent auction where bids are submitted in writing and tallied at the specified close of the sale. Live auctions feature bidding that occurs in real time—online—and are won by the highest bidder at the closing time. Some sellers claim that diamond producers' increasing use of tenders and live auctions, instead of the De Beers sight model of selling at a fixed price, has encouraged speculative buying and caused rough prices to become much more volatile, especially since 2009. Proponents claim that tenders and auctions reflect "true" market prices, opening access to rough to more diamond manufacturers and dealers. The evidence supports the volatility theory, although other factors such as the world economic crisis and the lending policies of leading diamond industry banks also created turbulence and unstable prices within the diamond pipeline.

See end of article for About the Author and Acknowledgments.
Gems & Gemology, Vol. 50, No. 4, pp. 252–267,
http://dx.doi.org/10.5741/GEMS.50.4.252.

BACKGROUND

In 1888, De Beers Consolidated Mines succeeded in taking control of the diamond mining operations around Kimberley, South Africa, following a lengthy battle that pitted its founder, Cecil Rhodes, against rival Barney Barnato. The Kimberley mines, discovered in the early 1870s, yielded millions of carats each year, most of which were sold into the market at wildly fluctuating prices ("Diamonds," 1935). Rhodes and Barnato both believed that controlling production was essential to stabilizing prices. After Rhodes prevailed, gaining control of Barnato's Kimberley Central Diamond Mining Company, De Beers signed a contract with 10 distributors in London that would buy all of its production. This group of diamond houses was dubbed The London Syndicate ("Diamonds," 1935).

The idea originated with Barnato's nephew, Solly Joel, a De Beers director and diamond wholesaler whose firm was part of the original Syndicate. Joel believed that regulating sales through a small number of noncompetitive outlets was the key to main-

Figure 1. Diamond producers are increasingly selling their rough goods through auctions rather than the traditional set-price sights. These rough diamonds from the Kao mine in Lesotho were auctioned in Antwerp in November 2014. They include three light pinks (1.10 carats total), eight yellows (3.13 carats total), and a large group of colorless diamonds (68.79 carats total). Photo by Robert Weldon/GIA.

taining stable rough diamond prices and an orderly supply chain. Another member of the original syndicate was Dunkelsbuhler & Company, managed by a young broker named Ernest Oppenheimer.

The Syndicate nearly collapsed during the financial crash of 1907 and again during World War I, when mining was suspended. Oppenheimer gained backers from the United States to take over the newly discov-

Figure 2. Sorting diamonds at De Beers's Diamond Trading Company headquarters at 17 Charterhouse Street in London. Photo courtesy of the De Beers Diamond Trading Company.

ered coastal mines that Great Britain wrested from the former German colony of South-West Africa (now Namibia) after the war. That venture was named the Anglo American Corporation. Oppenheimer eventually leveraged Anglo American's highly profitable operations to take over both the Syndicate and De Beers by 1929, in effect controlling most African diamond production directly through mine ownership or indirectly through the Syndicate, which also distributed production from other mining operations outside De Beers's ownership.

Six years later, with the Great Depression causing a drastic drop in diamond sales, Oppenheimer dissolved the Syndicate and directed all rough sales through a new marketing subsidiary called the Diamond Trading Company (DTC). The DTC mixed rough diamonds from all sources, sorting them by quality, shape, and weight (figure 2). This allowed the DTC to set standard selling prices for each category of rough instead of charging different prices from each producer. It also established the modern sight system, in which selected clients would be permitted to buy directly from the DTC at 10 six-day sight periods during the year. All sales were "take it or leave it," with immediate payment required and no negotiating permitted. Prices were adjusted upward when market conditions warranted, but never downward. The DTC also served as a market regulator: In periods of slack demand or overproduction, it would stockpile rough diamonds or impose production quotas on mining operations ("Diamonds," 1935).

De Beers operated its sight system with few changes until 2001, when it overhauled the sightholder selection process as part of its Supplier of Choice initiative (Shor, 2005). The overhaul established two-year term limits for each client (later raised to 30 months), after which clients could apply for renewal and adopt "downstream" marketing requirements, which included spending funds on brand creation and advertising. Eight years later, in response to the economic crisis of 2008–2009, De Beers waived its traditional "take it or leave it" requirement and allowed its clients to defer all, or portions of, their sight allotments.

De Beers's approach to rough market control changed as well. Through nearly all of the last century, the company commanded 75–80% of world rough diamond sales. De Beers controlled not only production from its own mines but also the output from the former Soviet Union, starting around 1963, as well as Australia's Argyle mine from 1983 and a small portion of Canada's Ekati mine from 1998. In addition, the company operated buying offices in a number of African countries with large alluvial production, including Angola, Zaire (now the Democratic Republic of the Congo), and Sierra Leone, to take in portions of diggings from artisanal miners (Even-Zohar, 2007a).

In Brief

- Diamond mining companies now sell about 30% of world production through auctions instead of fixed-price sights.
- These auctions have a strong effect on rough diamond prices.
- Critics believe these auctions cause price volatility and encourage speculation, to the detriment of manufacturers who require consistent supplies of rough diamonds.
- Proponents maintain auction sales provide a truer market barometer that is more beneficial to the market in the long run.

Until the early 21st century, the 15–20% of rough diamonds sold outside De Beers's sales offices were generally traded through long-established networks of dealers in source countries. These were distributed to large rough brokers in Antwerp, who in turn sold them into the diamond pipeline. Some of these transactions were completed in Antwerp's legally sanctioned diamond clubs, and others were off-the-books "gray market" deals (King, 2009).

While the Soviet Union classified its yearly production figures as a state secret (including its sales arrangement with the DTC), it was generally estimated to account for one-fourth of DTC sales, making it the world's third-largest diamond producer by value behind South Africa and Botswana (where production began in 1970). Thus, while De Beers's own operations accounted for about 45% of rough production by value through the 1980s, the share it actually controlled was 80% ("The diamond cartel…," 2004).

The DTC's control over the rough diamond market began to wane in the early 1990s, after the breakup of the Soviet Union ended the central government's tight grip on provincial resources. The Kremlin, in cooperation with the Sakha Republic, where most of the country's diamonds are mined, created a mining and marketing organization called Alrosa (Shor, 1993). While Alrosa was still in its formative stages, some Russian government officials began releasing millions of carats of gem-quality diamonds into the world market under the guise of "technical" (industrial) stones that had been exempt from the sales agreement with De Beers (Shor, 1993). This depressed polished diamond prices for several years, especially with the smaller stones comprising the vast majority of these goods.

In 1996, Australia's Argyle operation, owned by Rio Tinto, became the first major producer to leave the DTC sales arm. Argyle was then the largest source of diamonds by volume—more than 40 million carats yearly—though the material was predominantly lower in quality. Rio Tinto, whose executives had long chafed over the production and sales quotas De Beers levied on its operation, established its own sales office in Antwerp, as well as a selling system similar to De Beers's sights (Shor, 1996).

In 1998, the large mining company BHP Billiton commissioned the first Canadian diamond mine, Ekati. BHP signed a three-year agreement to market 35% of its production through the DTC while selling the remainder through its own sales channel at fixed prices, a system akin to De Beers's sight system (figure 3). When Diavik, another large Canadian mine majority owned by Rio Tinto, came on line three years later, BHP ended its sales agreement with De Beers, marketing all of its production through its own offices. Rio Tinto integrated the production from Diavik into its Argyle sales operation.

Figure 3. Diamonds from BHP's Ekati mine were the first major production sold by tender auction. Photo courtesy of BHP Diamonds Inc.

Beginning in 2000, De Beers radically restructured its operations and strategic role in the diamond market. The company closed its African buying offices in 2000. Two years later, it signed an agreement with the European Monopolies and Mergers Commission to phase out its marketing of Russia's diamond production over seven years. De Beers also sold its diamond stockpile and curtailed its market custodianship by declining to limit sales during slower demand periods (Harden, 2000).

At the same time, De Beers itself contributed to the rough market's fragmentation by divesting most of its aging South African mines to smaller companies. It sold its Premier mine (now called the Cullinan), the Finsch mine, its Kimberley operations, and several smaller prospects to Petra Diamonds, while its Namaqualand properties went to Trans Hex.

These changes brought a sharp decline in De Beers's market share and, with it, the ability to dictate rough prices. In 2003, De Beers's mines, which it owned outright or in partnership with the governments of Botswana and Namibia, produced just under 43.95 million carats and still commanded a 65% market share by value, 55% by volume. By 2012, De Beers's production had declined to 27.9 million carats (De Beers Group, 2012); with no contract sales, the company's share of the rough diamond market slipped to approximately 40% by value and 29% by volume.

Thus, within a decade, the production and sale of rough diamonds passed from the control of one major company with a stated priority of maintaining price stability to a multichannel environment, with major players such as Rio Tinto, BHP, and Petra eschewing market custodianship in favor of maximizing sales by adjusting prices to market conditions. This policy required the creation of a flexible pricing mechanism, setting the stage for new avenues of marketing rough diamonds.

THE RISE OF TENDER AND AUCTION SALES

Before 2000, the use of tender auctions to sell rough diamonds was limited primarily to Rio Tinto's small production of fancy pink diamonds. Starting in 1985, the company held an annual sale of these stones at a luxury hotel in Geneva, surrounding the event with a strong publicity push. Producers of saltwater cultured pearls had been using the tender auction model for decades, conducting sales in Japan and Hong Kong and experiencing, over the long term, much greater price volatility than rough diamond producers (Shor, 2007).

Smaller mining companies that entered the market during the early 21st century began adopting tender/auction sales instead of dealing through brokers as their predecessors had done. Some of these companies, such as Petra Diamonds and Gem Diamonds (figure 4), were publicly traded and required a more transparent pricing model to comply with securities regulators. Meanwhile, the emerging diamond center of Dubai began hosting rough tenders in 2005 through the newly formed Dubai Diamond Exchange. Global Diamond Tenders, based in the United Arab Emirates, conducted the first sales from production of small mining operations in southern Africa, selling 435,000 carats for US$66 million. That year, Dubai saw the trading of 1.9 million carats of rough, valued at $2.36 billion (Golan, 2005).

Major diamond producers, however, were reluctant to alter the fixed-price sight system because it guaranteed a steady, predictable cash flow. This continued until early 2009, when BHP Billiton, after three years of trials, became the first major producer to fully convert to the tender auction system, citing the desire to sell at "true" market prices. In 1998, its first year of diamond mining, BHP established a multi-tier distribution system, with 50% of the production sold to eight "regular" clients and 20% to nine "elite" customers. Elite customers paid a premium over BHP's price book in exchange for the right to reject a portion of their allocations. Like the DTC, BHP held sights every five weeks, each totaling about $60 million (Cramton et al., 2012). Also like the DTC, it divided rough stones into about 4,000 categories (called "price points") according to weight, shape, size, clarity, and color. BHP then grouped 200 price points into aggregate lots called "deals," which were then subdivided into parcels called "splits." Thus, a client could buy several splits from a variety of deals representing different sizes and qualities.

The remaining 30% of the rough went, through direct sale, to cutting firms in the Northwest Territories and to some retailers. Beginning in 2004, BHP added a trial tender sale, a market window channel (a limited sales channel for sellers to gauge prices and demand), and a separate channel for "special" stones over seven carats. The trial tender sales, which consisted of 20 assortments, ranged from $200,000 to $500,000 each. Generally the bids from customers came in a few percentage points above BHP's price for comparable goods over the trial period, so the company expanded its tender auction to 60% of production (mostly melee goods) in September 2008, with a full conversion to tender sales in February 2009 (Golan, 2008).

Figure 4. Operations at the Letseng mine in Lesotho. Gem Diamonds, which owns a 70% stake in the mine and markets all of its production, began selling all of its approximately 100,000-carat yearly production by tender auction after restarting operations in 2006. Photo by Russell Shor/GIA.

BHP's Ekati mine produced 6% of the world's diamond supply in fiscal year 2007—3.3 million carats—with a revenue of $583 million. BHP's tender system was divided into three channels: a spot auction, term auctions, and special sales. The spot auction was based on single transactions. Because there were a number of similar parcels or splits offered at each sale, all bids above the minimum reserve price were averaged out to what BHP called the "clearing price" and sold at that price. While the final sale price would be the same for all winning bidders, the reward for higher bidders was that they received larger allocations if the demand exceeded available supply for a particular deal. In a term auction, the company offered an 18-month supply contract with auctions conducted in a different system, as well as special sales for large stones over seven carats. Term auctions employed what is known as an ascending clock, lasting for three hours during each sale period. Prices for each split opened at a small discount below the prices set by the spot auctions and steadily rose via online bidding until the three hours expired, or until prices reached the point where bidders declined to raise their offers.

BHP conducted the third type of auction for special stones larger than seven carats in three sales each year. Stones were offered individually or in small lots that grouped several similar rough stones. The sale

used the ascending clock format, which was believed to provide the truest price discovery (Cramton et al., 2012).

The bidding process was designed to achieve "true" market prices by averaging the clearing price, which would reduce the influence of speculative bidders and ensure that all serious bidders received goods. This process would also prevent buyers from colluding to limit prices by keeping a large client base spread around the world and establishing reserve prices based on extensive market knowledge (Cramton et al., 2012).

BHP began phasing in its regular tender auction sales in July 2008, selling more than half of its production through this avenue. It completed the process by February 2009. The move's timing, coming as it did in the midst of the gravest financial crisis since the 1930s, ensured controversy.

In the fall of 2008, after news of the near collapse of the global financial system, the rough diamond market, along with most other economic activity, saw a plunge in demand. De Beers continued to hold its regular sights but at a greatly diminished level, announcing it would reduce rough sales to 50% of pre-crisis levels. But sights in early 2009 were down much more—just $135 to $150 million compared to $750 million the previous year (Golan, 2009a). The company also suspended or severely curtailed its Botswanan and Namibian operations, for which there was little demand. De Beers found itself in the extraordinary position of having to borrow $500 million from its shareholders to maintain cash flow (Even-Zohar, 2009a).

Other major players in the industry were also affected. Russia's Alrosa, the world's second-largest diamond producer, continued mining at pre-crash levels but sold most of its goods at unspecified discounts to Gokhran, the Kremlin's stockpile of precious materials. Rio Tinto cut back production in its Argyle and Diavik mining operations by 12% in the fourth quarter of 2008. The next year, it shut portions of Argyle for maintenance (Golan, 2009b) while adjusting prices downward—nearly to the levels of BHP tenders. Rio Tinto made no formal announcement on prices, so the extent of its discounting did not become known until early 2010.

BHP, however, continued to sell Ekati's full production. Prices at its October 2008 tender fell 35–45% from the previous month and continued to slide another 10–15% through February 2009. Critics of BHP's move to the tender system blamed the company for undermining the market and adding to the diamond industry's difficulties (Golan, 2008). Yet the company benefited greatly; BHP's revenues during this period actually exceeded De Beers's because it was able to sell its entire output instead of restricting sales and curtailing production (Cramton et al., 2012). Conversely, when prices began recovering after June 2009, BHP's prices accelerated much more rapidly than those of other producers.

The economists who created the tender sale model for BHP wrote in a 2010 evaluation that the process offered a number of advantages to mining companies over the fixed-price sales employed by De Beers and other large producers, including:

- True market price discovery. The study claimed that De Beers had underpriced its rough for many years, which helped create the supply-driven market.
- Getting the premium value from bidders who wanted only the quantities and qualities of rough they needed, as well as a consistent supply. In short, buyers would be bidding highest for their preferences. Under the De Beers sight system, clients were usually obliged to purchase goods for which they had no current use, requiring them to sell that material to other diamond firms.
- A competitive bidding environment, which usually resulted in higher prices and getting goods into the hands of clients who valued them the most.
- Pricing transparency (Cramton et al., 2012).

Many BHP clients and veteran diamond manufacturers criticized the tender system, citing several of the reasons enumerated by Moti Ganz, then president of the International Diamond Manufacturers Association:

- The competitive nature of bidding could compromise the regular supplies necessary to maintain a stable diamond manufacturing business. Without such supply stability, diamond industry banks would be reluctant to finance manufacturers' operations.
- The bidding process encouraged speculative buying, especially from large companies that might want to dominate sales and push prices beyond the reach of smaller manufacturers. Ultimately this would work against the mining companies by putting them at the mercy of a few large buyers.

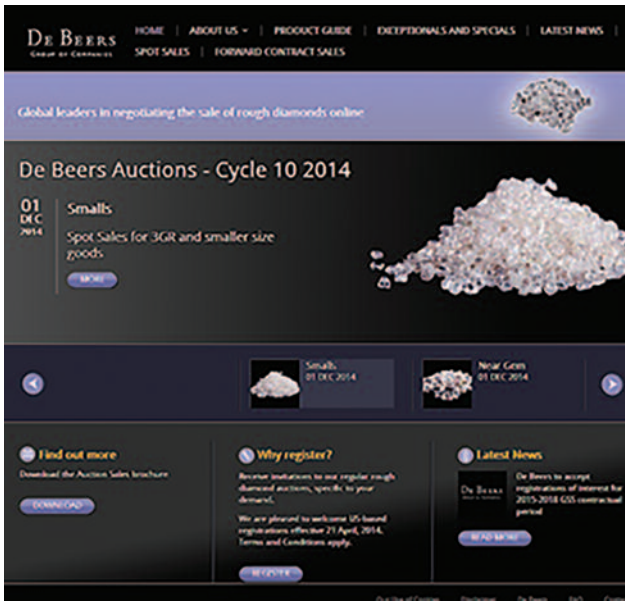

Figure 5. Through its online auctions, De Beers Diamond Auctions (formerly Diamdel) is now the single largest distributor of rough diamonds by tender.

- Prices could become very volatile, cutting into profits and further discouraging banks from financing rough purchases (Ganz, 2011).

As BHP Billiton converted to the tender system, De Beers began its own tender auction system through its Diamdel subsidiary. De Beers had formed Diamdel in the mid-1960s to provide rough diamonds at set prices to smaller manufacturers who could not qualify for sightholder status. By 2007, however, the venture was costing a great deal of money (Even-Zohar, 2007b), prompting De Beers to close Diamdel's offices and reorganize it to sell rough via online auctions. The reorganized Diamdel (figure 5) was charged with selling 10% of De Beers's run-of-mine production. Of that 10%, 70% would be sold by auction and the remainder by set-price sale (Shishlo, 2010).

The first sale, in 2008, consisted of 16 lots grouped by size and quality, with buyers able to view them online. Since then, the auctions have been spread out over each calendar month, with one day dedicated for each size and quality lot. The auctions were conducted online through the offices of Curtis Fitch in England, an e-commerce auction service provider in which De Beers acquired a 25% stake in 2013. As with other online auctions, potential buyers could examine parcels and then place bids in a time window on the scheduled ending day (Robinson, 2013a).

The first auction realized prices ranging 12–18% above comparable goods sold at De Beers's sights, because most of the buyers believed that rough prices were rising sharply enough for them to recoup their premiums over the long run (Even-Zohar, 2008). Eighty companies based in Hong Kong, Tel Aviv, Antwerp, and Mumbai bid on the 300 lots offered at online auctions (De Beers Group, 2008). By the year's end, Diamdel had reported sales of $444 million, but the percentage sold at auction remained unspecified because the company had included set-price transactions by the Hindustan Diamond Company (the Mumbai branch of Diamdel).

The following year, Diamdel did not report a sales figure, noting the rapidly deteriorating demand for rough as the world economic crisis took hold. The company revealed that it had sold 85% of the 695 lots offered at its first presentations, with 88 companies participating. By 2011, sales had increased 30% over the previous year to $405 million, with 2,614 auction lots offered and 152 firms placing winning bids (De Beers Group, 2011). Using Diamdel's 70% auction sales as a guide, an estimated $310 million worth of rough was sold through this channel.

In 2012, Diamdel was renamed De Beers Auction Sales and began selling 100% of its rough through online auctions. That year, however, saw the company's production reduced by a severe accident at its largest mine, Jwaneng in Botswana. Furthermore, growing liquidity problems in the diamond industry forced De Beers Auction Sales's total down 12% to $356 million, from 151 online auctions that offered 3,807 lots totaling an estimated 2.7 million carats. The company noted that despite the slowdown in the rough market, "competition in short-term rough diamond buying opportunities is intensifying as more players adopt the auction sales and pricing approach" (De Beers Group, 2012).

In 2013, Diamdel and its online provider, Curtis Fitch, instituted forward contract sales in addition to its spot-market bidding system to help clients develop supply continuity. The first contracts, for three-month supplies of specific sizes and qualities, began in December 2013. The company planned to extend contracts to one year in 2014.

According to De Beers, the new forward contract sales would provide customers the opportunity to secure longer-term supply at auction events and enable more effective planning and commitment to longer-term agreements with their own customers. "The forward contract sales offer customers the opportunity to bid for future supply of the types and quantities of

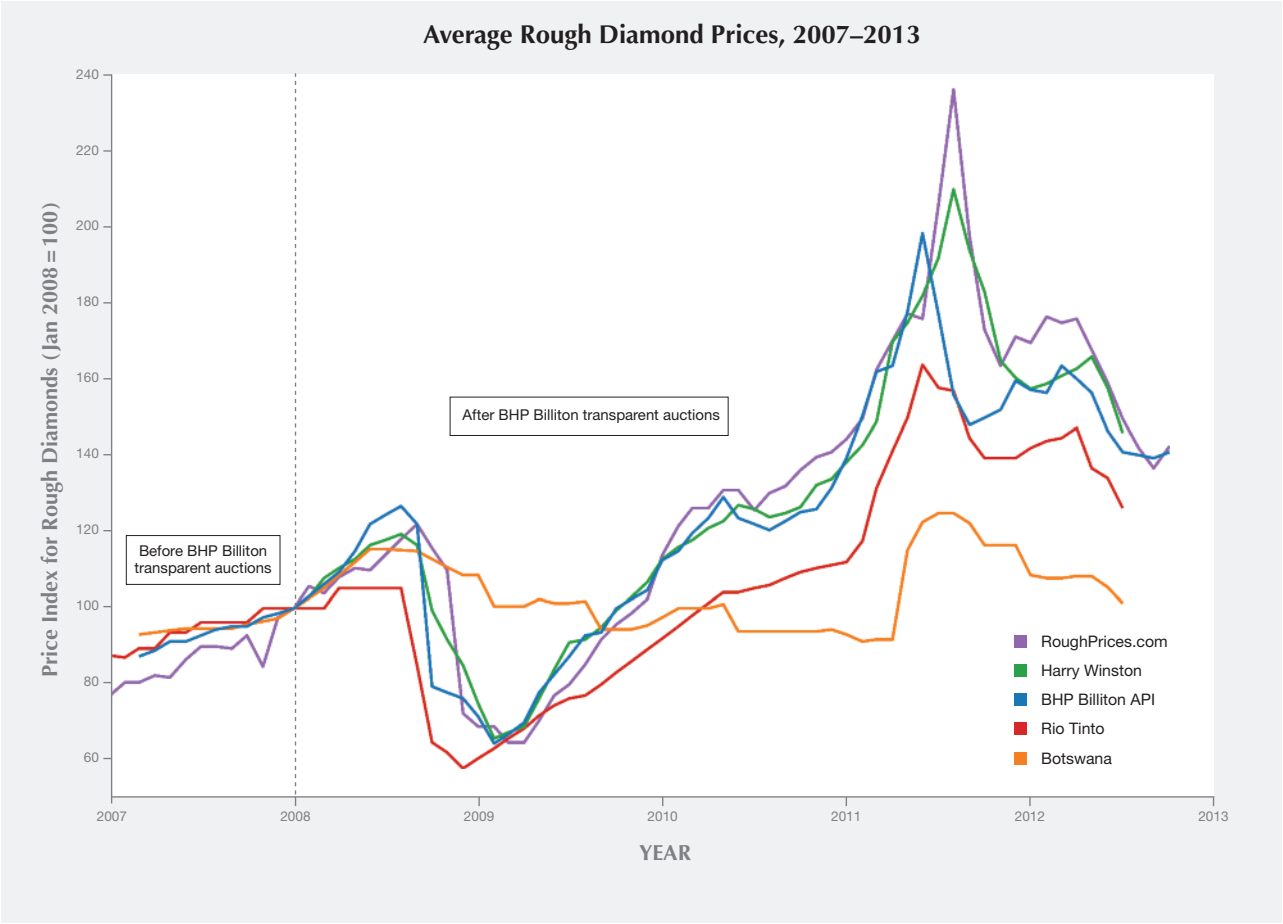

Figure 6. This chart shows average prices of rough diamonds from major producers. In 2008, prices became volatile after BHP converted to a tender auction system, as its rates influenced the set-price market as well. Source: Cramton et al. (2012).

rough diamonds they require, when they require them. The new proposition will complement current spot auction events," announced De Beers Auction Sales senior vice president Neil Ventura. The purchase price for the volume of rough diamonds in a forward contract would be determined by a customer's bid relative to the spot price for the same type of goods at the De Beers Auction Sales spot auction when the contract matured (Odendaal, 2013).

Within two years of BHP's and Diamdel's adoption of the tender system, most smaller mining companies, seeing how the returns had improved, moved from selling through contracted rough dealers to tendering their own productions. By 2010, as much as 20% of all rough production worldwide was being sold through some form of auction, and this had become a key price driver in the rough market (R. Platt, pers. comm., 2013). Rio Tinto, currently the world's third-largest diamond producer, announced in early 2010 that it would tender a "small percentage" of its Diavik production to gauge price levels. After the initial sale, several longtime Rio Tinto clients claimed they were priced out of the tender by the newer companies invited to bid (Golan, 2010).

A BHP economic study confirmed the volatility of the rough market from mid-2009 through 2012. The study found that average prices, which had been slowly rising through most of the past decade (with the exception of the deep plunge late in 2008), more than tripled between June 2009 and March 2011. BHP tender prices led these increases by one month, suggesting that bidders in other tenders, as well as set-sale producers, were following its ascent. Similarly, in early 2011, after disappointing Christmas sales of diamond jewelry in the U.S. cooled the market, BHP's sales were the first to fall, giving up about

one-third of their gains by year's end. Fixed-price producers De Beers and Rio Tinto showed much less volatility, but their prices remained well below the tender sellers' (figure 6). But in December 2010, Diamdel chief executive Mahiar Borhanjoo denied that the company's auction results were causing the rapid rise of rough prices at De Beers's sights, claiming that auction results were only one of many data sources the company used in pricing its set-sale sights (Shishlo, 2010).

As the number of smaller producers proliferated—in 2013, there were 27 active diamond mining companies operating 40 mines (B. Janse, pers. comm., 2014)—so did the number of tender sales. This led to the creation of several tender auction consolidators such as Fusion Alternatives, which handled the production from multiple sources. Formed in 2010 in cooperation with diamond brokerage I. Hennig & Co., Fusion Alternatives offered a platform for small producers and dealers of artisanal production to market rough diamond in both online and physical auctions. To attract the latter, the London-based company established offices in Antwerp and Israel and later Dubai and Johannesburg. The company vetted buyers' credentials and bank references to ensure they operated legally and ethically and were financially qualified.

Fusion Alternatives holds several consolidated producers' sales each week in its offices. Each sale consists of about 25,000 to 30,000 carats, including larger stones from Namakwa Diamonds' Kao mine in Lesotho, with 30 to 50 buyers participating. Company executives say that prices fluctuate from one sale to the next but maintain that competitive pressure in the auction setting is only one reason.

"Of course some buyers will overpay to obtain certain goods," says Raphael Bitterman, a partner in the company. "But there are many factors at work to affect prices and demand today: the wild changes in exchange rates, particularly the rupee; the credit standing of the buyer; and, of course, the banks' changing credit requirements."

Tenders are often more focused on specific sizes and qualities than the larger sights, where clients are usually obliged to buy rough for which they have no immediate use. Larger companies can absorb these goods and sell them—often profitably—into the secondary market, but small operations cannot assume this financial burden up front. Similarly, manufacturing is becoming more specialized for niche markets, and manufacturers now have very specific needs. Tender sales give smaller players access to direct supplies of rough. For instance, Fusion Alternatives will sell rough parcels as small as $25,000 to $50,000 (about 10% of a minimum De Beers sight) to small cutting firms (figures 7 and 8). This helps small manufacturers source rough to grow their business, says Bitterman, while staying price-competitive with larger firms.

By 2013, tender and auction sales had become an established source of rough supply. This was mainly because of the quality and variety of material offered, but also because many key rough dealers had come to understand how the process worked. They knew which tender/auction sales offered the goods they needed and could adjust their businesses to the sales schedules (Golan, 2014; R. Bitterman, pers. comm., 2013).

Another significant move toward the auction system came at the end of 2013, when De Beers began auctioning a portion of its Botswana production through a newly formed government enterprise called the Okavango Diamond Company. Okavango is actually a hybrid set-price/auction setup that purchases rough allocations from Debswana—the fifty-fifty joint venture between De Beers and the Botswana government—for a fixed price and then sells the rough in auctions held every five weeks.

Figure 7. These large stones (upwards of 10.8 ct) from the Kao mine in Lesotho were offered by Fusion Alternatives at a December 2013 tender sale in Antwerp. Photo by Russell Shor/GIA.

Okavango's plan is to market 12% (increasing to 15% within two years) of Debswana's production, representing about $400 million yearly, or 2.5 to 3 million carats (Robinson, 2013b).

While the company vets each potential client that registers to buy, the process is not nearly as cumbersome as the lengthy application De Beers requires for its sightholders. Consequently, about half of the clients are nonsightholders. As with other tender sales, rough is divided into various size, shape, and quality categories and then subdivided into parcels. Special stones 10.8 carats and larger are auctioned separately. Every lot is available for a full day of viewing before the scheduled auction. The auction is held online during a three- to four-hour period (M. ter Haar, pers. comm., 2013; Robinson, 2013b).

The first pilot sale of 123,000 carats, held in August 2013, netted a total of nearly $20 million (Wyndham, 2013). Some categories of rough sold as much as 51% higher than comparable De Beers goods. These prices were surprising, considering that throughout 2013, De Beers clients had deferred buying as much as one-quarter of their regular sight allocations, presumably because prices were too high. Okavango's first full auction in November saw prices more in line with De Beers's sight goods, possibly because the banks that finance the diamond trade had announced they would fund only 70% of rough purchases going forward, instead of 100% (Shor, 2013).

Okavango executives acknowledge that auctions can create short-term price volatility but insist that over the long term, auctions reflect market prices. Besides driving higher prices for its rough diamonds, the Botswana government is hoping the Okavango tenders will help supply the growing diamond-manufacturing industry around the capital city of Gaborone (Weldon and Shor, 2014). This would increase traffic of smaller and midsize diamond manufacturers into Botswana while boosting revenues (M. ter Haar, pers. comm., 2013).

Like De Beers, Alrosa and Rio Tinto still market most of their rough to specific clients in set-price sale contracts. Both companies have been auctioning their "specials"—rough diamonds larger than 10.8 carats—and very specific types of rough for more than a decade. Alrosa, mostly in conjunction with major trade shows where there is a concentration of diamond firms, sells about 25% of its production by value through such sales (figure 9). Through its Antwerp sales office, Rio Tinto sells about 10% of its production by value through auctions or tenders (Bain & Company, 2013).

Since 2011, one of the drivers of tender/auction sales by volume has been the huge production from Zimbabwe's Marange deposit. This output is mainly industrial—8% gem and an additional 8% near-gem—but sizable in volume, totaling an estimated 17 million carats in 2013 (Shor, 2014). In 2007–2008, Marange drew controversy after Zimbabwean forces evicted thousands of artisanal miners from the area, resulting in an estimated 180 deaths. Although mining continued, the Kimberley Process officially banned exports until lifting the embargo in November 2011. Subsequently, the four licensed mining firms began holding regular tender sales in the capital city of Harare and in Dubai. At the end of 2013, the Antwerp World Diamond Centre, working with the Kimberley Process, succeeded in aggregating some of these tenders and moving them to a newly commissioned tender/auction facility in the AWDC headquarters building.

Figure 8. This 41.76 ct rough diamond from the Kao mine in Lesotho, classified as light brown, was sold by Fusion Alternatives at a December 2013 tender in Antwerp. Photo by Russell Shor/GIA.

A 280,000-carat pilot tender in December 2013, consisting of mainly lower-quality material, was deemed a success by Zimbabwe's government and the AWDC, which led to the scheduling of a second sale in February 2014. While that tender in Antwerp exceeded 960,000 carats, the licensed producers have continued to hold separate tenders in Dubai and Zimbabwe while also providing goods for the Antwerp sales (Shor, 2014).

THE TENDER DEBATE

In the fall of 2013, a resurgence of prices at the tenders and auctions, while polished prices remained soft, prompted the International Diamond Manufacturers Association (IDMA) to ask that mining companies allocate "reasonably large amounts" of their goods for sale outside of the tender system (Robinson, 2014). The IDMA blamed such sales for the speculation that has further reduced industry profits, except at the mining level.

The IDMA complained that the system was especially hard on the small and medium-sized companies that comprise the bulk of its membership. These firms did not have the financial muscle to compete with larger companies, which often push prices beyond an affordable range. IDMA members added that tender sales made it difficult to plan for the long term and fulfill their customer needs because they could not be assured of a consistent supply of rough diamonds. IDMA further argued that producers might benefit from high prices in the short run, but in the long run a healthy diamond market is in their best interest as well.

By late 2014, nearly every diamond mining company was conducting either a portion or all of its sales by tender and auction. An estimated 30% of world diamond production was sold by tender and auction events, compared to almost none a decade earlier. This was despite the fact that Dominion Resources, which acquired BHP's diamond operations at the end of 2012, reverted to the set-price model (R. Platt, pers. comm., 2013). In mid-2014, however, the company reported that it planned to resume tenders for a small portion of its production to monitor market prices. The major producers such as De Beers, Alrosa, and Rio Tinto have adopted a mixed model that allows them to reap the steady cash flow from contracted set-price sales while adjusting prices (mainly upward) based on the results of their auction sales ("Times are changing," 2013).

Lukoil, a new Russian producer that owns a majority stake in the Grib diamond deposit in the Arkhangelsk region adjoining Finland, began selling its production at auction in Antwerp in the fall of 2014. The sales were operated by several former BHP executives using the ascending clock format that had characterized most of that company's rough sales until the end of 2012 (Miller, 2014).

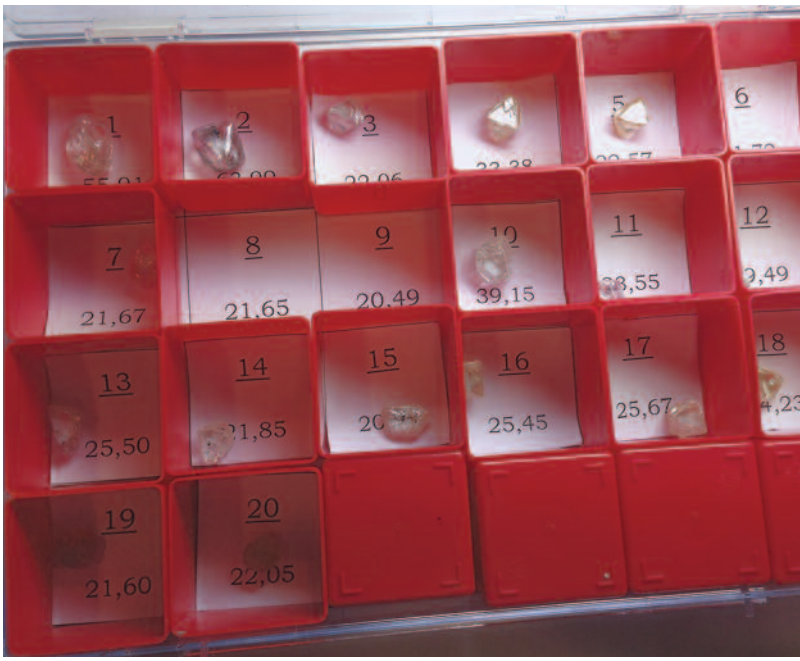

Figure 9. This array of large rough diamonds was presented at an Alrosa tender held in Hong Kong in September 2013. Photo by Russell Shor/GIA.

While tender and auction sales still comprise a minority of rough sold into the market, they have become the driving force of rough prices. Nearly all diamond producers, including De Beers, apply the results of their own tenders or auctions to the rough prices at their traditional sights. As one analyst explained, De Beers's use of the tenders means that, in effect, the prices realized at these sales influence the pricing for 40% of total diamond production by value. Likewise, Alrosa tenders a small percentage of its run-of-mine production to gauge price levels, and this influences the prices for the goods it sells by contract sales (Wyndham, 2013; M. ter Haar, pers. comm., 2013).

PRICE VOLATILITY AND ITS EFFECT ON THE MARKET

While the debate over the effect on rough prices continues, proponents still argue that, speculation aside, tender sales more accurately reflect prevailing market prices. Opponents maintain that the stability afforded by the sight system is necessary for a healthy

diamond market. But as figure 10 shows, rough diamond prices over the past decade were stable only at the sources: De Beers, Alrosa, and Rio Tinto. In the secondary rough market, where the rest of the players operated, volatility was high. The chart, which lists average premiums De Beers sightholders got for selling their sight goods to diamond manufacturers, shows fluctuation between +13% and –11% between the second half of 2003 and the second half of 2006, well before tender/auction sales had a pronounced effect on the market. Of particular note is the 35% premium during the first half of 2008. The extraordinary events of 2008, after BHP Billiton's full conversion to the tender auction system, touched off a credit-fueled speculative bubble, mainly on larger goods, that drove prices of both rough and polished to unprecedented highs just before the late-year economic crisis (Even-Zohar, 2009b). After the crash, prices fell to a 2.5% deficit one year later.

By mid-2009, the BHP effect as described by Cramton et al. (2012) had taken hold, with premiums on De Beers sight rough soaring to 15% by year's end. Outside events also served to influence market prices. In India, where the diamond industry was hit hard by the economic crisis, banks had established a credit program to fund diamond manufacturers' operations until the industry recovered, thus restoring jobs to hundreds of thousands of workers (Shor, 2009). At the same time, rumors of rough shortages swept the market, touching off a buying spree with bank-advanced funds ("Rough shortages looming," 2009).

By 2010, bank financing was fueling a speculative boom in both rough and polished prices. Much of this boom was caused by a practice later dubbed "round-tripping," in which some Indian diamond manufacturers secured higher credit lines by inflating export totals by as much as three to four times to make it appear their business was growing at that rate (Golan, 2012).

In the second half of 2011 (again, see figure 6), rough prices abruptly declined. The catalyst that broke the bubble was disappointing economic news from the United States, which caused banks to issue their first round of credit tightening. The Indian government announced it would impose a 2% duty on polished diamond imports to discourage round-tripping (Golan, 2012).

How volatile these prices would have been under the De Beers–dominated sight system is open to debate. Evidence shows that during difficult economic circumstances, the company reduced sales volume in an effort to maintain rough prices. As noted earlier, price stability at the primary (i.e., sightholder) level did not always carry over to the secondary rough market or the polished market, both of which

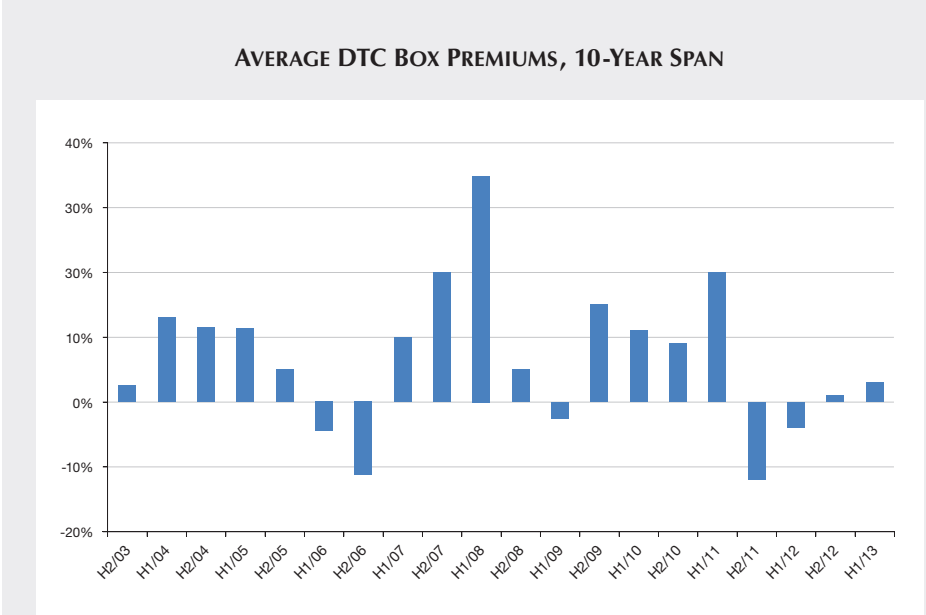

Figure 10. This chart shows the average premiums of De Beers DTC rough obtained by dealers during each six-month period between the second half of 2003 and the first half of 2013. While De Beers and other major producers kept rough diamond prices relatively stable in the years before tender auctions, they were quite volatile in the secondary market. A large percentage of rough sold by De Beers still goes to rough dealers, who then sell the rough to manufacturers at a premium. Source: WWW International Diamond Consulting Services.

Figure 11. These nine rough diamonds from the Kao mine, 75.37 carats total, were among those auctioned at Fusion Alternatives' November 2014 sale in Antwerp. Photo by Robert Weldon/GIA.

showed high volatility during the early 1980s, when commodity markets crashed after a bubble, and in the Asian financial crisis of the late 1990s.

Looking back on the 2013 results, De Beers CEO Philippe Mellier said the company had no plans to increase the percentage it sells through auctions (pers. comm., 2014) but noted that its sales allowed many newcomers and nonsightholders the opportunity to purchase rough diamond directly from a producer. He said that several customers were named sightholders in 2012 based on their participation in De Beers auctions. Between its direct auction sales and indirect sales through Okavango, De Beers is, ironically, the largest seller of rough at auction and tender, with an estimated total of 5.75 million carats in 2013 (Anglo American Corp., 2013).

CONCLUSION

The diamond industry is in the midst of numerous transitions as it moves from single-source to multi-channel supply, with more pressure from governments, regulatory agencies, and financial institutions, in addition to the trend toward tender and auction sales. There is general agreement that the evolution to tender/auction sales of rough diamonds has caused considerable price volatility at the producer level, particularly as the shift occurred during one of the most turbulent economic periods in recent history. Yet volatility has always been a part of the secondary rough market, reflected in the premiums that De Beers sightholders received for their goods, so the true effect may not be fully apparent until the world economy is on a surer footing and the industry has adjusted to stricter banking policies. It is reasonable to conclude that tender sales have considerably widened the quantity and selections of rough available to smaller diamond manufacturers (figure 11), because the purchase requirements are lower and the application processes are less complex (and less expensive) compared to traditional sight contracts. It is certain that rough diamond tenders and auctions, combined with these other forces, will continue to influence how these goods are priced and traded in the coming years.

ABOUT THE AUTHOR

Mr. Shor is senior industry analyst at GIA in Carlsbad, California.

ACKNOWLEDGMENTS

The author thanks Richard Platt of WWW International Diamond Consulting Services in London, Raphael Bitterman and Adam Schulman of Fusion Alternatives in Antwerp, Marcus ter Haar of the Okavango Diamond Company in Gaborone, and Dr. Bram Janse of Archon Exploration Pty Ltd. in Perth.

REFERENCES

Anglo American Corp. (2013) Annual report. http://www.angloamerican.com/~/media/Files/A/Anglo-American-Plc/reports/annual-report-2013/annual-report2013.pdf.

Bain & Company (2013) The global diamond report 2013: Journey through the value chain. http://www.bain.com/publications/articles/global-diamond-report-2013.aspx.

Cramton P., Dinkin S., Wilson R. (2012) Auctioning rough diamonds: A competitive sales process for BHP Billiton's Ekati Diamonds. In Z. Neeman, A. Roth, and N. Vulkan, Eds., *Handbook of Market Design*. http://www.cramton.umd.edu/papers2010-2014/cramton-dinkin-wilson-auctioning-rough-diamonds.pdf.

De Beers Group (2008) Operating and financial review. http://debeersgroup.com/content/dam/de-beers/corporate/documents/Archive%20Reports/DeBeers_OFR_2008_Feb_2009.pdf.

——— (2011) Operating and financial review. http://debeersgroup.com/content/dam/de-beers/corporate/documents/articles/reports/2012/OFR_2011.pdf.

——— (2012) Operating and financial review. http://debeersgroup.com/content/dam/de-beers/corporate/documents/articles/reports/2013/OFR_2012.pdf.

The diamond cartel: The cartel isn't for ever (2004) *The Economist*, Vol. 372, No. 8384, July 17, pp. 60–62, www.economist.com/node/2921462.

Diamonds (1935) *Fortune*, Vol. 11, No. 5, pp. 65–78.

Even-Zohar C. (2007a) *From Mine to Mistress: Corporate Strategies and Government Policies in the International Diamond Industry*. Mining Communications Ltd., London.

——— (2007b) Will Diamdel become a mini-Enron? *Idex*, June 21, www.idexonline.com/portal_FullEditorial.asp?id=27732.

——— (2008) Diamdel markets Pandora's boxes. *Idex*, Jan. 31, www.idexonline.com/portal_FullEditorial.asp?id=29486.

——— (2009a) Giving credit to De Beers. *Idex*, Feb. 26, www.idexonline.com/portal_FullEditorial.asp?TextSearch=&KeyMatch=0&id=31980.

——— (2009b) Just think what might have happened… *Idex*, Dec. 24, www.idexonline.com/portal_FullEditorial.asp?TextSearch=&KeyMatch=0&id=33387.

Ganz M. (2011) Too much sugar in the tea. *International Diamond Manufacturers Association Bulletin*, http://www.idma.co/downloads/press/Interview%20Moti%20Ganz%20%28July%202011%29.pdf

Golan E. (2005) Dubai Exchange. *Idex*, Oct. 10, www.idexonline.com/portal_FullNews.asp?TextSearch=&KeyMatch=0&id=24705.

——— (2008) Sharp drop in prices at BHP rough tender. *Idex*, Oct. 23, www.idexonline.com/portal_FullNews.asp?TextSearch=&KeyMatch=0&id=31366.

——— (2009a) DTC Sight 1: Reduced supply, shine: Christmas sales below expectations. *Idex*, Jan. 22, www.idexonline.com/portal_FullNews.asp?id=31806.

——— (2009b) Rio Tinto diamond production declines 20% in 2008. *Idex*, Jan. 15, www.idexonline.com/portal_FullNews.asp?TextSearch=&KeyMatch=0&id=31763.

——— (2010) Rio Tinto Diamonds starts rough diamond tenders. *Idex*, April 8, www.idexonline.com/portal_FullNews.asp?id=33891.

——— (2012) The real cost of round-tripping. *Idex*, Jan. 19, www.idexonline.com/portal_FullEditorial.asp?id=36336.

——— (2014) A year of surprises—Banks, prices, profitability. *Idex*, Jan. 12, www.idexonline.com/portal_FullNews.asp?id=38992.
Harden B. (2000) De Beers halts its hoarding of diamonds. *New York Times*, July 13, www.nytimes.com/2000/07/13/business/de-beers-halts-its-hoarding-of-diamonds.html.
King E. (2009) *Transfer Pricing and Corporate Taxation: Problems, Practical Implications and Proposed Solutions*. Springer Science+Business Media, New York.
Miller J. (2014) Lukoil schedules first rough diamond auction for Sept. 23. Diamonds.net, www.diamonds.net/News/NewsItem.aspx?ArticleID=47787&ArticleTitle=LUKOIL+Schedules+First+Rough+Diamond+Auction+for+Sept.+23
Odendaal N. (2013) De Beers to offer forward contract sales. *Mining Weekly*, Dec. 3, www.miningweekly.com/article/de-beers-to-offer-forward-contract-sales-2013-12-03.
Robinson A. (2013a) De Beers buys 25% of online service provider Curtis Fitch. *Idex*, Sept. 3, www.idexonline.com/portal_FullNews.asp?id=38561.
——— (2013b) Okavango Diamond Company explains sales process at IDE. *Idex*, Nov. 12, www.idexonline.com/portal_FullNews.asp?id=38827.
——— (2014) Tenders a tough sell for many diamantaires. *Idex*, Feb. 20, www.idexonline.com/portal_FullEditorial.asp?id=39143.
Rough shortages looming (2009) Polished Prices.com, Oct. 9, http://polishedprices.com/go/market-news/news~4806.
Shishlo A. (2010) Industry debates the hard reality of diamond tenders. *Rough & Polished*, Dec. 10, http://rough-polished.com/en/expertise/43223.html.
Shor R. (1993) Russia to De Beers: We want more control. *JCK*, Vol. 164, No. 1, pp. 50–60.
——— (1996) Thinking the unthinkable. *JCK*, Vol. 167, No. 5, pp. 98–105.
——— A review of the political and economic forces shaping today's diamond industry. *G&G*, Vol. 41, No. 3, pp. 202–233, http://dx.doi.org/10.5741/GEMS.41.3.202.
——— (2007) From single source to global free market: The transformation of the cultured pearl industry. *G&G*, Vol. 43, No. 3, pp. 200–226, http://dx.doi.org/10.5741/GEMS.43.3.200.
——— (2009) DTC raises prices in "hot" rough market. *GIA Insider*, July 17, http://app.e2ma.net/campaign/13748.add8618e3c4af0d6092da2d8be7d5bc6#article1.
——— (2013) Banks move to curb rough speculation. *GIA Insider*, Oct. 28, www.gia.edu/research-news-banks-move-curb-rough-speculation.
——— (2014) Taming Zimbabwe's diamond production. *GIA Research & News*, March 7, www.gia.edu/gia-news-research-zimbabwe-diamonds-shor.
Times are changing (2013) *Mining Journal*, Sept. 13, www.mining-journal.com/reports/diamonds-times-are-changing.
Weldon R., Shor R. (2014) Botswana's scintillating moment. *G&G*, Vol. 50, No. 2, pp. 96–113, http://dx.doi.org/10.5741/GEMS.50.2.96.
Wyndham C. (2013) Apricot or raspberry? *Rubel & Ménasché Diamantaires*, July 15, www.rubel-menasche.com/insiders/charles-wyndham/apricot-or-raspberry.

THANK YOU, REVIEWERS

GEMS & GEMOLOGY requires each manuscript submitted for publication to undergo a rigorous peer review process, in which each paper is evaluated by at least three experts in the field prior to acceptance. This is an essential process that contributes to the accuracy, integrity, and readability of *G&G* content. In addition to our dedicated editorial review board, we extend many thanks to the following individuals, who devoted their valuable time to reviewing manuscripts in 2014.

- Tara Allen
- Donna Beaton
- Edward W. Boehm
- Guy Borenstein
- John Chapman
- Seavy Chen
- P.G.R. Dharmaratne
- Chanaka Ellawala
- Robyn Ellison
- Ronnie Geurts
- Al Gilbertson
- Hertz Hasenfeld
- Bin He
- Richard W. Hughes
- Dorrit Jacob
- Josephine Johnson
- Sellakumar Kandasamy
- Guanghua Liu
- Yun Luo
- Lainie Mann
- Derek Palmer
- Richard Platt
- Sheriff Rahuman
- Peter Raucci
- Ilene Reinitz
- Menahem Sevdermish
- Russell Shor
- Nicholas Sturman
- Tim Thomas
- Rose Tozer
- Nai Wang
- Pornsawat Wathanakul
- Jian Zhang
- J.C. "Hanco" Zwaan

EXCEPTIONAL PINK TO RED DIAMONDS: A CELEBRATION OF THE 30TH ARGYLE DIAMOND TENDER

John King, James E. Shigley, and Claudia Jannucci

Over the past three decades, more than one thousand pink diamonds from Rio Tinto's Argyle mine in Western Australia have been offered for sale at annual invitation-only events known as tenders. These diamonds, selected from the mine's large annual production of rough, are cut and polished at the company's factory in Perth for the tenders. These diamonds have all been graded by GIA, as their color grade is a crucial value consideration. This article summarizes each year's collection and presents some pertinent statistical information on color grade and description for this important group of rare colored diamonds.

Diamonds are among the rarest and most valuable of all gems. Those exhibiting noticeable color are rarer still. It is estimated that they make up just 0.01% of the world's total production (King, 2006). Such diamonds have been celebrated throughout history as defining treasures of nobility and prized possessions of the wealthy. Of all the colors, pink diamonds are among the most alluring and sought after. For much of history they were recovered only sporadically in India, Brazil, Indonesia, and southern Africa (King et al., 2002). Even rarer was the recovery of diamonds described as red or predominantly red, of which only a handful have ever been documented (Shigley and Fritsch, 1993; Wilson, 2014).

The situation changed dramatically in the mid-1980s with the emergence of the Argyle mine, located in a remote region of Western Australia (Smith, 1996; Shigley et al., 2001). Argyle Diamonds Ltd. was formed by the parent company CRA Ltd., later Rio Tinto Ltd., to develop the mine and market the product. This mine became one of the world's largest sources of diamonds (Bevan and Downes, 2004), including a small production of valuable pink to red stones (figure 1). This limited but consistent supply has intensified interest in these colored diamonds.

The late 1970s and 1980s were a pivotal time in the world of colored diamonds. Through a confluence of events—including the Argyle mine coming on line—colored diamonds gained much greater publicity and desirability than ever before. The late 1970s witnessed a period of unprecedented experimentation in diamond cutting. This proved beneficial to colored diamonds, as many of the proportion sets that were developed served to maximize face-up color appearance. Auction sales and museum exhibitions also drove interest, drawing widespread media coverage. For example, Christie's New York sold the Hancock Red for almost US$1 million per carat in 1987. Andre Gumuchian's Spectrum Collection and Eddy Elzas's Rainbow Collection were also shown at the American Museum of Natural History in New York during these years.

With its high yield of colored diamonds, Argyle joined in this mix of activity by developing innovative advertising and marketing campaigns. These efforts, while bringing attention to their brown "champagne" and "cognac" as well as rare pink diamonds, also heightened awareness of colored diamonds overall.

See end of article for About the Authors and Acknowledgments.
GEMS & GEMOLOGY, Vol. 50, No. 4, pp. 268–279,
http://dx.doi.org/10.5741/GEMS.50.4.268.

Figure 1. A selection of Argyle pink diamonds from the 2007 tender shows a range of color depth. The weights range from 0.66 to 1.74 ct. Photo by Robert Weldon/GIA.

ARGYLE DIAMOND MINE

The Argyle mine (figure 2) is in the East Kimberley region of Western Australia, 500 km (340 mi) southwest of Darwin and more than 2,200 km (1,400 mi) northeast of Perth. Systematic exploration began in 1969, following the discovery of a few alluvial diamonds in the area, but another decade of careful fieldwork passed before geologists recognized the host rock as a diamond-bearing lamproite pipe (Chapman et al., 1996). Several more years were required to de-

Figure 2. In this early photo of Rio Tinto's Argyle mine in Western Australia, taken in the late 1980s, the production plant is seen in the center and the open-pit mine in the upper left. Photo by James Lucey/GIA.

Figure 3. A recent view of underground operations at the Argyle mine, where 40 kilometers of tunneling have been built to access the diamond-bearing lamproite ore. Photo courtesy of Rio Tinto.

velop the site, and the mine became fully operational in late 1985 (Shigley et al., 2001). Over the next 25 years, mining was carried out from a large open pit. In the early years of the 21st century, recognition of the finite economic lifetime of this open pit led to feasibility studies of underground mining operations, which began in 2013 (figure 3).

This decision is expected to extend the life of the mine until at least 2020, with expected production of up to 20 million carats per year over the life of the underground mine. The output is dominated by near-colorless to brown diamonds, but from the beginning there has been a small but consistent supply of pinks, comprising less than 0.1% of the mine's total annual production. This deposit now supplies more than 90% of the pink diamonds in the marketplace, and no other source is known to produce these goods in quantity on a regular basis.

ARGYLE TENDERS

The autumn of 2014 marked the 30th Argyle pink diamond tender. Each year has witnessed increasing participation and competition among diamantaires for invitations to the tender and the opportunity to place sealed bids on these select goods. While most of the diamonds tendered over the years have been pink and purplish pink, a few reds (and even other colors such as blue, violet, orange, and yellow) are occasionally offered.

The first tender, consisting of 33 diamonds, took place in Antwerp in 1985. The following year, Geneva was added as a viewing venue. As interest in these events has grown, previews have been held in New York, Hong Kong, London, Perth, and Tokyo. The number of venues continues to change over the years, as does the number of diamonds on view—some tenders have included 70 or more. The rarity of the items selected for these events is readily apparent from Argyle's estimate that for every half million carats of rough produced, only one carat is suitable for tender.

In Brief

- For the past 30 years, the Argyle mine in Western Australia has been the world's only consistent source of extremely rare pink diamonds.
- Each year a limited selection of Argyle's pink diamond production is sold through highly anticipated closed-bid tenders.
- With mining at Argyle drawing to a close in approximately 2020, the future of the pink diamond tenders is an intriguing question.

Argyle's tender process only adds to the excitement that surrounds these diamonds. The tender is by invitation only, and the list of invitees is not made public. Those invited to bid are provided limited-edition catalogs highlighting key information on each diamond. While they have ample time to review the data from the catalog, an invitation to view allows a time slot of approximately one hour in which to make bidding decisions. Despite this time constraint, the participants are seasoned professionals who know the range of pink diamond color appearances and how they relate to value. In any given city, the site remains unknown until just before the viewings. When setting up to show 30 to 80 pink diamonds in one location, security is crucial.

Upon arrival, the observer finds the diamonds displayed in small individual cases with clear fronts (figure 4). Weight and color grade are noted on each case. Loupe and tweezers are supplied, but many diamantaires bring their own. In some instances, they bring samples for comparison. As is typical in many diamond offices, white paper desk pads are in place, and desk lamps with fluorescent lights are available as well as daylight. While this arrangement does not represent the standard used in a laboratory, most dealers are comfortable with it as it resembles their own office conditions.

Following the viewing, participants make decisions about individual stones or, in some instances, the entire lot. Argyle does not publish the winning bidders or final prices; when reported in the press, it is at the discretion of the buyer.

While GIA has graded all the tender stones, the refinement of its color grading system for colored diamonds in 1995 (see King et al., 1994) allowed a more detailed, boundary-distinct color language for these pink diamonds than ever before. With the addition of grades such as Fancy Deep, Fancy Intense, and Fancy Vivid, the tender diamonds were better recognized for their uniqueness and rich color appearances.

Interest in Argyle pink diamonds certainly expands beyond the activity surrounding tenders. Over the past five years, GIA's laboratory has produced custom monograph reports for exceptional diamonds, colored gemstones, pearls, and jewelry pieces. One such monograph was created in 2010 for the Majestic Pink Diamond Bracelet. The bracelet's 204 pink diamonds, though not tender stones, did come from the Argyle mine. In recent years, notable "hero" stones from the tender have been named. In 2013 a GIA monograph was created for such a diamond, the Argyle Phoenix, a 1.56 ct Fancy red (figure 5).

Figure 4. GIA's John King and Tom Moses (left) join David Fardon of Rio Tinto in examining the 1998 Argyle tender in New York.

Over the years, several authors have described the gemological characteristics of pink diamonds from the Argyle mine, including Hofer (1985), Chapman et al. (1996), Deljanin et al. (2008), and Rolandi et al. (2008). Shigley et al. (1990) detailed the quantity and quality of diamonds discovered in Western Australia during the mine's first five years of operation. Particularly noted was the Argyle mine's dramatic impact on the world market: In 1986, one year after the mine became fully operational, Australia was the largest source of diamonds.

PINK DIAMOND TENDER OVERVIEW

The summaries noted below are based on Argyle press materials highlighting the first 13 tenders (1985 to 1997) as well as annual tender catalogs produced by the company from 1995 to 2014. Tender diamonds have encompassed a wide range of color depths, as well as colors other than pink (figure 6). Note that throughout this article, the term *pink* is applied broadly to the entire color range of pink diamonds. This includes stones with brown, purple, or orange modifying components. In each of these instances, however, the predominant color appearance is pink.

Figure 5. The Argyle Phoenix, a 1.56 ct Fancy red round brilliant diamond, was a highlight of the 2013 tender. Photo by Josh Balduf/GIA.

1985: The inaugural tender offered 33 diamonds with a total weight of 18.03 carats. Never had such a large group of pink diamonds been assembled for sale, a noteworthy preview of things to come.

1986: This collection of 56 stones totaling 32 carats was divided into two groups: 12 diamonds of fine color and 44 lower-quality pink and brownish pink diamonds. Two gems in particular stood out. One of them, a 0.52 ct emerald cut, was noted to be the finest purple-pink diamond Argyle had ever offered. The other, a 2.11 ct cushion cut, was said to be remarkable not only for its size but also its deep color and fine VS clarity. According to Argyle, the prices achieved at this sale were thought to be strong, considering this was only the second tender.

1987: With 83 diamonds weighing a combined 59.65 carats, this tender nearly doubled the total weight from the preceding year. The overall quality of the goods was also markedly improved. One memorable 0.50 ct diamond appeared to be so saturated that it bordered on red, eclipsing all other Argyle pink diamonds seen up to that point.

1988: The fourth tender set new standards for size, color, and quality, featuring 53 diamonds with a combined weight of 64.08 carats. The average stone size was 7% larger, including 26 diamonds over one carat and three diamonds over two carats. Highly saturated colors were also found in a 0.66 ct diamond and a 1.00 ct round.

1989: Although Argyle's fifth tender offered fewer diamonds, the average carat weight rose 26% over the prior year: 67 diamonds were offered at 64.38 total carats, for an average weight of 1.04 ct. This tender included two stones over three carats. One, a 3.16 ct round, boasted a saturation previously found only in much smaller diamonds. The second, a 3.20 ct kite-shaped diamond described as lilac-colored, was notable for its size and exquisite saturation. Another memorable pink was a 1.04 ct round, described by Argyle as "the single finest example of color, size, make, and clarity, striking the most ideal balance, that ever had, or possibly ever will, come out of Australia."

In April 1989, a separate auction of Argyle pink diamonds was held at Christie's New York. Argyle chose this method of sale—a first for a mine—hoping to reach a new audience of private buyers. The auction featured 16 unmounted pink diamonds ranging from 0.41 to 3.14 ct. At this time, the "end grade" for pinks in GIA's system was Fancy. Therefore, diamonds with the greatest depth of color were all described as Fancy, with others noted as Light or Fancy Light. Color descriptions included pink, purplish pink, brownish pink, brown-pink, and pink-brown.

1990: In the first tender of the 1990s, 36 diamonds totaling 40.93 carats were offered. The average weight remained above one carat, but this tender was a departure from previous years in that no stones over two carats were offered. Nevertheless, record bids for this smaller collection reflected the continued emphasis on quality.

1991: The seventh tender consisted of 47 gems weighing a total of 40.15 carats: 43 pinks, three blues, and one Fancy grayish greenish yellow diamond. The entire collection was sold to a single buyer, Robert Mouawad of Geneva.

1992: The 1992 tender began with a preview in Tokyo. Fifty diamonds with a total weight of 43.39 carats were offered for sale. A record number of bidders demonstrated the continuing demand for Argyle's unique diamonds. Winning bids went to 15 clients from countries including the United States, the UK, Belgium, Switzerland, Japan, and Italy.

Figure 6. Highlights from the 2007 tender include (left to right) a 0.66 ct Fancy Vivid purplish pink cut-cornered rectangular modified brilliant, a 1.02 ct Fancy Intense pink round brilliant, a 0.91 ct Fancy Intense purplish pink triangular brilliant, a 1.74 ct Fancy purplish red oval brilliant, a 0.77 ct Fancy Dark gray-violet shield cut, a 0.69 ct Fancy purplish red emerald cut, and a 1.22 ct Fancy Vivid purplish pink emerald cut. Photo by Robert Weldon/GIA.

1993: Strong competition characterized this tender, which saw the entire collection sold again to Robert Mouawad. This time, Mouawad announced that he paid more than US$2.25 million to purchase the 46-diamond selection, totaling 41.48 carats.

1994: The entire collection of 47 diamonds, weighing a total of 45.17 carats, was sold to an international consortium. Argyle reported that the per-carat price surpassed that of all previous tenders but did not disclose the amount of the sale.

More than 35% of the 1994 tender diamonds were above one carat. These included two Fancy pink diamonds weighing more than three carats, a 3.00 ct round brilliant and a 3.04 ct emerald cut. For the first time, the tender collection was viewed in Hong Kong and Singapore.

1995: This tender featured the most pink diamonds over one carat since 1990. Its 47 diamonds weighing 45.22 carats total brought more than US$4.5 million, over US$100,000 per carat. Seven fancy-color diamond dealers from Asia and Europe purchased the collection. Showings in Tokyo, Hong Kong, and Geneva brought unprecedented levels of publicity to the tender, and 17 leading dealers and jewelers placed more than 180 bids for individual diamonds. Noted highlights included a 1.05 ct Fancy Deep purplish pink round brilliant and three heart shapes weighing 0.70, 0.75, and 0.90 ct, as well as the collection's largest diamond, a 2.80 ct Fancy Deep pink emerald cut.

1996: Two new venues were added this year: Perth and London. The 47.82 carat collection of 47 stones featured the largest polished pink diamond ever tendered by Argyle up to that point, a 3.66 ct Fancy Intense pink-purple cushion cut. The second-largest diamond at this tender was a 3.06 ct Fancy Intense pink emerald cut. Prior to 1996, only six pink diamonds in the three-carat-plus category had ever been offered by Argyle.

1997: Featuring 59 diamonds totaling 58.64 carats, the 1997 tender set a new record for total sale price. Although Argyle also reported a new record per-carat price for the 55 pink diamonds offered, neither figure was made public. Almost half the diamonds (27) were one carat or larger. The most outstanding offering was a 1.78 ct oval, the largest Fancy purplish red diamond ever graded by GIA at the time. Other significant stones were a 1.41 ct Fancy Intense purple-pink emerald cut with VVS clarity (pinks with such high clarity grades are extremely rare), a 1.01 ct Fancy Deep pink round brilliant, and a 2.82 ct Fancy Intense purplish pink round brilliant (the tender's largest diamond). A viewing was conducted in Sydney for the first time, in response to growing demand for fancy-color diamonds in the Australian market.

1998: This year saw the introduction of New York as a viewing location. This edition included 63 diamonds, ranging from 0.44 to 3.15 ct, with a total weight of 58.20 carats. Lot 62, a 2.66 ct heart-shaped diamond, truly captured the soul of the tender with its Fancy Vivid purplish pink hue. Almost a quarter of the diamonds received a Fancy Vivid classification from GIA, the most since the revision of the fancy-color grading system in 1995.

1999: For the 15th tender, 51 diamonds with a total weight of 52.61 carats were presented, in sizes ranging from 0.50 to 2.76 ct. A highlight of this tender was its largest diamond, a stunning 2.76 ct Fancy Intense purplish pink oval brilliant. This sale also included the first Argyle diamond graded by GIA as Fancy red, a 0.73 ct emerald cut.

2000: To start the new millennium, Argyle assembled 47 diamonds totaling 46.43 carats. With a size range from 0.50 to 2.10 ct, the tender included 22 diamonds of at least one carat. Five of the diamonds were Fancy Vivid; the two largest of these, both graded as Fancy Vivid purplish pink, were a 1.66 ct oval and a 1.75 ct princess cut.

2001: Of the 41 diamonds featured, 17 were larger than one carat. One highlight of the tender was an impressive 4.15 ct Fancy Intense purplish pink radiant, the first stone over four carats to appear in an Argyle tender. The collection had a total weight of 41.92 carats.

2002: Of the 43 diamonds offered at this tender, nearly half were graded by GIA as either Fancy Vivid purplish pink or Fancy Intense purplish pink, with an additional three Fancy purplish reds. The colors represented an impressive palette, ranging from Fancy Vivid purplish pink to Fancy Deep gray-violet. Two highlights of this tender were a magnificent 2.14 ct round brilliant Fancy Intense purplish pink and a rare Fancy purplish red 1.00 ct oval. The total weight of the lots was 40.13 carats, with sizes ranging from 0.40 to 2.52 ct.

2003: This stunning collection was comprised of 48 pink diamonds weighing a total of 45.60 carats. Two of these are considered among the finest from any tender: a 2.06 ct round brilliant graded as Fancy Vivid purplish pink and a 2.04 ct radiant graded as Fancy Vivid purple-pink. This tender, with sizes ranging from 0.49 to 2.07 ct, also featured the second-ever Fancy red diamond, a 0.54 ct oval.

2004: For the 20th edition, Argyle unveiled an impressive selection of 60 pink diamonds totaling 55.53 carats. This sale featured an extraordinarily rare 1.00 ct Fancy red radiant-cut diamond, only the third Fancy red ever tendered. There were four stones larger than two carats, most notably a 2.31 ct Fancy Vivid purplish pink cushion cut. The collection also featured two diamonds graded as Fancy purplish red: a 0.52 ct lozenge cut and a 0.69 ct emerald cut.

2005: With 60 diamonds totaling 58.81 carats, this collection featured an extraordinary number of red hues, as well as nine diamonds designated as Fancy Vivid. There were also 27 diamonds larger than one carat, and four greater than two carats.

Another notable event that year was the formal registering of the Argyle Participation Agreement, signed by both Argyle and the traditional owners of the land. This agreement acknowledged the indigenous owners as the mining lease custodians, recognizing Argyle's right to mine while also laying the foundation for a shared commitment to employment, education, and business development in East Kimberley.

2006: This tender featured the largest gathering of pink diamonds in well over a decade, consisting of 65 diamonds weighing a total of 61.43 carats. Thirteen received the Fancy Vivid color grade. Rounding out this splendid collection were three radiant cuts, each weighing exactly 2.03 ct, graded as Fancy Deep pink, Fancy Intense pink, and Fancy Intense purplish pink. Also in 2006, Argyle announced that an underground mine would be constructed below the existing open pit. At the time it was estimated that underground operations would extend the life of the mine to 2018.

2007: The 2007 tender was viewed in only three locations: Perth, Hong Kong, and New York, half the number of venues seen in the previous three years. Many of the 65 stones had a deeper, more vivid color than in years before. With 62.20 carats total, the tender offered several highlights, including a rare Fancy Dark gray-violet diamond, a 0.77 ct shield cut (figure 7). The selection also featured 22 stones with a Fancy Deep grade and 15 others graded as Fancy Vivid. Other featured diamonds included a 1.51 ct octagonal Fancy Deep pink, an octagonal 2.02 ct Fancy Deep pink, and a 1.74 ct oval-shaped Fancy purplish red (again, see figure 7).

2008: This tender was comprised of 64 lots weighing a total of 62.46 carats. It included a number of highly sought-after rounds and two notable diamonds: a 1.01 ct round Fancy purplish red (the Argyle Aphrodite) and a 1.41 ct Fancy Deep gray-violet octagon (the Argyle Ocean Seer). For the first time in seven years, the collection also included a heart-shaped diamond, a 1.33 ct Fancy Intense purplish pink.

2009: Titled "Grand Passions," the 25th tender comprised 43 stones and a total weight of 34.74 carats. One of the four hearts offered, a 2.61 ct Fancy Intense pink, was the most valuable heart-shaped pink diamond ever to come from the Argyle mine. Exuding passion, romance, and warmth, it was named the Argyle Amour. Also highlighted were the Argyle Shalimar, a 1.25 ct Fancy Vivid purplish pink round, and the Argyle Scarlett, a 1.10 ct Fancy red oval.

For this tender, Argyle produced a magnificent two-volume oversized catalog. The first volume showed all 43 stones, while the second gave background on the Argyle mine and its pink diamonds, including many beautiful illustrations. The collection also had its first-ever viewing in India. Mumbai had established itself as the manufacturing center for champagne-colored Argyle diamonds, and the tenders had seen an enthusiastic response from Indian diamantaires.

2010: Showcased for the first time in mainland China (Shanghai and Beijing), the 2010 "Earth Magic" tender comprised 55 diamonds totaling 46.42 carats. A 2.02 ct round Fancy Vivid purplish pink named the Argyle Mystra intrigued bidders with its depth of color. Argyle used the move into new tender locations to educate potential collectors through its publication of *Rare and Collectable*. This book, which accompanied the tender catalog and was distributed through authorized partners, examined the rarity of Argyle pink diamonds relative to global supply, capturing their allure and value.

2011: This year's theme was hearts and flowers. For the first time, a matching suite of stones was presented. As each Argyle diamond is unique, a trio of matching colors is exceptionally rare. The Argyle Semper Suite, consisting of three Fancy Intense pink heart-shaped diamonds (0.58, 0.60, and 1.31 ct) was rarer still. Also shown was the Argyle Alanya, a 1.06 ct Fancy Vivid purplish pink oval named after one of the world's rarest tulip species. Fifty-five diamonds appeared in the 2011 tender, with a total weight of 47.61 carats.

2012: Inspired by Queen Elizabeth II's Diamond Jubilee, Argyle showcased its 2012 collection in a unique exhibition at Kensington Palace in London. The queen's association with pink diamonds dated back to 1947, when she and Prince Phillip were given a 54.5 ct rough pink crystal from the Williamson (or Mwadui) mine in Tanzania as a wedding present. The diamond, now known as the Williamson Pink, was cut in 1948 and set as a 23.6 ct round brilliant into a flower spray brooch by Cartier in 1953. Those attending the Kensington Palace exhibition were granted the unusual privilege of viewing a selection from this very private collection of rare stones. Of the 70 diamonds in the 2012 tender, which totaled 42.79 carats, 40 were on display in this special exhibition. A notable stone from the tender was the Argyle Siren, a 1.32 ct Fancy Vivid purplish pink square radiant cut.

2013: The 2013 tender was known as the "Red Edition" for its three Fancy reds weighing 0.20, 0.58, and 1.56 ct, all round brilliants. Sixty-four diamonds were showcased that year, ranging from 0.20 to 2.03 ct, with a total weight of 54.99 carats. Two significant records were broken. The Argyle Phoenix, a 1.56 ct Fancy red, brought in the highest per-carat price for any diamond from the mine. The Argyle Dauphine, a 2.51 ct Fancy Deep pink radiant cut, achieved the

Figure 7. Two important diamonds from the 2007 tender were a 1.74 ct Fancy purplish red oval brilliant and a 0.77 ct Fancy Dark gray-violet shield cut. Photo by Robert Weldon/GIA.

highest overall price paid for an Argyle diamond. According to Argyle, this was also a world record for a Fancy Deep pink tender diamond.

Though plans for underground mining at Argyle had been announced in 2006, it did not start until April 2013. As underground mining became operational and testing was completed, the expected life of the mine was extended from its original estimate of 2018 to at least 2020.

2014: To celebrate the 30th tender, and in keeping with that year's bird theme, a limited-edition set of diamond-encrusted feather pendants was created with over one carat of pavé-set Argyle pinks. The tender comprised 54 pink diamonds totaling 46.88 carats. The featured diamond of the collection was the 1.21 ct radiant-cut Fancy red Argyle Cardinal, named after the North American bird known for its bright color. This tender also included four red diamonds. To date, there have only been 13 red diamonds in the history of the tender.

Two other exceptional diamonds were the Argyle Toki, a 1.59 ct Fancy Intense purplish pink emerald cut, and the Argyle Rosette, a 2.17 ct Fancy Intense purple-pink emerald cut. The 2014 sale achieved the highest average price per carat since the tender's inception.

EXAMINATION OF PINK TENDER DIAMONDS

As noted earlier, each of the pink diamonds tendered has been examined by GIA's laboratory. But the 1995 modifications to GIA's colored diamond color grading system (see King et al., 1994) added new classifications to better describe face-up color appearance. With this in mind, our analysis of the pink tender diamonds will focus on the years 1995 to 2014. During that time, 1,100 Argyle stones were sold by tender. Included in that number are very limited examples of color other than predominantly pink. For the purposes of our analysis, we will focus on the 1,065 diamonds described as predominantly pink (again, the term *pink* is used to describe the entire range of pink diamonds).

Over the years, strong depth of color has become a trademark of the Argyle diamonds seen at tender. This is clear from the chart in figure 8, where the grades related to stronger depth of color—Fancy Intense, Fancy Deep, and Fancy Vivid—dominate.

To determine the color grade, the overall face-up color appearance is observed under controlled lighting and viewing conditions (King et al., 1994). The assigned grade is a combination of tone (the color's lightness or darkness) and saturation (its strength or purity). Pink diamonds occur throughout the entire range of fancy grades, from pale colors associated with grades such as Faint, Very Light, and Light to the grades noted above for stronger colors. Red or purplish red diamonds are limited to the grade "Fancy" because they occur in a limited range of tone and saturation (King et al., 2002).

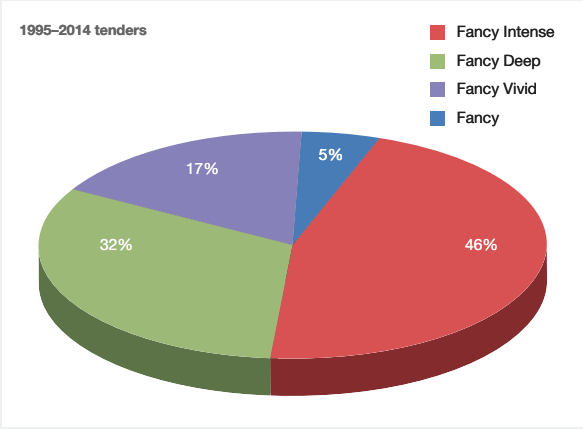

Figure 8. This chart shows the distribution of fancy color grades for the 1,065 pink diamonds from the 1995–2014 tenders. The vast majority (95%) had Fancy Deep, Fancy Intense, and Fancy Vivid color grades.

In our analysis, the grade of "Fancy" represents the very small percentage of red or purplish red diamonds. Of the 1,065 pink diamonds selected for the tender from 1995 through 2014, 95% were graded as Fancy Intense, Fancy Vivid, and Fancy Deep (see figure 8). In the last five years, there has been a steady increase in the number of Fancy Intense color grades chosen, while the number of Fancy Vivids has fallen to levels seen in the first decade of the 2000s. Similarly, diamonds described as Fancy Deep represented 70% of the grades in 2000 but just 3% in 2014. Such shifts can occur for many reasons, including variations in the yearly mine output, cutting decisions to brighten or darken color near grade boundaries, or attempts to address current market trends in desirability.

Figure 9 shows that the color descriptions chosen for tender diamonds have been quite consistent over the 20-year period. In GIA's system, the color appearance of pink diamonds extends across six different hues, from pink-purple to pinkish orange (King et al., 2002). As shown in figure 9, the overwhelming majority of the 1,065 diamonds sampled (91%) occurred

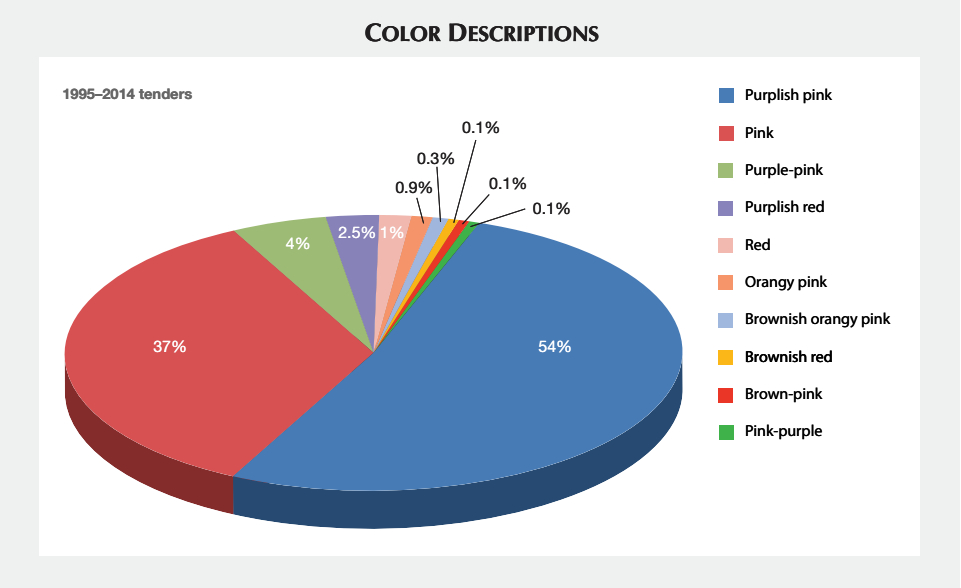

Figure 9. While the tender diamonds displayed a range of color hues, the majority (91%) were described as having pink or purplish pink hues. A total of 1,065 diamonds were included in this analysis (excluding those with blue, violet, gray, green, and yellow colors).

in a narrower range of hues: pink to purplish pink. Of this group of samples, 40 were described on grading reports as purplish red (27) or red (13). The largest of the red diamonds, the Argyle Phoenix, a 1.56 ct round brilliant, was included in the 2013 tender.

With regard to carat weight, figure 10 notes that 95% of the tender diamonds have weighed less than 2.00 ct, with the majority (56%) in the 0.50–0.99 ct range. The smallest weighed 0.20 ct, the largest 4.15 ct. Only 5% of this group weighed 2.00 ct or more. This faceted size range is typical of diamonds from the Argyle deposit. While larger rough pink diamonds have originated from kimberlites in India, Brazil, Indonesia, and southern Africa, it is unclear in geological terms why similar larger crystals do not occur here. Pink diamond crystals from Argyle tend to display irregular or strongly resorbed shapes (Chapman et al., 1996), and there is no indication that they represent broken cleavage pieces of larger crystals.

The shape and cutting style descriptions of the Argyle diamonds from the 1995–2014 tenders are compared in figure 11. Four shapes—rectangular, round, square, and oval—account for 89% of the

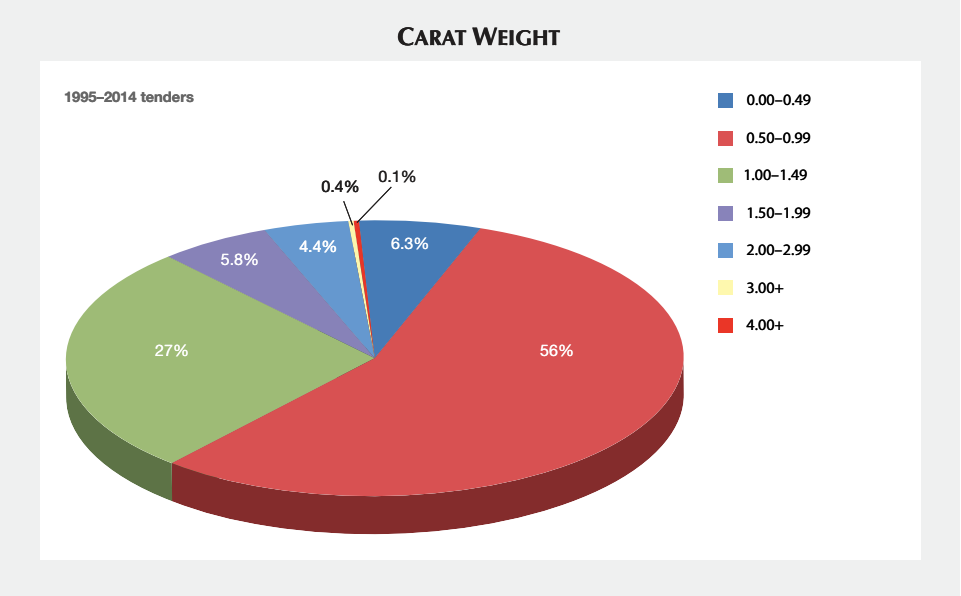

Figure 10. Most of the tender diamonds (95%) weighed less than 2.00 ct, and 62% were less than 1.00 ct.

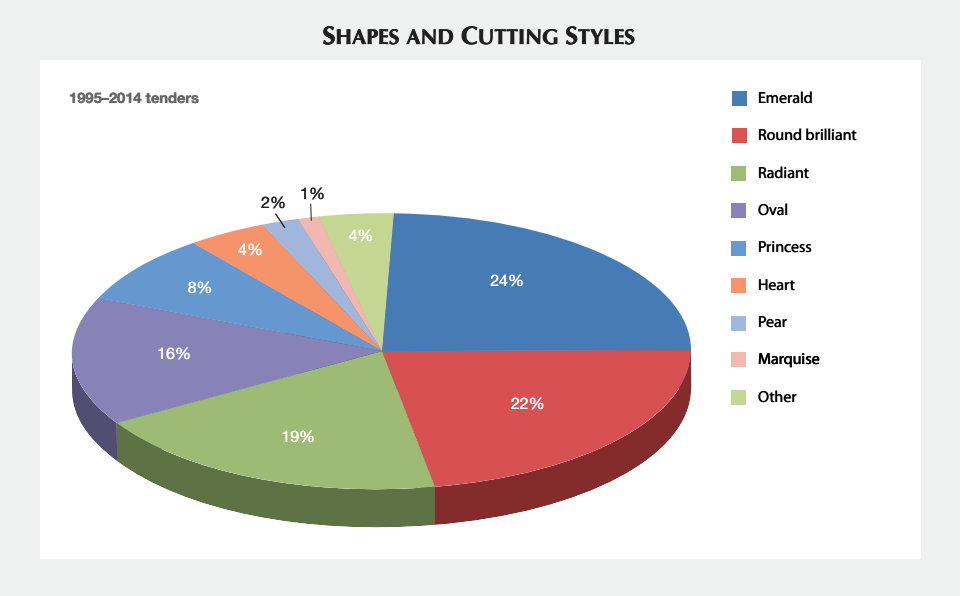

Figure 11. Argyle uses a combination of shape and cutting style descriptions in labeling diamonds for the tender catalogs. Most of the tender diamonds (89%) were rectangular, round, square, and oval. The overwhelming majority of stones are cut in the modified brilliant style, including all diamonds described as round, radiant, and princess.

samples. The square and rectangular stones were most often cut as emerald cuts or cut-cornered modified brilliants (often referred to in the trade as "radiants"). While the step faceting of emerald cuts was the most common style, with round brilliants a close second, the other fancy shapes (square and rectangular modified brilliants and oval brilliants or modified brilliants) are often chosen by the manufacturer to maximize weight retention from the original crystal and accentuate the face-up color appearance.

These cutting choices reflect the tremendous rarity of pink to red diamonds in that clarity grades have relatively little impact on their market value. With per-carat prices easily reaching US$100,000 or more based primarily on color, achieving high clarity is of less concern. Most pink to red diamonds seen in the Argyle tenders correspond to an SI to I clarity range. On the rare occasion that one is accompanied by high clarity, it is usually the talk of the tender, such as the exceptional 2.04 ct Fancy Vivid purple-pink radiant offered in 2003, which possessed VVS_1 clarity. More recently, the 2014 tender featured a 0.51 ct round brilliant Fancy Intense pink diamond with VVS_1 clarity.

CONCLUSION

For centuries, pink diamonds have been cherished as true rarities of nature, and their great beauty has made them sought-after possessions. For the past 30 years, Australia's Argyle mine has been the only consistent source of this gem material. Through Argyle's effort to market these and other colored diamonds from the mine, the industry and public have gained much greater awareness of these fascinating gems. This article presented an overview of 30 years of tender diamonds, as well as a 20-year summary of their characteristics. As Argyle looks ahead to the 30th anniversary of its pink diamond tender, we are left to wonder about the course of future tenders with the shift to underground mining operations. How will pink diamonds' desirability and value be shaped by an end-of-mining scenario in the near future? Such intriguing questions only add to the fascination that surrounds this unique product.

ABOUT THE AUTHORS

Mr. King is chief quality officer, and Mrs. Jannucci is project manager of laboratory services, at GIA's laboratory in New York. Dr. Shigley is a Distinguished Research Fellow at GIA in Carlsbad.

ACKNOWLEDGMENTS

The authors wish to thank John Chapman, Josephine Johnson, and Robyn Ellison of Argyle Pink Diamonds for their comments and assistance on background information.

REFERENCES

Bevan A., Downes P. (2004) In the pink: Argyle's diamond gift to Australia. *Australian Gemmologist*, Vol. 22, No. 4, pp. 150–155.

Chapman J., Brown G., Sechos B. (1996) The typical gemmological characteristics of Argyle diamonds. *Australian Gemmologist*, Vol. 19, No. 8, pp. 339–346.

Deljanin B., Simic D., Chapman J., Dobrinets I., Widemann A., DelRe N., Middleton T., Deljanin E., de Stefano A. (2008) Characterization of pink diamonds of different origin: Natural (Argyle, non-Argyle), irradiated and annealed, treated with multi-process, coated and synthetic. *Diamond and Related Materials*, Vol. 17, No. 7/10, pp. 1169–1178, http://dx.doi.org/10.1016/j.diamond.2008.03.014.

Hofer S.C. (1985) Pink diamonds from Australia. *G&G*, Vol. 21, No. 3, pp. 147–155, http://dx.doi.org/10.5741/GEMS.21.3.147.

King J.M., Ed. (2006) *Colored Diamonds*. Gemological Institute of America, Carlsbad, CA.

King J.M., Moses T.M., Shigley J.E., Liu Y. (1994) Color grading of colored diamonds in the GIA Gem Trade Laboratory. *G&G*, Vol. 30, No. 4, pp. 220–242, http://dx.doi.org/10.5741/GEMS.30.4.220.

King J.M., Shigley J.E., Guhin S.S., Gelb T.H., Hall M. (2002) Characterization and grading of natural-color pink diamonds. *G&G*, Vol. 38, No. 2, pp. 128–147, http://dx.doi.org/10.5741/GEMS.38.2.128.

Rolandi V., Brajkovic A., Adamo I., Fontana I. (2008) Argyle type Ia pink diamonds. *Australian Gemmologist*, Vol. 23, No. 5, pp. 194–203.

Shigley J.E., Chapman J., Ellison R.K. (2001) Discovery and mining of the Argyle diamond deposit, Australia. *G&G*, Vol. 37, No. 1, pp. 26–41, http://dx.doi.org/10.5741/GEMS.37.1.26.

Shigley J.E., Dirlam D.M., Schmetzer K., Jobbins E.A. (1990) Gem localities of the 1980s. *G&G*, Vol. 26, No. 1, pp. 4–31, http://dx.doi.org/10.5741/GEMS.26.1.4.

Shigley J.E., Fritsch E. (1993) A notable red-brown diamond. *Journal of Gemmology*, Vol. 23, No. 5, pp. 259–266.

Smith R. (1996) Jewel of the Kimberley. *Australian Geographic*, No. 41 (January–March), pp. 88–107.

Wilson W.E. (2014) Red diamond. *Mineralogical Record*, Vol. 45, No. 2, pp. 201–214.

Study of the Blue Moon Diamond

Eloïse Gaillou, Jeffrey E. Post, Keal S. Byrne, and James E. Butler

The Blue Moon diamond, discovered in January 2014 at the historic Cullinan mine in South Africa, is of significance from both trade and scientific perspectives. The 29.62 ct rough yielded a 12.03 ct Fancy Vivid blue, Internally Flawless gem. The authors were provided the opportunity to study this rare diamond at the Smithsonian Institution before it went on exhibit at the Natural History Museum of Los Angeles County. Infrared spectroscopy revealed that the amount of uncompensated boron in the diamond was 0.26 ± 0.04 ppm, consistent with measurements of several large type IIb blue diamonds previously studied. After exposure to short-wave ultraviolet light, the Blue Moon displayed orange-red phosphorescence that remained visible for up to 20 seconds. This observation was surprising, as orange-red phosphorescence is typically associated with diamonds of Indian origin, such as the Hope and the Wittelsbach-Graff. Time-resolved phosphorescence spectra exhibited peaks at 660 and 500 nm, typical for natural type II blue diamonds. As with most natural diamonds, the Blue Moon showed strain-induced birefringence.

The Blue Moon diamond drew widespread media attention when the discovery of the 29.62 ct rough (figure 1, left) at the Cullinan mine in South Africa was announced in January 2014. This mine, formerly known as the Premier, is also the source of the historic Cullinan diamond, as well as two other important blue diamonds: the Smithsonian Institution's Blue Heart, a 30.62 ct Fancy Deep blue gem discovered in 1908, and the 27.64 ct Fancy Vivid blue Heart of Eternity, unveiled by Steinmetz in 2000. The publicity only increased when the rough was purchased a month later by Cora International LLC for $25.6 million, setting a record price per carat for a rough stone (Bronstein, 2014). In June 2014, after a few months of examination, the diamond was cut into a 12.03 ct cushion, graded by GIA as Fancy Vivid blue and Internally Flawless (figure 1, right). Cora International named it the Blue Moon diamond as a tribute to its rarity. The Blue Moon made its first public appearance at the Natural History Museum of Los Angeles County (NHMLAC) on September 13, 2014, for a temporary exhibit running through January 6, 2015.

The Cullinan mine produces the most type II diamonds of any mine (King et al., 1998). In 2014 alone it yielded the Blue Moon as well as a 122.52 ct type IIb light blue diamond and a 232.08 ct type IIa colorless diamond, both of them rough stones. Additionally, the largest rough diamond of all time was discovered at the Cullinan mine in 1905. The Cullinan diamond, a 3,106.75 ct type IIa colorless stone, was eventually cut into several stones. The two largest (545.67 and 317.40 ct) reside in the British Crown Jewels (Balfour, 2009). Because of its rare color and size, the Blue Moon can be added to the list of significant diamonds from the Cullinan mine.

The Blue Moon represents a noteworthy blue diamond discovery, as an exceptional gem and as a rare specimen for scientific study. In a recent study that investigated the relationships among color saturation, phosphorescence properties, and concentrations of boron and other impurities in type IIb blue diamonds (Gaillou et al., 2012), one variable was largely excluded: geographic origin. Among the 76 stones studied, only a dozen were of known origin. This is not surprising, as information about a diamond's mine or even country of origin is rarely retained. The exceptions are stones such as the Hope and the Wittelsbach-Graff diamonds, which are known to be alluvial stones from near Golconda in India, and the Blue Heart and the nine blue diamonds in the Cullinan necklace, which are from the Cullinan mine. The Blue Moon adds to this list of important blue diamonds with a known origin. It is also the first Fancy Vivid blue that the authors have been able to examine in detail.

See end of article for About the Authors and Acknowledgments.
Gems & Gemology, Vol. 50, No. 4, pp. 280–286,
http://dx.doi.org/10.5741/GEMS.50.4.280.

Figure 1. Left: The Blue Moon diamond as the 29.62 ct rough discovered in January 2014 at the Cullinan mine in South Africa. Right: The faceted Blue Moon diamond, a 12.03 ct cushion modified brilliant, graded by GIA as Fancy Vivid blue and Internally Flawless; photo by Tino Hammid. Photos © Cora International.

MATERIALS AND METHODS

The Blue Moon diamond has a cushion modified brilliant cut, weighs 12.03 ct, and measures 15.57 × 13.47 × 7.55 mm. Its small culet facet enabled us to perform spectroscopy through the parallel faces of the table and the culet. Analyses were conducted at the Smithsonian Institution's Department of Mineral Sciences (figure 2). Fourier-transform infrared spectra were acquired using a Thermo Scientific Nicolet 6700 FTIR spectrometer and Nicolet Continuum microscope (figure 2, left). Spectra were collected with a spectral resolution of 4 cm^{-1} and an accumulation of 128 scans. The IR light was focused on the culet facet with an aperture of 150 × 150 µm.

Phosphorescence was visually observed using portable short-wave and long-wave ultraviolet lights, with main excitation wavelengths of 254 and 365 nm, respectively. Phosphorescence spectra were col-

Figure 2. Left: The Blue Moon under the microscope of the FTIR spectrometer, which identified it as a type IIb diamond with an uncompensated boron concentration of 0.26 ± 0.04 ppm. Center: A view of the Blue Moon and the phosphorescence equipment, composed of a deuterium lamp source, a spectrometer, and fiber optics. Right: The Blue Moon under the tip of a fiber-optic bundle used for the phosphorescence experiments. All analyses were conducted at the Smithsonian Institution. Photos by Jeffrey Post (left) and Eloïse Gaillou (center and right).

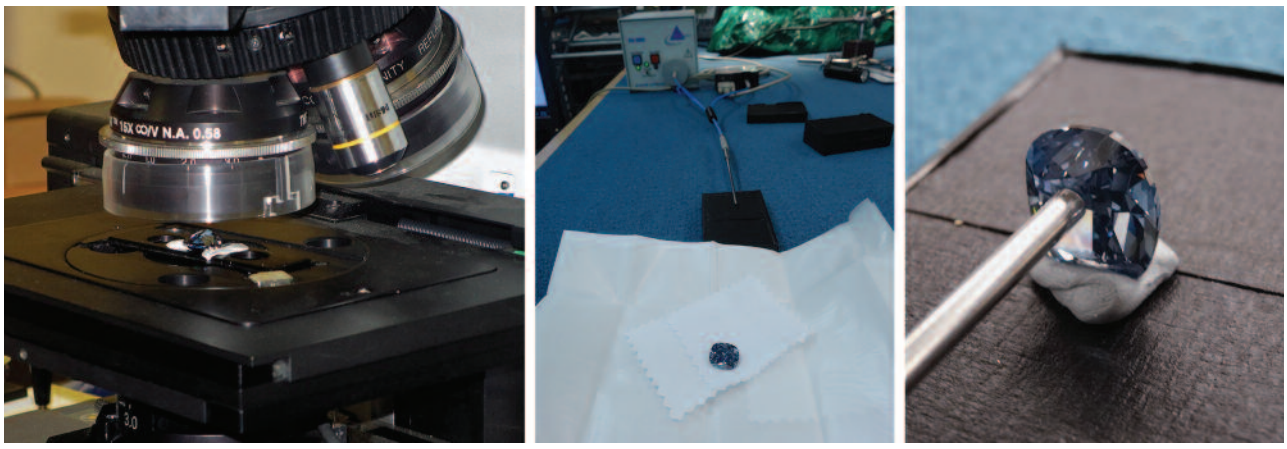

lected using the portable spectrometer described by Eaton-Magaña et al. (2008) and shown in figure 2, center. The diamond was excited with an Ocean Optics DH-2000 deuterium UV lamp (215–400 nm), and the signal was acquired with an Ocean Optics USB2000 charge-coupled device (CCD) spectrometer through a fiber-optic bundle. The UV radiation was transferred through a bundle of six optical fibers, each 600 µm in diameter. A seventh fiber in the core of the bundle collected the emitted light from the diamond and delivered it to the entrance aperture of the CCD spectrometer. The tip of the fiber-optic bundle was placed directly in contact with four different areas of the diamond (figure 2, right) to sample possible spatial variations in the spectra. The phosphorescence spectra were collected after 10 seconds of UV light exposure. The spectra acquisition began 500 ms after the light was turned off. During decay, the spectra were integrated and recorded at 2.0, 1.0, and 0.5 second intervals, respectively. Only the results for the spectra with 1.0 second intervals are presented here, as it is the most representative data.

To examine birefringence resulting from internal strain in diamond, we placed the stone between crossed polarizers and observed it using transmitted light.

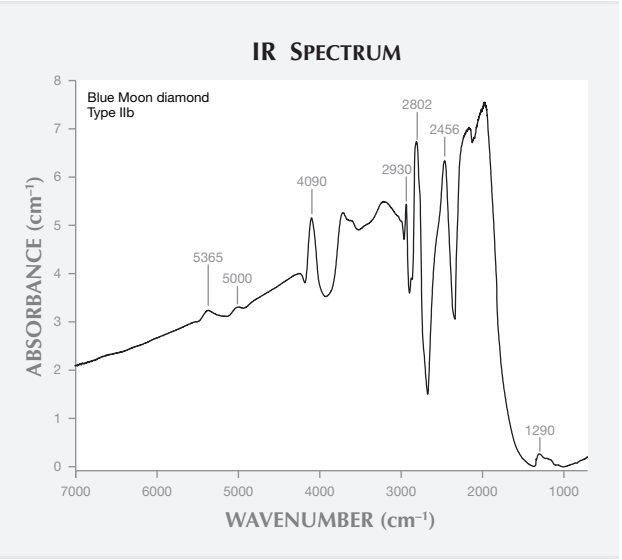

Figure 3. The Blue Moon's infrared spectrum exhibits peaks associated with boron. The 1290 cm^{-1} peak was used to determine the boron concentration. The absorption coefficient is normalized per centimeter of optical path length.

In Brief

- The type IIb Blue Moon diamond is a 12.03 ct Fancy Vivid blue, Internally Flawless diamond. The 29.62 ct rough was mined at the Cullinan mine in South Africa in January 2014.
- The concentration of uncompensated boron, which gives the diamond its blue color, is 0.26 ± 0.04 ppm.
- The Blue Moon shows a red phosphorescence for about 20 seconds after UV excitation; spectroscopy reveals an intense broad emission centered at 660 nm and a weak, quickly fading 500 nm emission.

RESULTS

FTIR spectrometry (figure 3) confirmed that the Blue Moon is a type IIb diamond—in other words, it lacks nitrogen observable by FTIR in the 900–1400 cm^{-1} region, and it contains boron. Due to the diamond's long IR beam path (7.55 mm) from the culet facet through the table, most of the spectral features related to boron showed almost complete absorption. The boron peaks were positioned at 1290, 2456, 2802, 2930, 4090, 5000, and 5365 cm^{-1}. The area near the 2802 cm^{-1} peak is typically used to calculate the concentration of uncompensated boron (Collins and Williams, 1971; Fisher et al., 2009), but this peak was saturated and could not be used to estimate boron concentration. Instead we used a secondary peak at 1290 cm^{-1}, as in the method developed by Collins (2010). After normalization, the boron peak at 1290 cm^{-1} had an absorption height of 0.115 cm^{-1}, corresponding to a boron concentration of 0.26 ± 0.04 ppm (Collins, 2010). As this value represents only uncompensated boron—not charge-compensated by other impurities such as nitrogen—the total boron content is at least equal to this measured value, plus potentially some unknown amount of compensated boron. The Blue Moon's value of 0.26 ppm is within the average of several notable blue diamonds. Compare this with the uncompensated boron averages of 0.36 ± 0.06 ppm for the 45.52 ct Hope, 0.19 ± 0.03 ppm for the 31.06 ct Wittelsbach-Graff, 0.24 ± 0.04 ppm for the 30.62 ct Blue Heart, and 0.31 ± 0.003 ppm for the 2.60 ct Cullinan Blue (Gaillou et al., 2012).

The Blue Moon did not show any obvious fluorescence (i.e., there was no visible emission of light while the diamond was excited by a UV light), in keeping with the type IIb blue diamonds we have examined. It did show phosphorescence, in the form of an intense orange-red glow after exposure to UV

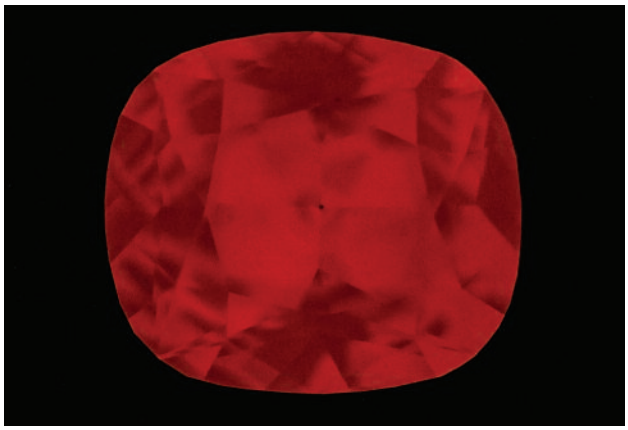

Figure 4. After exposure to short-wave ultraviolet light, the Blue Moon displayed orange-red phosphorescence for up to 20 seconds. Photo by Tino Hammid, © Cora International.

light. The phosphorescence was most intense after exposure to short-wave UV light and remained visible to dark-sensitized eyes for up to 20 seconds (figure 4).

Time-resolved spectra for the light emitted during phosphorescence are presented in table 1 and in figure 5. As previously observed for all natural, untreated type IIb blue diamonds, the Blue Moon's phosphorescence spectra showed two emission bands: one at 660 nm and another at 500 nm that decreased more rapidly. Previous studies (Gaillou et al., 2012) have demonstrated that different diamonds can have different relative intensities of those two bands. Diamonds with a dominant 500 nm band exhibit a brief bluish phosphorescence; if the 660 nm peak is more intense, the diamond shows an orange-red glow (Eaton-Magaña et al., 2008; Eaton-Magaña and Lu, 2011; Gaillou et al., 2012). The Blue Moon displayed an intense 660 nm band and a weak 500 nm band (hence the observed orange-red phosphorescence). The 500 nm peak disappeared completely within seconds, while the 660 nm band faded away after 25 seconds (with a half-life of about four seconds). Only a third of the type IIb diamonds examined by Gaillou et al. (2012) showed a stronger emission at 660 nm than at 500 nm (figure 6). The Blue Moon belongs to this minority, along with the Hope and the Wittelsbach-Graff (Gaillou et al., 2010; figure 7). Several spectra were acquired across the stone: in the center of the table, on the edge of the table, on the girdle, and on the culet (table 1). The slight differences are not significant, indicating that the phosphorescence is homogeneous, at least to the resolution of our measurements.

The cause of the 500 and 660 nm emissions is not fully understood, but it has been suggested that

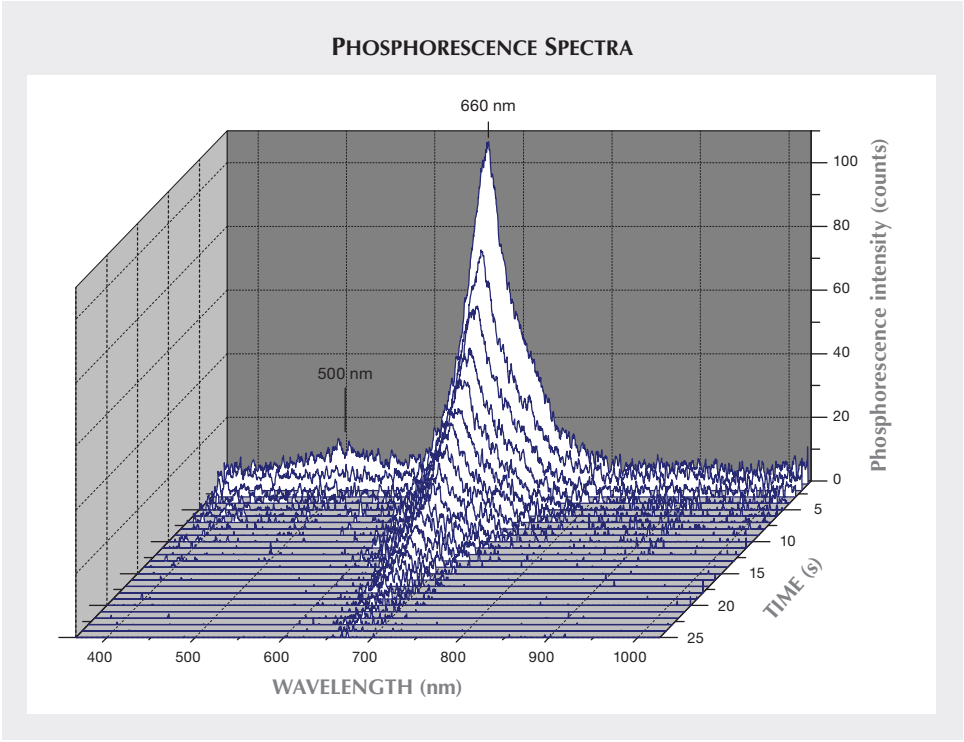

Figure 5. Time-resolved phosphorescence spectra of the Blue Moon diamond after excitation by a deuterium lamp. An area on the girdle was probed for these spectra. The weaker 500 nm band decreased faster than the more intense 660 nm peak.

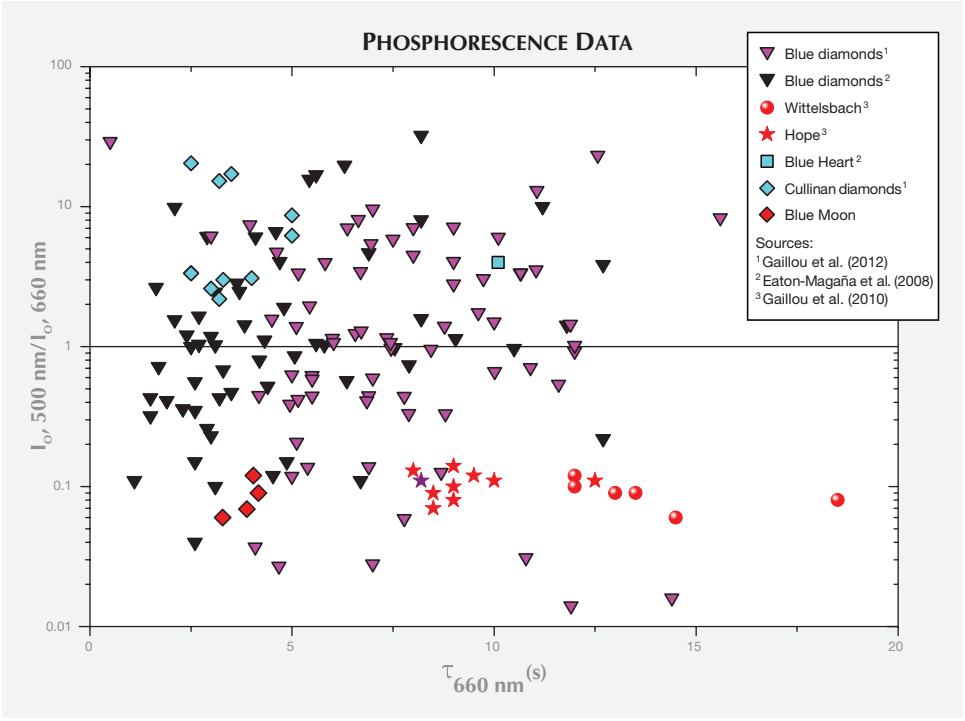

Figure 6. Phosphorescence data from natural type IIb diamonds shows the ratios of initial intensities of the 500 and 660 nm bands plotted against the measured half-lives of the 660 nm emission. For y-axis values greater than 1, the blue band dominates; for values less than 1, the red band dominates. Except for the Blue Moon, blue diamonds from South Africa such as the Blue Heart and the diamonds in the Cullinan necklace ("Cullinan diamonds") plot in the upper part of the graph. The Hope and Wittelsbach-Graff, which have an Indian origin, plot with the Blue Moon in the lower part of the graph.

they might be produced by the recombination of donor-acceptor pairs (nitrogen and boron, respectively). The 660 nm band may also have a component influenced by plastic deformation (Eaton-Magaña et al., 2008; Eaton-Magaña and Lu, 2011; Gaillou et al., 2012).

Finally, the Blue Moon was examined between crossed polarizers with transmitted light to observe the anomalous birefringence found in many diamonds, especially type II samples (Lang, 1967). While diamonds are cubic and should not show any birefringence, most do display some birefringence due to residual strain in the diamond structure (e.g., Lang, 1967; Hanley et al., 1977; Collins et al., 2000; Kanda et al., 2005). The Blue Moon displayed the typical "tatami" pattern (two directions of strain lamination) with gray and blue interference colors (figure 8). The tatami pattern was visible in every direction through the diamond. The laminations of the tatami patterns are oriented in the [111] planes, the "weak" planes of diamonds corresponding to the octahedral faces.

Figure 7. A selection of type IIb blue diamonds previously studied. Left: the 31.06 ct Wittelsbach-Graff (width = 23.23 mm) and 45.52 ct Hope (width = 25.60 mm). Center: the 30.62 ct Blue Heart diamond (width = 20.15 mm). Right: The Cullinan necklace's detachable brooch, containing nine blue diamonds (width of brooch = 55.54 mm). Photos by Chip Clark, © Smithsonian Institution.

TABLE 1. Phosphorescence data acquired from the Blue Moon diamond.

Area probed	Initial intensity, 500 nm band (counts)	Initial intensity, 660 nm band (counts)	Ratio of initial intensities, 500 nm/660 nm bands	Half-life, 500 nm band (seconds)	Half-life, 660 nm band (seconds)
Table off-center	5.34	77.34	0.07	2.28	3.88
Table center	5.00	90.43	0.06	1.00	3.28
Culet	7.22	78.65	0.09	1.19	4.17
Girdle	13.00	107.00	0.12	1.75	4.04

DISCUSSION AND CONCLUSION

While the Blue Moon diamond has a Fancy Vivid blue color, its uncompensated boron concentration of 0.26 ppm is in the lower range of values of blue diamonds recorded in a previous study (Gaillou et al., 2012). But the value is similar to that of other large type IIb blue diamonds such as the Hope, the Wittelsbach-Graff, and the Blue Heart (Eaton-Magaña et al., 2008; Gaillou et al., 2012; again, see figure 7). While the uncompensated boron concentration might not represent the total boron content, it is the only boron that is active in the infrared and visible parts of the spectrum and contributes to the blue bodycolor (e.g., Collins, 1982). Gaillou et al. (2012) showed a lack of a strong correlation between color saturation (as graded by GIA on a scale from light to deep saturation) and uncompensated boron content. For a parallel slab of type IIb diamond, the bodycolor is a function of the uncompensated boron concentration and the thickness of the slab, and maybe other components; for a faceted gem the perceived color also depends on the shape and the cut.

Figure 8. Placed between crossed polarizers and viewed in transmitted light, the Blue Moon diamond shows anomalous birefringence with the crossed laminations called "tatami" features. Photo by Eloïse Gaillou.

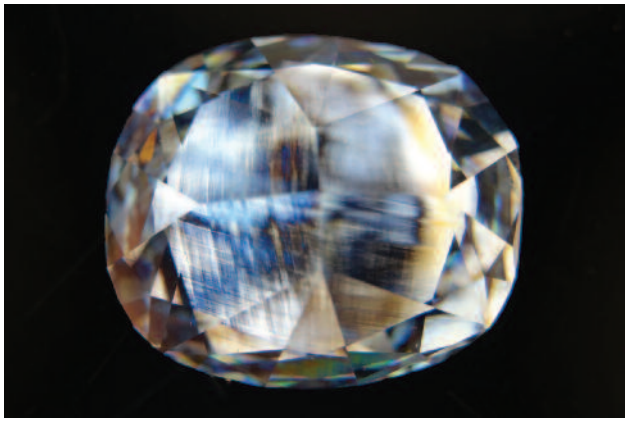

Perhaps the most surprising result is that the Blue Moon shows an intense and relatively long-lasting orange-red phosphorescence. We are aware of only one other type IIb diamond from the Cullinan mine with orange-red phosphorescence (King et al., 2003). Type IIb diamonds with orange-red phosphorescence more commonly originated in India or Venezuela (Gaillou et al., 2010, 2012; personal communication with Thomas Hainschwang in 2011 on the Indian blue diamond collection of the Natural History Museum in Vienna). The nine diamonds from the Cullinan mine studied by Gaillou et al. (2012) showed the more typical brief bluish phosphorescence (again, see figures 6 and 7). The Blue Moon underscores the fact that the phosphorescence behavior of type IIb diamonds is not tied to a specific geographical source.

ABOUT THE AUTHORS

Dr. Gaillou (eloise.gaillou@gmail.com) is associate curator at MINES ParisTech (School of Mines, Paris) and a research associate at the Smithsonian Institution's National Museum of Natural History in Washington, DC. At the time of the study, she was the associate curator in mineral sciences at the Natural History Museum of Los Angeles County. Dr. Post is curator of the National Gem and Mineral Collection, and Dr. Byrne is a postdoctoral fellow, at the Smithsonian's National Museum of Natural History. Dr. Butler, retired from the Naval Research Laboratory in Washington, DC, is a consultant in Huntingtown, Maryland, and a research associate at the Smithsonian's National Museum of Natural History.

ACKNOWLEDGMENTS

The authors are grateful to Cora International for the unique opportunity to study the Blue Moon diamond.

REFERENCES

Balfour I. (2009) *Famous Diamonds*. Antique Collectors' Club Ltd., Woodbridge, Suffolk, UK, 335 pp.

Bronstein A. (2014) The tale of the Blue Moon diamond. *CampdenFB*, http://www.campdenfb.com/article/sponsored-feature-tale-blue-moon-diamond [date accessed: 12/1/2014].

Collins A.T. (1982) Colour centres in diamond. *Journal of Gemmology*, Vol. 18, No. 1, pp. 37–75.

Collins A.T. (2010) Determination of the boron concentration in diamond using optical spectroscopy. *Proceedings of the 61st Diamond Conference*, Warwick, UK.

Collins A.T., Williams A.W.S. (1971) The nature of the acceptor centre in semiconducting diamond. *Journal of Physics C: Solid State Physics*, Vol. 4, pp. 1789–1799, http://dx.doi.org/10.1088/0022-3719/4/13/030.

Collins A.T., Kanda H., Kitawaki H. (2000) Colour changes produced in natural brown diamonds by high-pressure, high-temperature treatment. *Diamond and Related Materials*, Vol. 9, No. 2, pp. 113–122, http://dx.doi.org/10.1016/S0925-9635(00)00249-1.

Eaton-Magaña S., Lu R. (2011) Phosphorescence in type IIb diamonds. *Diamond and Related Materials*, Vol. 20, No. 7, pp. 983–989, http://dx.doi.org/10.1016/j.diamond.2011.05.007.

Eaton-Magaña S., Post J.E., Heaney P.J., Freitas J., Klein P., Walters R., Butler J.E. (2008) Using phosphorescence as a fingerprint for the Hope and other blue diamonds. *Geology*, Vol. 36, No. 1, pp. 83–86, http://dx.doi.org/10.1130/G24170A.1.

Fisher D., Sibley S.J., Kelly C.J. (2009) Brown colour in natural diamond and interaction between the brown related and other colour-inducing defects. *Journal of Physics: Condensed Matter*, Vol. 21, No. 36, pp. 1–10, http://dx.doi.org/10.1088/0953-8984/21/36/364213.

Gaillou E., Wang W., Post J.E., King J.M., Butler J.E., Collins A.T., Moses T.M. (2010) The Wittelsbach-Graff and Hope diamonds: Not cut from the same rough. *G&G*, Vol. 46, No. 2, pp. 80–88, http://dx.doi.org/10.5741/GEMS.46.2.80.

Gaillou E., Post J.E., Rost D., Butler J.E. (2012) Boron in natural type IIb blue diamonds: chemical and spectroscopic measurements. *American Mineralogist*, Vol. 97, No. 1, pp. 1–18, http://dx.doi.org/10.2138/am.2012.3925.

Hanley P.L., Kiflawi I., Lang A.R. (1977) On topographically identifiable sources of cathodoluminescence in natural diamonds. *Philosophical Transactions of the Royal Society of London A: Mathematical, Physical, and Engineering Sciences*. Vol. 284, No. 1324, pp. 329–368, http://dx.doi.org/10.1098/rsta.1977.0012.

Kanda H., Ahmadjan A., Kitawaki H. (2005) Change in cathodoluminescence spectra and images of type II high-pressure synthetic diamond produced with high pressure and temperature treatment. *Diamond and Related Materials*, Vol. 14, No. 11–12, pp. 1928–1931, http://dx.doi.org/10.1016/j.diamond.2005.08.015.

King J.M., Moses T.M., Shigley J.E., Welbourn C.M., Lawson S.C., Cooper M. (1998) Characterization of natural-color type IIb blue diamonds. *G&G*, Vol. 34, No. 4, pp. 246–268.

King J.M., Johnson E.A., Post J.E. (2003) Gem News International: A comparison of three historic blue diamonds. *G&G*, Vol. 39, No. 4, pp. 322–325.

Lang A.R. (1967) Causes of birefringence in diamond. *Nature*, Vol. 213, No. 5073, pp. 248–251, http://dx.doi.org/10.1038/213248a0.

A Preliminary Study on the Separation of Natural and Synthetic Emeralds Using Vibrational Spectroscopy

Le Thi-Thu Huong, Wolfgang Hofmeister, Tobias Häger, Stefanos Karampelas, and Nguyen Duc-Trung Kien

More than 300 natural and synthetic emeralds from various sources were examined with Raman spectroscopy. Of this set, 36 KBr pellets of different samples were also examined with FTIR spectroscopy. In many cases, the presence or absence of specific Raman and FTIR bands, and the exact position of apparent maxima, are correlated to the weight percentage of silicon and/or alkali. This can help determine whether an emerald is natural or synthetic.

Both vibrational Raman and FTIR spectroscopy have been widely applied in identifying synthetic and natural beryl (Wood and Nassau, 1968; Schmetzer and Kiefert, 1990; Huong et al., 2010). These methods are used to characterize the water molecules present in the beryl channel sites, known as type I and type II water molecules. Type I water molecules occur independently of alkalis, while type II are associated with nearby alkalis. In most natural beryl, Raman bands arising from both types are visible, though some natural beryls with relatively low alkali present weak type II–related bands. Most hydrothermal synthetic samples display the Raman signal of type I water (the type II signal is barely visible in most cases). Neither band is visible in flux-grown synthetic beryl, which has no water in its structure (Schmetzer and Kiefert, 1990). These methods are not effective in cases such as relatively low-alkali natural beryl, where the type I water band is observed almost exclusively (Huong et al., 2011), and some hydrothermal synthetic beryl that contains a small amount of alkalis and can show a weak type II water Raman signal as well.

This article presents some additional differences that could be used to distinguish between natural and synthetic emeralds. These features, mostly generated by silicon- and/or alkali-related vibrations, include a Raman band at about 1070 cm^{-1} (Adams and Gardner, 1974) and an FTIR band around 1200 cm^{-1} (Aurisicchio et al., 1994) and its shoulder at about 1140 cm^{-1}.

BACKGROUND

Beryl—$Be_3Al_2Si_6O_{18}$—has a structure composed of six-membered rings of $[SiO_4]^{4-}$ tetrahedra. The silicate rings are aligned precisely over one another, forming open channels parallel to the c-axis of the crystal (Huong et al., 2010). The diameter of the channels has the capacity to hold large ions and molecules such as alkalis (Na^+, K^+) and water (Goldman et al., 1978; Aines and Rossman, 1984). Alkalis act as charge compensators for the substitution of main elements such as Al^{3+} and Be^{2+}. The ideal composition of the main elements to match the exact stoichiometry of beryl is 67.0 wt.% SiO_2, 18.9 wt.% Al_2O_3, and 14.1 wt.% BeO. In beryl, Al^{3+} in octahedral sites and Be^{2+} in tetrahedral sites are commonly substituted with other elements including Cr^{3+}, V^{3+}, Fe^{3+}, Fe^{2+}, Mg^{2+}, Mn^{2+}, Be^{2+}, and Li^+. Additionally, charge compensation by alkalis (including Cs, Rb, K, and Na) and water in the ring channels diminishes the weight % of Si in the formula. These additions affect the silicon-related vibrational signals.

Because growers of synthetic beryl follow the exact stoichiometric formula, unlike nature, some differences in silicon-related vibrations would be expected. Therefore, Raman and FTIR spectroscopy could provide valuable information for assessing the origin of emeralds (figure 1).

See end of article for About the Authors.
Gems & Gemology, Vol. 50, No. 4, pp. 287–292,
http://dx.doi.org/10.5741/GEMS.50.4.287.

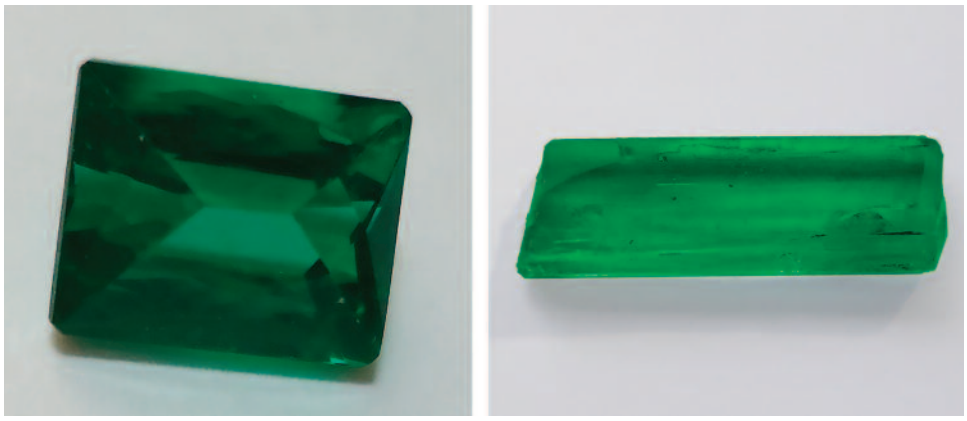

Figure 1. Representative samples from this study include faceted synthetic emeralds (Biron, 0.61 ct, 5.5 × 4.6 mm) and natural emeralds (Zambia, 0.48 ct, 6.5 × 2.3 mm). Photos by Nguyen Duc-Trung Kien.

MATERIAL AND METHODS

We collected 326 natural and synthetic emerald samples for Raman analysis. The natural samples consisted of 260 crystals obtained directly from mines in Brazil (20 from Santa Terezinha and 15 each from Carnaíba, Capoeirana, Itabira, and Socotó); Colombia (30 from Chivor); Austria (10 from Habachtal); Russia (10 from the Ural Mountains); Madagascar (30 from Mananjary); South Africa (30 from Transvaal); Zambia (30 from Kafubu); Nigeria (30 from Gwantu); and China (10 from Malipo). The 66 faceted synthetic emeralds consisted of hydrothermally grown (15 Tairus and 10 Biron) and flux-grown (20 Gilson, 20 Chatham, and 1 Lennix) samples provided by the producers.

Raman spectra from 200 to 1200 cm^{-1} were collected with a Jobin Yvon (Horiba) LabRam HR 800 spectrometer equipped with an Olympus BX41 optical microscope and a Si-based CCD (charge-coupled device) detector. All samples (except the faceted ones) were polished on two sides, oriented parallel to the c-axis. They were polished with corundum paste to obtain a smooth surface and ultrasonically cleaned with acetone. The instrumentation used an Ar^{+} ion laser (514 nm emission), a grating with 1800 grooves/mm, and a slit width of 100 mm. These parameters, and the optical path length of the spectrometer, yielded a spectral resolution of 0.8 cm^{-1}. The spectral acquisition time was set at 240 seconds for all measurements, and sample orientation was carefully controlled. The electric vector of the polarized laser beam was always parallel to the c-axis.

For FTIR measurements, we chose 36 samples (27 natural emeralds from various sources and 9 synthetics from different producers; see table 1). FTIR spectra were recorded in the 400–1400 cm^{-1} range by a PerkinElmer 1725X FTIR spectrometer with 100 scans and 4 cm^{-1} spectral resolution using the KBr pellet method (2 mg of powder drilled from each sample mixed with 200 mg of KBr). Peak analysis of both Raman and FTIR results was performed with an OriginLab Origin 7.5 professional software package, and the peaks were fitted using a Gauss-Lorentz function.

Chemical analysis of the same 36 samples was carried out with electron microprobe for Si and laser ablation–inductively coupled plasma–mass spectrometry (LA-ICP-MS) for all other elements studied. Microprobe analyses were performed with a JEOL JXA 8900RL instrument equipped with wavelength-dispersive spectrometers, using 20 kV acceleration voltage and a 20 nA filament current. Silicon was analyzed by microprobe, with wollastonite used as the standard. For most elements, including silicon, the detection limit for wavelength-dispersive (WD) spectrometers is between 30 and 300 parts per million (ppm). The precision depends on the number of X-ray counts from the standard and sample and the reproducibility of the WD spectrometer mechanisms. The highest obtainable precision is about 0.5%.

In Brief

- The presence or absence of Raman and FTIR bands, and the exact position of apparent maxima, often correspond to the silicon and/or alkali content in natural and synthetic emerald.
- The Raman band in synthetic emerald samples shows an apparent maximum at 1067–1066 cm^{-1} and FWHM between 11 and 14 cm^{-1}. In natural samples, the apparent maximum ranges from 1068 to 1072 cm^{-1} and FWHM varies from 12 to 26 cm^{-1}.
- The FTIR band in synthetic emeralds shows an apparent maximum at about 1200–1207 cm^{-1}, while natural samples show an apparent maximum at about 1171–1203 cm^{-1}.

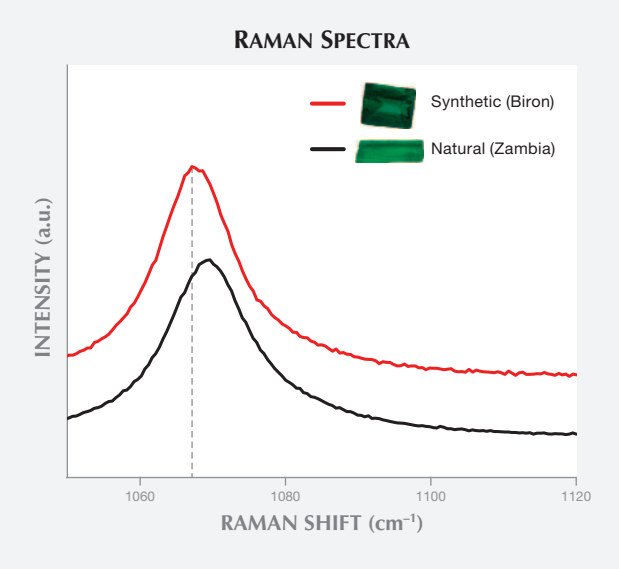

Figure 2. The Raman peak of a representative natural sample is at a higher wavenumber than that of a representative synthetic emerald sample.

LA-ICP-MS quantitative analysis for all elements except Si (including Li, Be, B, Na, Mg, Al, P, K, Ca, Sc, Ti, V, Cr, Mn, Fe, Co, Ni, Ga, Ge, Rb, Sr, Y, Zr, Nb, Mo, Cs, Ba, La, and Ta) was conducted using an Agilent 7500ce ICP-MS in pulse-counting mode. Ablation was performed with a New Wave Research UP-213 Nd:YAG laser ablation system, using a pulse repetition rate of 10 Hz, an ablation time of 60 seconds, a dwell time of 10 milliseconds per isotope, a 100 µm crater diameter, and five laser spots averaged for each sample. Silicon (determined with the microprobe) was used as the internal standard. Data reduction was carried out using Glitter software. The amount of material ablated in laser sampling varied in each spot analysis. Consequently, the detection limits were different for each spot and were calculated for each acquisition. Detection limits for the analyzed elements ranged between 0.0001 and 0.5 ppm. For trace elements such as Ta, La, Nb, and Y, the detection limit was 0.0001 ppm. The detection limit was 0.01 ppm for minor elements such as alkalis and 0.5 ppm for main elements, including Be and Al. Analyses were calibrated using the NIST 612 glass standard. BCR-2G glass was also measured as a reference material.

RESULTS AND DISCUSSION

The Raman Peak at Approximately 1070 cm^{-1}. Earlier studies attributed this peak to either Si-O stretching (e.g., Adams and Gardner, 1974; Charoy et al., 1996) or Be-O stretching in the beryl structure (e.g., Kim et al., 1995; Moroz et al., 2000). Recent results have shown that this peak is mainly due to Si-O stretching (Huong, 2008).

Figure 2 presents Raman spectra from 1050 to 1120 cm^{-1} for a hydrothermal synthetic emerald (Biron) and a natural emerald (Kafubu, Zambia). The exact posi-

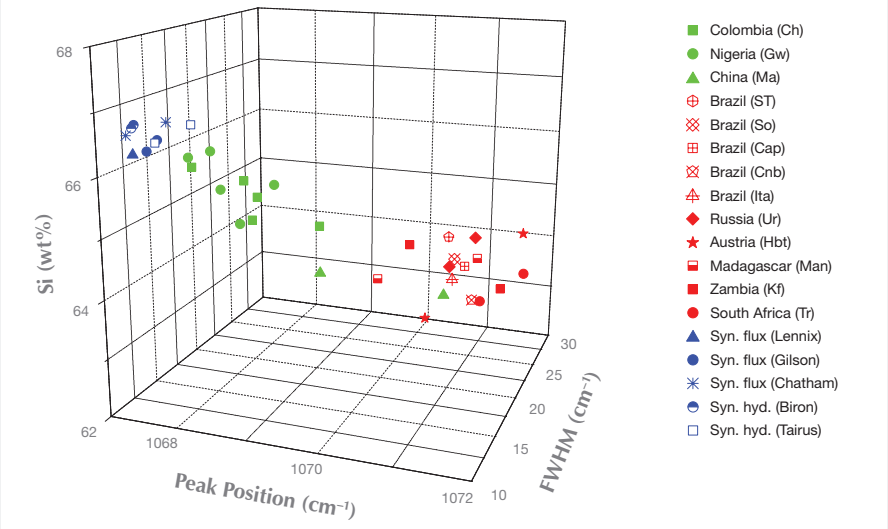

Figure 3. This diagram shows the correlation among FWHM, Raman shift (peak position), and Si (wt.%). Higher Raman shifts and FWHM values correspond to a lower wt.% of Si.

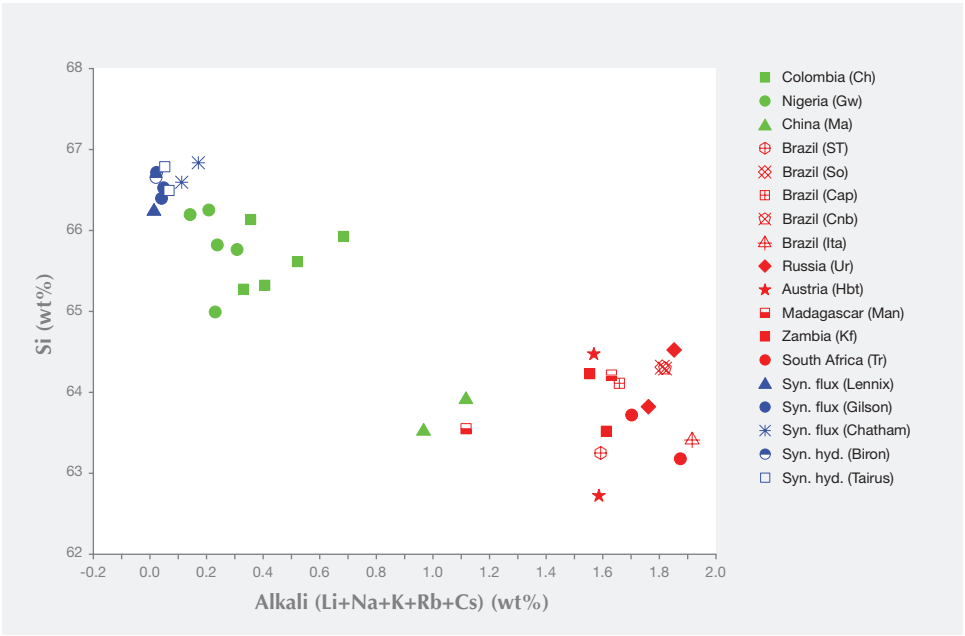

Figure 4. This diagram shows the correlation between silicon and alkali (Li+Na+K+Rb+Cs) weight percentage (wt.%) in natural and synthetic samples. Samples with lower wt.% of Si show higher alkali wt.%.

tion and shape of the observed peaks differ. For the synthetic sample, the apparent maximum is situated at around 1067.5 cm^{-1}, with a full width at half maximum (FWHM) of 12 cm^{-1}. The apparent maximum for the synthetic samples is positioned at 1067.0–1068.0 cm^{-1}, and the FWHM varies between 11 and 14 cm^{-1}. There is no variation between the different growth methods (hydrothermal vs. flux) or manufacturers regarding this peak (figure 3). The natural sample presented in figure 2 shows an apparent maximum at approximately 1070 cm^{-1} and a FWHM of 18 cm^{-1}. In the natural samples, the apparent maximum ranged from 1068 to 1072 cm^{-1} and FWHM varied between 12 and 26 cm^{-1} (with no clear difference among geographic origins; figure 3). The variation in the exact position (shifting) and shape (broadening) of this peak is probably due to the presence of at least two different bands; the peak's position and shape are linked to the relative intensities of these bands. Peak position and FWHM show overlap between some natural and synthetic samples (when the apparent maxima overlap at 1068 cm^{-1} and the FWHM at 12–14 cm^{-1}). Thus, only the natural samples have presented peak maxima above 1068 cm^{-1} with a FWHM >15 cm^{-1}, and only synthetic emeralds have maxima at 1067 cm^{-1} with a FWHM of 11 cm^{-1}. When they are not within overlap ranges, peak position and FWHM can help identify natural and synthetic emerald.

Correlation diagrams of chemical composition data, 1070 cm^{-1} Si-related Raman peak positions, and FWHMs showed that the Si-O band broadened and shifted to higher wavenumbers when the Si wt.% decreased (figure 3). The shifting and broadening of the peak probably result from chemical substitution.

In figure 4, the correlation between Si and alkali ion weight percentages is observed; samples with lower than stoichiometric Si show high alkali wt.%. As silicon is the main element in the beryl structure, only a relatively significant decrease of silicon wt.% (i.e., a relatively significant increase of alkali wt.%) causes a detectable change in the Raman band properties. When the wt.% of silicon (as well as the sum of alkalis) is significantly different (for example, up to 3 wt.% variance between natural and synthetic samples), the difference in band properties can be observed. When the silicon wt.% is more similar (around 1 wt.% variance among natural samples; i.e., "low" alkali wt.%), the difference in band properties is not visible. In "high-alkali" emeralds (>1.5% alkali content), this band shifts at about 1069–1072 cm^{-1} (FWHM of 16–26 cm^{-1}). In "low-alkali" emeralds with <0.5% alkali content (e.g., Nigerian and Colombian) and in synthetic samples with <1.5% alkali content, these bands shift at about 1068–1070 cm^{-1} (FWHM of 12–18 cm^{-1}) and 1067–1068 cm^{-1} (FWHM of 11–14 cm^{-1}), respectively.

The 1200 cm^{-1} FTIR Absorption Band and Its Shoulder. This band was attributed to Si-O stretching in the beryl structure (Aurisicchio et al., 1994). Figure 5 presents the FTIR absorption spectra of a synthetic emerald (flux-grown, Gilson) and a natural emerald (Ural Mountains, Russia) from 400 to 1600 cm^{-1} (see inset from 1100 to 1300 cm^{-1}).

TABLE 1. Chemical data of natural and synthetic emeralds by electron microprobe (silicon content) and LA-ICP-MS (alkali content).

Source	Silicon (wt.%)	Total alkalis Li+Na+K+Rb+Cs (wt.%)
Natural		
Colombia/Chivor 1	65.272±0.333	0.330±0.024
Colombia/Chivor 2	66.134±0.081	0.355±0.030
Colombia/Chivor 3	65.609±0.392	0.521±0.041
Colombia/Chivor 4	65.921±0.312	0.683±0.031
Colombia/Chivor 5	65.306±0.284	0.405±0.053
Nigeria/Gwantu 1	66.254±0.168	0.208±0.021
Nigeria/Gwantu 2	66.188±0.056	0.142±0.018
Nigeria/Gwantu 3	64.986±0.409	0.230±0.041
Nigeria/Gwantu 4	65.755±0.220	0.208±0.035
Nigeria/Gwantu 5	65.820±0.081	0.238±0.052
China/Malipo 1	63.521±0.302	0.966±0.062
China/Malipo 2	63.914±0.472	1.116±0.036
Brazil/Santa Terezinha	63.245±0.221	1.591±0.041
Brazil/Socotó	64.306±0.162	1.809±0.032
Brazil/Capoeirana	64.109±0.093	1.657±0.081
Brazil/Carnaíba	64.287±0.178	1.819±0.032
Brazil/Itabira	63.410±0.254	0.914±0.011
Russia/Ural 1	63.823±0.213	1.760±0.070
Russia/Ural 2	64.521±0.243	1.850±0.021
Austria/Habachtal 1	64.470±0.151	1.567±0.072
Austria/Habachtal 2	62.719±0.083	1.585±0.045
Madagascar/Mananjary 1	63.554±0.412	1.116±0.017
Madagascar/Mananjary 2	64.209±0.244	1.629±0.029
Zambia/Kafubu 1	64.228±0.109	1.552±0.006
Zambia/Kafubu 2	63.523±0.372	1.611±0.012
South Africa/Transvaal 1	63.723±0.251	1.701±0.017
South Africa/Transvaal 2	63.178±0.222	1.872±0.045
Synthetic (hydrothermal)		
Biron 1	66.710±0.360	0.166±0.011
Biron 2	66.650±0.163	0.142±0.014
Tairus 1	66.489±0.214	0.067±0.009
Tairus 2	66.783±0.202	0.052±0.014
Synthetic (flux)		
Gilson 1	66.391±0.101	0.041±0.003
Gilson 2	66.524±0.323	0.049±0.010
Chatham 1	66.830±0.272	0.171±0.019
Chatham 2	66.591±0.130	0.112±0.012
Lennix 1	66.233±0.164	0.033±0.005

All synthetic samples showed an apparent maximum at around 1200 to 1207 cm^{-1}, while natural emeralds showed an apparent maximum at about 1171 to 1203 cm^{-1}. This peak appears to consist of more than one band, and its exact position and shape are linked to the relative intensities of these bands. An overlap of the apparent maxima was observed with some low-alkali natural and synthetic samples from 1200 to 1203 cm^{-1}. In addition, all high-alkali emeralds displayed a shoulder at about 1140 cm^{-1}. The shoulder has not been reported in previous studies. Among low-alkali samples, this shoulder could be seen in Colombian samples (Chivor) but not in Nigerian emeralds. Its exact position is also linked to the main peak position. The shoulder was not observed in any of the synthetic samples (again, see figure 5).

Correlating chemical data showed that the presence of the shoulder was also related to alkali content. In the samples with high alkali ion content, the

Figure 5. The FTIR weak absorption band (see inset) at around 1140 cm^{-1} is seen in natural samples with high alkali content but not in synthetic samples. The presence of this shoulder has not been reported by previous studies. Other bands between 400 and 1100 cm^{-1} have been reported and assigned to the bondings of main elements (i.e., Si, Al, and Be). The FTIR absorption spectra were acquired on KBr pellets of powdered emeralds.

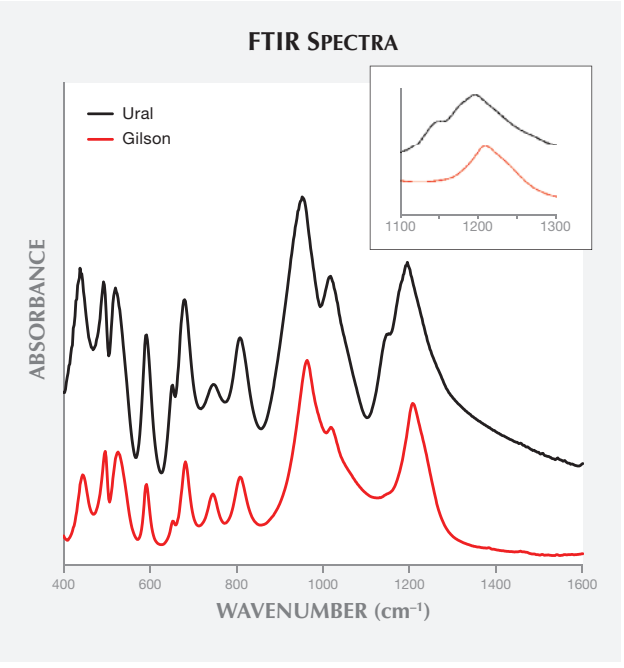

shoulder at 1140 cm^{-1} was distinct. Moreover, the apparent maximum of the peak at 1200 cm^{-1} shifted to lower wavenumbers. In samples with low alkali content, particularly synthetic samples, the shoulder disappeared and the apparent maximum at 1200 cm^{-1} shifted toward higher wavenumbers.

CONCLUSION

Natural and synthetic emeralds can sometimes be distinguished by the apparent maxima and FWHM of the silicon- and alkali-related Raman peak at 1070 cm^{-1}. Using FTIR spectroscopy on KBr pellets of powdered samples, the distinction can sometimes be made based on the silicon-related peak at 1200 cm^{-1}, as well as a shoulder, possibly linked to alkali content. Synthetic samples showed the Raman peak with apparent maxima from 1067 to 1068 cm^{-1} (FWHM of 11–14 cm^{-1}) and FTIR apparent maxima from 1200 to 1207 cm^{-1}. In natural emeralds, the Raman band displayed the band in the same range, but with apparent maxima from 1068 to 1072 cm^{-1}, FWHM varying between 12 and 26 cm^{-1}, and the FTIR band positioned from 1171 to 1203 cm^{-1}. All natural samples with high alkali content display a shoulder at 1140 cm^{-1}, while synthetic emeralds do not. Low-alkali natural samples from Colombia (Chivor) present this shoulder, but Nigerian emeralds do not. For more precise conclusions, a larger number of samples—namely synthetics with higher alkali content (>0.2%) and natural emeralds with lower alkali (<0.2%)—must be investigated.

ABOUT THE AUTHORS

Dr. Le Thi-Thu Huong (letth@vnu.edu.vn) is a lecturer in mineralogy and gemology at the Hanoi University of Science (Vietnam National University). Dr. Hofmeister is the dean of the Faculty of Chemistry, Pharmacy and Geosciences, and head of the Centre for Gemstone Research, at Johannes Gutenberg University in Mainz, Germany. He is also head of the Institute of Gemstone Research in Idar-Oberstein, Germany. Dr. Häger is senior scientist at the Centre for Gemstone Research at Johannes Gutenberg University, lecturer in the Gemstone and Jewellery Design Department at the University for Applied Sciences in Idar-Oberstein, and managing director of the Institute of Gemstone Research in Idar-Oberstein. Dr. Karampelas is a research scientist at the Gübelin Gem Lab in Lucerne, Switzerland. Dr. Nguyen Duc-Trung Kien is a scientist at the Advanced Institute for Science and Technology, Hanoi University of Science and Technology.

REFERENCES

Adams D.M., Gardner I.R. (1974) Single-crystal vibrational spectra of beryl and dioptase. *Journal of the Chemical Society, Dalton Transactions*, Vol. 1974, No. 14, pp. 1502–1505, http://dx.doi.org/10.1039/dt9740001502.

Aines R.D., Rossman G.R. (1984) The high temperature behavior of water and carbon dioxide in cordierite and beryl. *American Mineralogist*, Vol. 69, No. 3–4, pp. 319–327.

Aurisicchio C., Grubessi O., Zecchini P. (1994) Infrared spectroscopy and crystal chemistry of the beryl group. *The Canadian Mineralogist*, Vol. 32, No. 1, pp. 55–64.

Charoy B., de Donato P., Barres O., Pinto-Coelho C. (1996) Channel occupancy in an alkali-poor beryl from Serra Branca (Goias, Brazil): Spectroscopic characterization. *American Mineralogist*, Vol. 81, No. 3–4, pp. 395–403.

Goldman D.S., Rossman G.R., Parkin K.M. (1978). Channel constituents in beryl. *Physics and Chemistry of Minerals*, Vol. 3, No. 3, pp. 225–235.

Huong L.T.T. (2008) Microscopic, chemical and spectroscopic investigations on emeralds of various origins. PhD thesis, University of Mainz (Germany), 112 pp.

Huong L.T.T., Häger T., Hofmeister W. (2010) Confocal micro-Raman spectroscopy: A powerful tool to identify natural and synthetic emerald. *G&G*, Vol. 46, No. 1, pp. 36–41, http://dx.doi.org/10.5741/GEMS.46.1.36.

Huong L.T.T., Hofmeister W., Häger T., Khoi N.N., Nhung N.T., Atichat W., Arnond V.P. (2011) Aquamarine from the Thuong Xuan district, Thanh Hoa province, Vietnam. *G&G*, Vol. 47, No. 1, pp. 42–48, http://dx.doi.org/10.5741/GEMS.47.1.42.

Kim C., Bell M.I., McKeown D.A. (1995) Vibrational analysis of beryl ($Be_3Al_2Si_6O_{18}$) and its constituent ring (Si_6O_{18}). *Physica B: Condensed Matter*, Vol. 205, No. 2, pp. 193–208, http://dx.doi.org/10.1016/0921-4526(94)00290-C.

Moroz I., Roth M., Boudeulle M., Panczer G. (2000) Raman microspectroscopy and fluorescence of emeralds from various deposits. *Journal of Raman Spectroscopy*, Vol. 31, No. 6, pp. 485–490, http://dx.doi.org/10.1002/1097-4555(200006)31:6%3C485::AID-JRS561%3E3.0.CO;2-M.

Schmetzer K., Kiefert L. (1990) Water in beryl: A contribution to the separability of natural and synthetic emeralds by infrared spectroscopy. *Journal of Gemmology*, Vol. 22, No. 4, pp. 215–223.

Wood D.L., Nassau K. (1968) The characterization of beryl and emerald by visible and infrared absorption spectroscopy. *American Mineralogist*, Vol. 53, No. 5/6, pp. 777–800.

DIAMOND

Natural Colorless Type IaB Diamond with Silicon-Vacancy Defect Center

The silicon-vacancy defect, or $[Si\text{-}V]^-$, is one of the most important features in identifying CVD synthetic diamonds. It can be effectively detected using laser photoluminescence technology to reveal sharp doublet emissions at 736.6 and 736.9 nm. This defect is extremely rare in natural diamonds (C.M. Breeding and W. Wang, "Occurrence of the Si-V defect center in natural colorless gem diamonds," *Diamond and Related Materials*, Vol. 17, No. 7–10, pp. 1335–1344) and has been detected in very few natural type IIa and IaAB diamonds over the past several years.

Recently, a 0.40 ct round brilliant diamond with D color and VS_2 clarity (figure 1) was submitted to the Hong Kong laboratory for grading service. It was identified as a pure type IaB natural diamond. Infrared absorption spectroscopy showed low concentrations of the hydrogen peak (3107 cm^{-1}) and N impurities in the B aggregates. Photoluminescence spectra at liquid-nitrogen temperature with 514 nm laser excitation revealed $[Si\text{-}V]^-$ doublet emissions at 736.6 and 736.9 nm (figure 2), while 457 nm laser excitation revealed the H3 (503.2 nm) emission. DiamondView fluorescence images showed blue fluorescence with natural diamond growth patterns. These gemological and spectroscopic features confirmed the diamond's natural origin, despite the occurrence of $[Si\text{-}V]^-$ emissions. No treatment was detected.

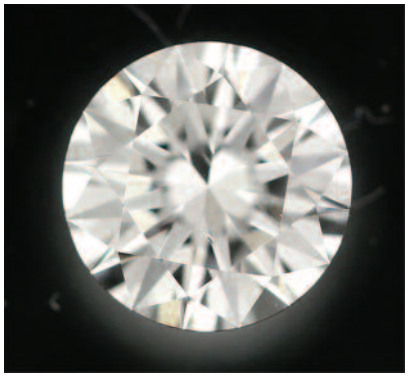

Figure 1. Emissions from the silicon-vacancy defect at 736.6 and 736.9 nm were detected in this 0.40 ct type IaB natural diamond.

Examination of this stone indicated that the $[Si\text{-}V]^-$ defect can occur, albeit rarely, in multiple types of natural diamonds. Therefore, all properties should be carefully examined in reaching a conclusion when $[Si\text{-}V]^-$ is present.

Carmen "Wai Kar" Lo

Screening of Small Yellow Melee for Treatment and Synthetics

Diamond treatment and synthesis have undergone significant developments in the last decade. During this time, the trade has grown increasingly concerned about the mixing of treated

Figure 2. The emission peaks at 736.6 and 736.9 nm from the $[Si\text{-}V]^-$ defect are shown in the type IaB diamond's photoluminescence spectrum. Identical peak positions are detected in CVD synthetic diamonds.

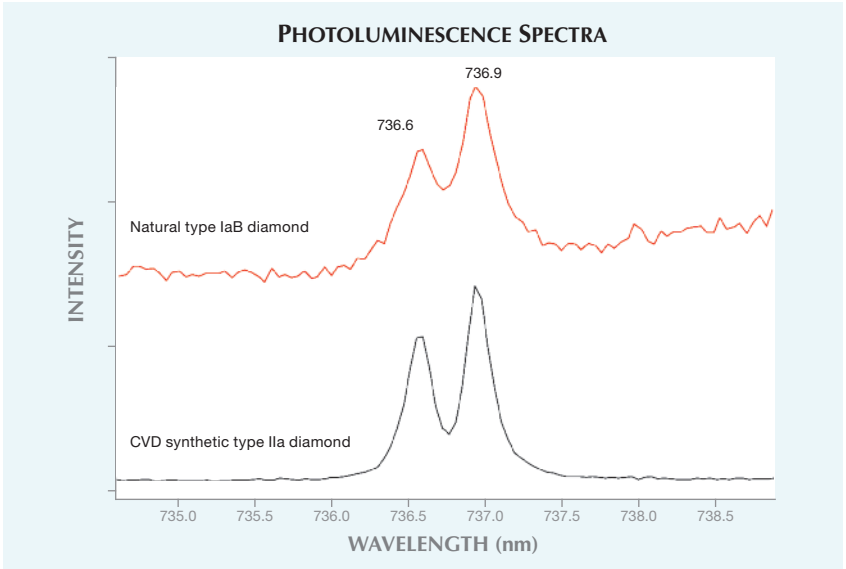

Editors' note: All items were written by staff members of GIA laboratories.

GEMS & GEMOLOGY, Vol. 50, No. 4, pp. 293–301.

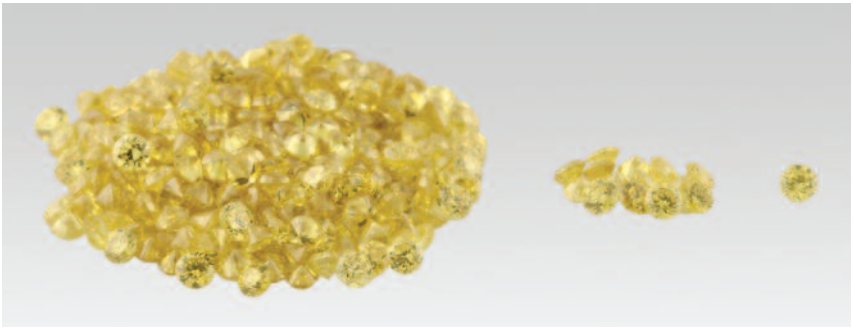

Figure 3. This group of 359 intensely colored round yellow diamonds (0.02–0.03 ct) was screened by GIA's New York laboratory. Among these, the majority were natural (left), 14 were HPHT synthetics (middle), and one was HPHT-treated natural diamond (right). They all displayed uniform appearance and could not be distinguished visually.

and/or synthetic diamonds with natural melee-sized goods. Because it is often not feasible to test every small diamond in a parcel, many of these products could be traded without being tested individually by a gem lab. GIA's New York laboratory recently tested two large groups of melee yellow diamonds submitted for screening of treatments and synthetics. The results will likely have profound implications for how melee diamonds are handled in the trade.

A parcel of 359 round diamonds between 0.02 and 0.03 ct was submitted for identification. They showed uniform appearance, intense yellow color, and good clarity. Based on spectroscopic analysis, each sample's color was attributed to trace concentrations of isolated nitrogen. Gemological observations, infrared absorption spectroscopy, and DiamondView analysis confirmed that 344 of them were natural diamonds, 14 were grown by HPHT (high-pressure, high-temperature) synthesis, and one was an HPHT-treated natural diamond (figure 3).

Of the 14 synthetic diamonds, eight were dominated by A-aggregate form nitrogen with trace isolated nitrogen, while the other six showed negligible amounts. All had widespread pinpoint inclusions, a feature typical of HPHT synthetic diamonds. Characteristic growth features of HPHT synthesis were confirmed using a DiamondView fluorescence instrument on six of them. The synthetic diamonds with a high concentration of A-aggregate form nitrogen were produced at much higher temperatures, indicating more than one producer.

To gain perspective on the surprisingly high prevalence of synthetic and treated diamonds found in this parcel, we analyzed an additional parcel containing 525 samples, with similar results. One of these was HPHT-processed, while 10 displayed the spectral, microscopic, and fluorescence characteristics typical of HPHT synthetics; we concluded that the remaining 514 were natural and untreated. Typical DiamondView characteristics of HPHT synthetics were observed, but most of the HPHT synthetics showed fluorescence patterns similar to those of natural diamonds (figure 4). This observation emphasizes the importance of infrared absorption spectroscopy, in addition to DiamondView imaging, when determining diamond origin.

This study indicates that melee diamonds in the marketplace are being contaminated by synthetic and treated diamonds. Screening analysis by gem labs is essential to ensuring the correct identification. An efficient and reliable screening can be performed using infrared absorption spectroscopy, DiamondView fluorescence imagery, and optical microscopy. From our analysis of 883 melee samples in all, we concluded that 857 were natural diamond (97.1%), 24 were HPHT synthetic diamond (2.7%), and two were HPHT-processed natural diamonds (0.2%).

Wuyi Wang, Martha Altobelli, Caitlin Dieck, and Rachel Sheppard

Figure 4. These DiamondView fluorescence images show (A) growth sector patterns typical of HPHT synthetic diamonds, (B) HPHT treatment, and (C and D) uncharacteristic HPHT synthetic patterns.

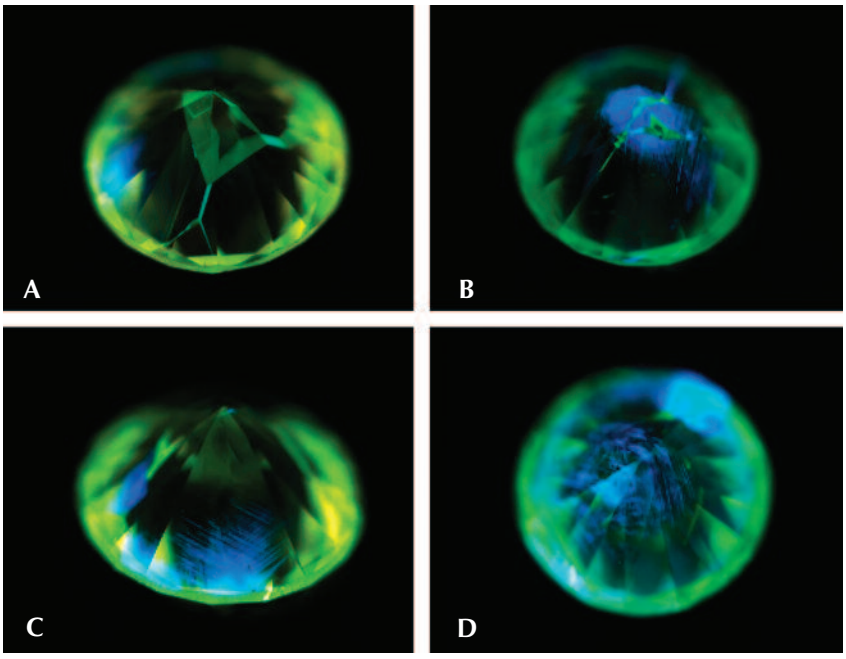

Very Large Irradiated Yellow

Artificial irradiation, with or without annealing, has been used to improve the color of natural diamonds for several decades. This technique is usually applied to brownish or light yellow diamonds of relatively small size. The New York lab recently tested a very large yellow diamond that had been artificially irradiated.

This emerald-cut stone weighed 22.27 ct and was color graded as Fancy Vivid yellow (figure 5). Faint color concentration was observed along the culet. The diamond showed medium yellow-green, slightly chalky fluorescence to long-wave UV and weak orange fluorescence to short-wave UV. No obvious internal features were observed. Its infrared absorption spectrum showed high concentrations of nitrogen and weak absorptions from defects H1b (4935 cm^{-1}) and H1c (5165 cm^{-1}). A weak hydrogen-related absorption at 3107 cm^{-1} was also detected. In the Vis-NIR region, the absorption spectrum collected at liquid-nitrogen temperature showed strong absorptions from the N3, H4, H3, and 595 nm optical centers (figure 6). These spectroscopic and gemological features demonstrated that the diamond had been artificially irradiated and annealed to introduce additional absorptions from the H3/H4 defects, enhancing its yellow color. This Fancy Vivid yellow color would have been much lighter and less saturated before the treatment.

Artificially irradiated diamonds of this size and attractive color are rarely examined in gem laboratories.

Wuyi Wang

Figure 5. This 22.27 ct Fancy Vivid yellow diamond was identified as artificially irradiated and annealed. Treated diamonds of this size and attractively saturated color are rare.

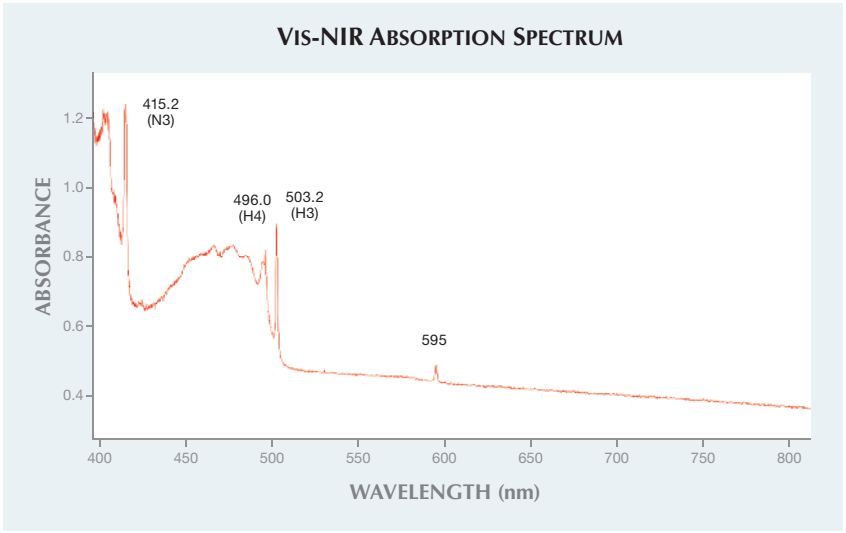

Figure 6. The irradiated yellow diamond's Vis-NIR absorption spectrum, collected at liquid-nitrogen temperature, showed strong absorption from the H3 and H4 defects, which were artificially introduced to enhance the yellow color.

Natural PEARL Aggregates from *Pteria* Mollusks

Both natural and cultured pearls of *Pteria*-species mollusks from the Gulf of California, Mexico (M. Cariño and M. Monteforte, "History of pearling in La Paz Bay, South Baja California," Summer 1995 *G&G*, pp. 88–104; L. Kiefert et al., "Cultured pearls from the Gulf of California, Mexico," Spring 2004 *G&G*, pp. 26–38) are examined in GIA laboratories from time to time. But a recent submission to the New York lab of 10 loose pearls, ranging from 8.17 × 7.65 × 3.89 mm to 17.85 × 11.16 × 6.80 mm (figure 7), proved interesting owing to their shapes and internal growth features. All the pearls had a "grapelike" cluster appearance, as if multiple smaller pearls had combined into aggregates. Their colors ranged from dark brown and purple to gray, with strong orient consisting of mainly bluish and pinkish overtones.

Microscopic examination revealed that the pearls formed with continu-

Figure 7. These 10 loose natural pearl aggregates from the Pteria *species ranged from dark brown and purple to gray.*

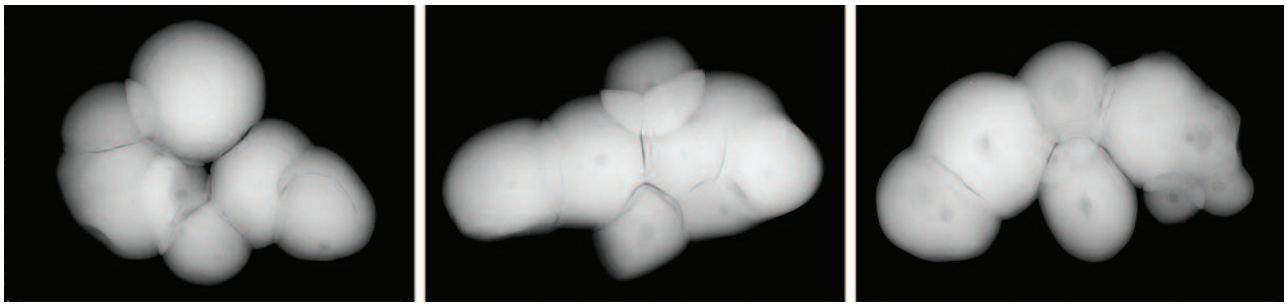

Figure 8. Microradiograph images of the pearls revealed multiple growth units with central conchiolin-rich cores in each unit.

ous nacre layers. Microradiography further demonstrated that their internal structures were composed of multiple small pearls related to their growth (figure 8). Conchiolin-rich centers were observed in all of the sub-units, indicating natural formation. Additional advanced testing (UV-Vis reflectance spectrophotometry, photoluminescence spectroscopy, and EDXRF spectrometry) showed that all 10 of the pearls had a natural color. More importantly, all 10 exhibited medium to strong orangy red to red fluorescence under long-wave UV, which is characteristic of pearls that form in *Pteria* mollusks (figure 9).

Pearls grown from the aggregation of smaller pearls are sometimes associated with freshwater culturing practices (Summer 2012 Lab Notes, pp. 138–139). Yet these samples clearly did not appear to be cultured. Our client later informed us that the pearls were obtained more than 40 years ago, reportedly off the Mexican coast, which further supports the identity of these unique pieces.

Sally Chan and Yixin (Jessie) Zhou

Figure 9. The pearls produced this striking characteristic red fluorescence under long-wave UV.

Lead-Glass-Filled Burmese RUBIES

Rubies filled with a high-lead-content glass as a clarity enhancement were first reported by the Gemmological Association of All Japan (GAAJ) laboratory in 2004. Since then, many of these stones have been examined by gemological laboratories around the world. They are identified by their numerous large, low-relief fractures and their blue or orange flashes easily seen at different angles, as well as their flattened gas bubbles and voids that are obvious under magnification (S.F. McClure et al., "Identification and durability of lead glass–filled rubies, Spring 2006 *G&G*, pp. 22–34).

The Carlsbad laboratory recently had the opportunity to examine a multi-strand necklace of graduated round ruby beads (figure 10), measuring 2.72 to 6.13 mm in diameter. Standard gemological testing showed properties consistent with natural ruby. Microscopic observations revealed typical inclusions for ruby: rutile silk, banded particulate clouds, twinning planes, red parallel planar zoning, and roiled graining. The ap-

Figure 10. The Burmese ruby beads in this multi-strand necklace were filled with lead glass.

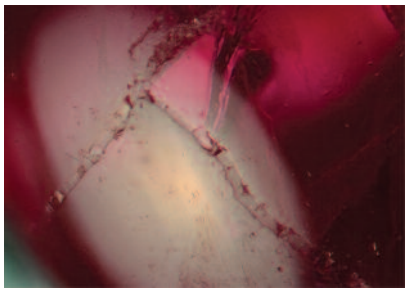

Figure 11. These wide fractures, filled with glass of relatively low lead content, showed a slightly lower luster than the host ruby. Field of view 2.96 mm.

pearance and chemical composition of the beads suggested that their geographic origin was Mogok, Myanmar. Their wide, low-relief fractures (figure 11) and cavities were filled with a foreign substance whose luster was slightly lower than that of the rubies. These observations suggested a lead-glass filler, although the lower luster was contrary to previous documentation and the filler did not display any flash effect. In some beads, the filler also showed a crazed appearance (figure 12) not typically observed in other rubies filled with high-lead glass.

This strange observation prompted us to carry out a chemical analysis of the glass filler. We tested two spots using laser ablation–inductively coupled plasma–mass spectrometry (LA-ICP-MS) on a relatively large glass-filled cavity. The results after normalization showed that the filler contained approximately 43 wt.% PbO, which was much lower than the lead content reported by McClure et al. in 2006 (71–76 wt.%). The diminished lead content would lower the refractive index of the glass and explain the lack of flash effect and the lower luster observed in this filler.

Figure 12. In some beads, the filler also showed a crazed appearance not typically observed in other rubies filled with lead glass. Field of view 2.96 mm.

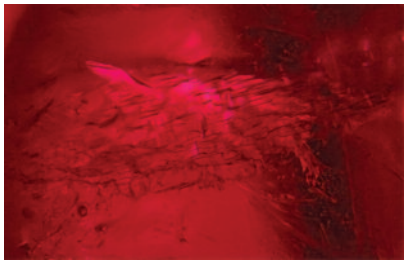

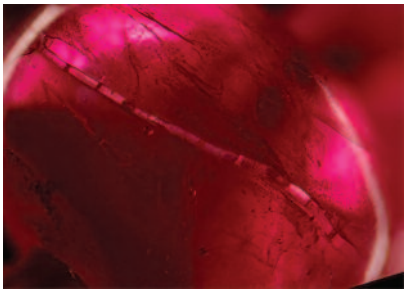

Figure 13. Some beads were so highly fractured and filled that they would be called "manufactured products consisting of lead glass and ruby." This material would easily disintegrate if the lead glass were removed. Field of view 2.96 mm.

These beads were the first examples of this lower-lead-content glass filling in Burmese rubies examined at the Carlsbad laboratory. On a GIA report, most of these beads would be identified as "rubies with significant clarity enhancement with lead glass filler." Yet some of the beads were so highly fractured and filled that they would be considered "manufactured products consisting of lead glass and ruby" (figure 13).

Najmeh Anjomani and Rebecca Tsang

Spinel Inclusion in SPINEL

A 26.73 ct transparent dark pink-purple oval mixed cut (figure 14) was submitted to the Carlsbad laboratory for identification services. Standard gemological testing showed a refractive index of 1.719 and a hydrostatic specific gravity of 3.59. The stone fluoresced very weak red to long-wave UV light and was inert to short-wave UV. Observed using a handheld spectroscope, the stone showed thin absorption bands near 680 nm, with fine absorption lines near 670 nm. These gemological properties were consistent with spinel.

Figure 14. This 26.73 ct dark pink-purple spinel contained a spinel crystal inclusion.

Interestingly, microscopic examination showed that the spinel was relatively free of inclusions except for a very low-relief solid inclusion that was only partially visible (figure 15). Examination with polarized light (figure 16) revealed the entire outline of the low-relief crystal. Unaltered crystals generally provide strong evidence that a stone has not been heated, and this inclusion showed no alteration. But it is also important to consider the identity of certain inclusions when using them as an indication for thermal treatment. Due to the low re-

Figure 15. Under diffused lighting, the outline of the spinel crystal was only partially visible. Image width 3.70 mm.

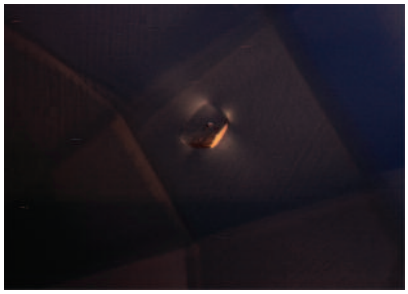

Figure 16. Under polarized lighting, the outline of the spinel crystal was clearly visible. Image width 3.70 mm.

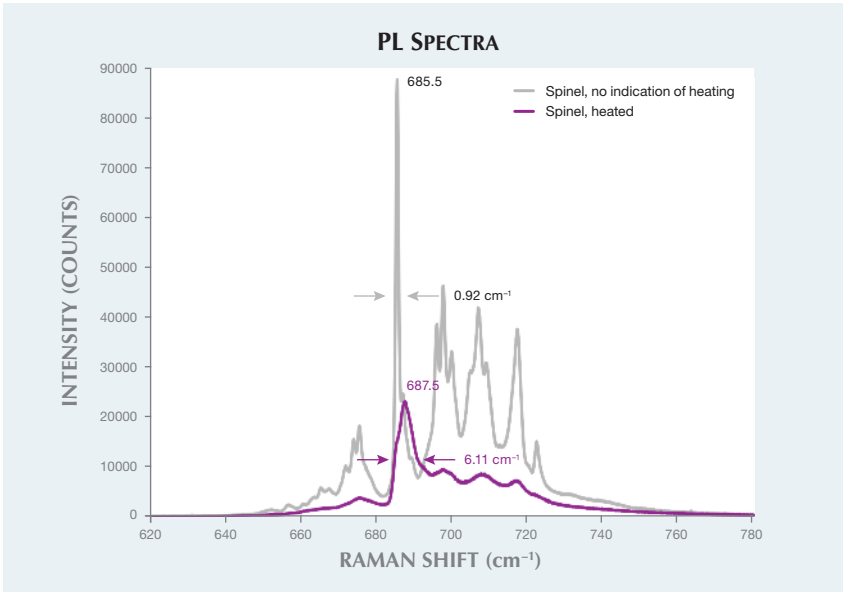

Figure 18. The gray spectrum of unheated spinel shows that the FWHM (full width at half maximum) of the peak with highest counts is 0.92 cm^{-1} and the position of the peak is at 685.5 cm^{-1}. The purple spectrum, representing the dark pink-purple spinel, shows that the FWHM of the peak with highest counts is 6.11 cm^{-1} and the peak is shifted from 685.5 to 687.5 cm^{-1}.

lief of this inclusion, it is very likely a spinel inside of spinel. Their matching refractive index explains why the inclusion is nearly invisible. Since the host and inclusion are the same material, we would not expect to see any alteration due to heat treatment. Therefore, the unaltered appearance of this inclusion cannot be used to determine that this spinel has not been heat treated.

The spinel's visible absorption spectrum revealed that its purple color results from the combination of Fe and Cr (figure 17). Absorption bands with a maximum at 400 and 550 nm are caused by Cr^{3+} (D.L. Wood et al., "Optical spectrum of Cr^{3+} ions in spinels," *The Journal of Chemical Physics*, Vol. 48, No. 11, 1968, pp. 5255–5262). Fe^{2+} causes the absorption band from 400 to 590 nm, while the Fe^{2+}/Fe^{3+} charge transfer and Fe^{2+} cause the absorption bands from 590 to 700 nm (S. Muhlmeister et al., "Flux-grown synthetic red and blue spinels from Russia," Summer 1993 *G&G*, pp. 81–98).

Figure 17. The spinel's visible spectrum revealed that its dark pink-purple color was caused by Cr and Fe.

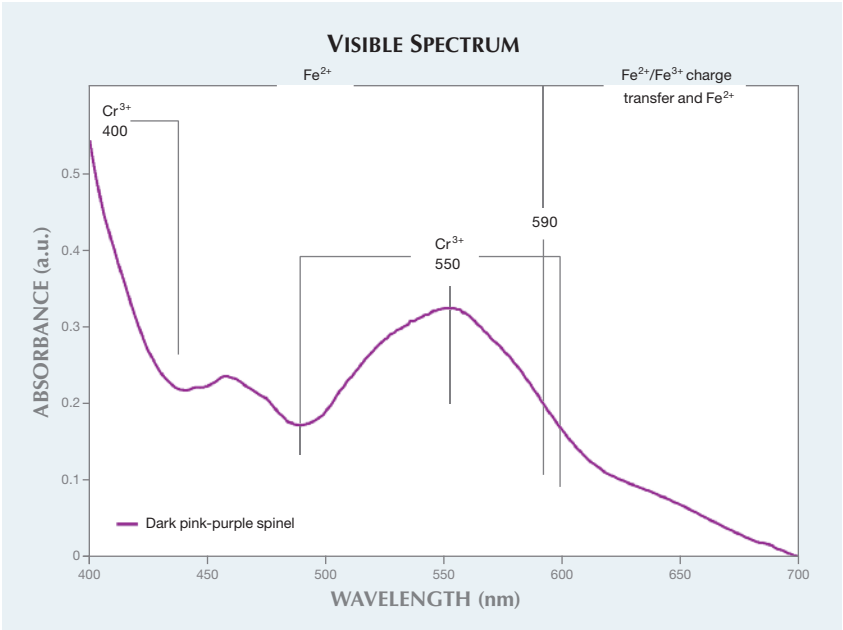

Spinels submitted to GIA's laboratory are routinely checked using advanced analytical tools. Laser ablation–inductively coupled plasma–mass spectrometry (LA-ICP-MS) was used to confirm the natural trace elements. Higher concentrations of Li (27.7 ppmw), Be (87.4 ppmw), Zn (133 ppmw), and Ga (63 ppmw) indicate a natural origin, and the specimen's photoluminescence (PL) spectrum was consistent with a heated spinel due to the broad full width at half maximum (FWHM) observed at 687.5 nm (figure 18; see S. Saeseaw et al., "Distinguishing heated spinels from unheated natural spinels and from synthetic spinels," GIA Research News, April 2009, http://www.gia.edu/gia-news-research-NR32209A). It was unusual to see a spinel with this dark pink-purple color showing evidence of heat, as we typically see only red spinels that have been heated. From careful microscopic examination and

advanced gemological testing, we were able to conclude that this was a natural spinel showing indications of heating.

Amy Cooper and Ziyin Sun

CVD SYNTHETIC DIAMOND with Fancy Vivid Orange Color

With the rapid improvement of CVD synthetic diamond quality in recent years, various colorations can be introduced after growth. The New York laboratory recently tested a CVD synthetic with a very attractive orange color.

This round-cut specimen weighed 1.04 ct and was color graded as Fancy Vivid pinkish orange (figure 19), a very rare color among natural and treated diamonds. Except for a few dark pinpoint inclusions, it showed no notable internal features. Under crossed polarizers, it displayed natural-looking "tatami" strain patterns. Absorption spectroscopy in the infrared region showed typical type IIa features, with no detectable defect-related absorption. At liquid-nitrogen temperature, a few absorption features were detected in the UV-Vis-NIR region (figure 20). The major ones include absorptions from N-V centers with ZPL at 575.0 and 636.9 nm, and their related side bands. We also recorded absorptions from some irradiation-related defects, including 594.4 nm, GR1 at 741.2 nm, ND1 at 393.4 nm, and the general radiation absorption features at 420–450 nm. Also observed were weak absorptions from the H3 defect at 503.2 nm, possible nickel-related defects at 516.1 nm, and [Si-V]$^-$ at 736.6/736.9 nm. Under the strong short-wave UV radiation of the DiamondView, the sample showed very strong red fluorescence with sharp linear growth striations, a unique feature of CVD synthetic diamond. Weak red phosphorescence was also detected. These observations confirmed that this was a CVD synthetic diamond with post-growth treatments. Nitrogen concentration, based on absorptions in infrared absorption spectroscopy, was below 1 ppm. After initial growth, the sample was artificially irradiated and then annealed at moderate temperatures to introduce the N-V centers. Strong absorptions from N-V centers are the main causes of the observed pinkish orange bodycolor.

The very attractive orange color was achieved by introducing the proper concentrations of N-V centers while limiting the formation of other defects. It should be pointed out that the relatively high concentration of [Si-V]$^-$ could be attributed to the treatment by combining preexisting Si impurity with artificially introduced vacancies. With further developments in after-growth treatment, it is highly likely that more colors in CVD synthetic diamonds will be introduced.

Wuyi Wang and Kyaw Soe Moe

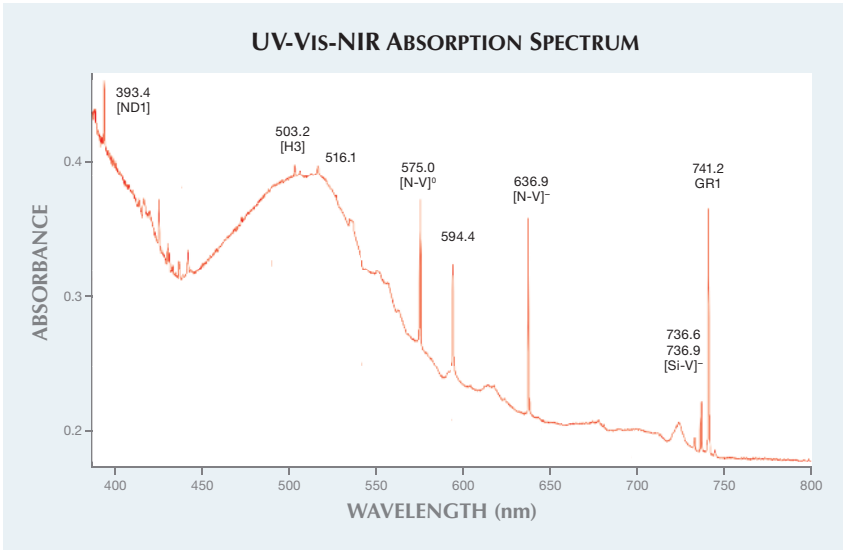

Figure 20. Several defects were detected in the CVD synthetic diamond's absorption spectrum in the UV-Vis-NIR region at liquid-nitrogen temperature. Strong absorptions from the N-V centers are the main cause of the observed pinkish orange color.

Figure 19. This 1.04 ct round was identified as a CVD synthetic diamond. Its Fancy Vivid pinkish orange color was introduced through post-growth irradiation and annealing.

Mixed-Type HPHT SYNTHETIC DIAMOND with Unusual Growth Features

A 0.28 ct round brilliant was submitted as synthetic moissanite to the Carlsbad lab for an identification report. At first glance, synthetic moissanite seemed like a possibility. The stone had a green-yellow color and contained numerous growth tubes visible through the table (figure 21). Yet it did not show doubling in the microscope, which is a characteristic feature of synthetic moissanite. Its infrared spectrum was a match for diamond. The infrared spectrum also showed a very unusual combination of boron and nitrogen impurities at 2804 and 1130 cm^{-1}, respectively (figure 22). These two impurities are not known to occur together in natural diamonds in measurable quantities.

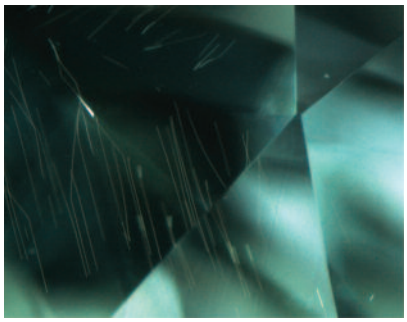

Figure 21. These growth tube features were visible through the table of the HPHT-grown synthetic diamond. Magnified approximately 90×.

This was a strong indicator of synthetic origin. A DiamondView image (figure 23) confirmed that it was synthetic, grown by the high-pressure, high-temperature (HPHT) method. It is noteworthy that after the sample was removed from the DiamondView, it showed very strong blue phosphorescence that was clearly visible in ambient room lighting and persisted for several minutes.

Unless special precautions are taken, diamond synthesis will incorporate nitrogen into the lattice, which leads to a yellow bodycolor. Certain chemicals can be added to prevent the incorporation of nitrogen, and this can lead to colorless diamonds. If boron is introduced to the growth of synthetic diamonds, it will become incorporated and produce a blue bodycolor. If both boron and nitrogen are allowed to incorporate into the lattice, the blue and yellow bodycolors will combine to produce a green color (J.E. Shigley et al., "Lab-grown colored diamonds from Chatham Created Gems," Summer 2004 *G&G*, pp. 128–145). Since boron is an electron acceptor and nitrogen is an electron donor, an excess of boron will compensate the nitrogen and the blue color will predominate. Because nitrogen and boron have slight preferences for different growth sectors, if the concentration of both nitrogen and boron is carefully controlled, nitrogen and boron will dominate different growth sectors. The colors will blend to create a face-up greenish color (R.C. Burns et al., "Growth-sector dependence of optical features in large synthetic diamonds," *Journal of Crystal Growth*, Vol. 104, No. 2, 1990, pp. 257–279).

Figure 23. This DiamondView image shows the characteristic growth pattern of an HPHT synthetic diamond.

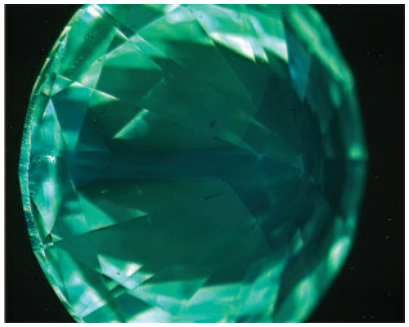

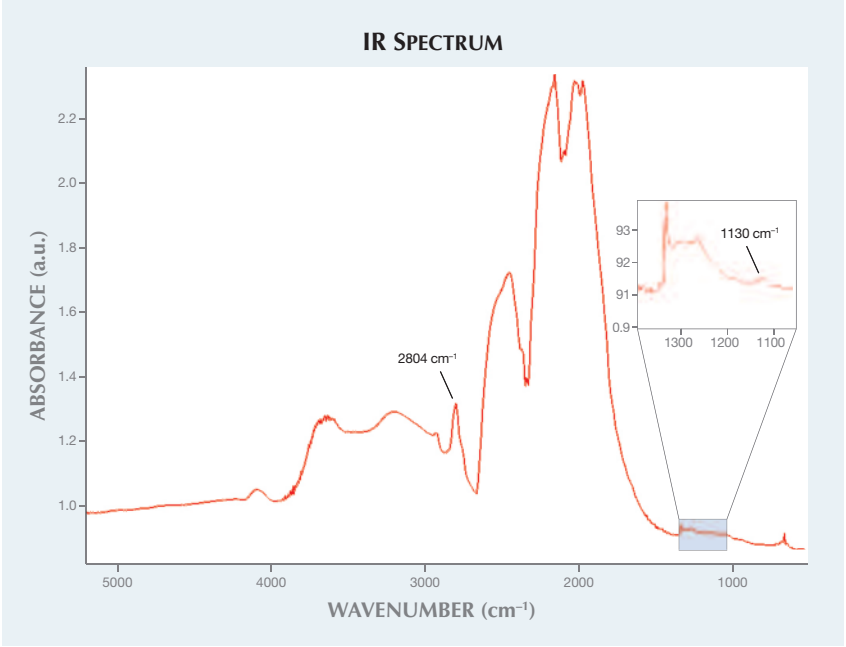

Figure 22. The HPHT-grown synthetic diamond's infrared spectrum shows peaks related to both boron and single nitrogen.

The growth tubes in this sample were an unusual feature, last seen in a selection of HPHT-grown synthetics several years ago at GIA's West Coast laboratory. They appear similar to synthetic moissanite growth tubes, though there are a few key differences. Whereas the growth tubes occur in only one direction in synthetic moissanite, they could be seen growing in different directions in this synthetic diamond. The tubes in synthetic moissanite also tend to be very straight, while the ones in this sample curved and changed direction. Although this stone bore some superficial resemblance to moissanite, its gemological properties were quite different, another reminder to avoid quick sight identifications.

Troy Ardon

A Larger, Higher-Quality NPD SYNTHETIC DIAMOND

In February 2014, these authors reported the first example of a synthetic nano-polycrystalline diamond (NPD) detected by a gemological laboratory (see www.gia.edu/gia-news-research-fancy-black-NPD-synthetic). The 0.9 ct marquise was small and so heavily included with graphite crystals as to receive a Fancy Black color grade. The East Coast laboratory recently detected another undisclosed NPD synthetic diamond, a 1.51 ct Fancy Black round.

This NPD specimen was larger and had a much better transparency than the previous NPD, though it still

Figure 24. This 1.51 ct Fancy Black nano-polycrystalline diamond (NPD) synthetic, submitted undisclosed, was larger and showed much better transparency than a previously detected NPD synthetic.

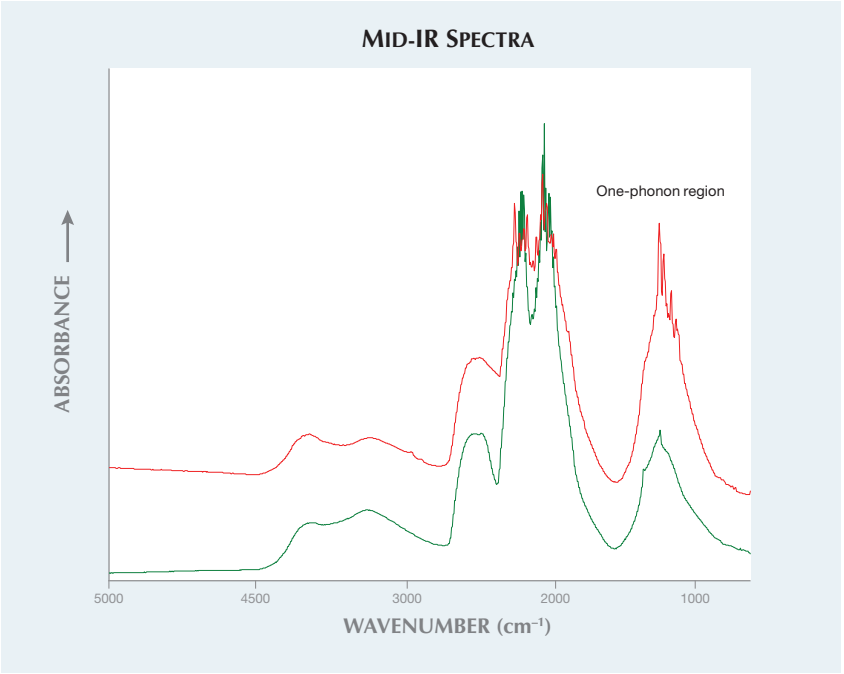

Figure 25. The mid-FTIR spectrum of the 1.51 ct black NPD synthetic diamond (red) displayed absorption in the one-phonon region similar to that of known NPD samples (green).

graded as Fancy Black (figure 24). Infrared spectroscopy showed a diagnostic absorption pattern for diamond, with strong absorption in the one-phonon region (approximately 400–1332 cm^{-1}). Absorption in this region is usually attributed to nitrogen impurity in different aggregation states, but careful observation showed otherwise.

The specimen's infrared absorption pattern matched that of known NPD samples (figure 25). Further testing, including Raman spectroscopy and DiamondView imaging, confirmed the sample to be a NPD synthetic diamond. Microscopic observation revealed that the host material had the yellow color typical of previously reported NPD samples (see E.A. Skalwold, "Nano-polycrystalline diamond sphere: A gemologist's perspective," Summer 2012 *G&G*, pp. 128–131). The sample was heavily included with graphite, but less so than the previously reported 0.9 ct marquise, and therefore it had a better transparency (figure 26).

The origin of this synthetic diamond is not known, but it showed obvious improvements in size and quality compared to the marquise reported in February 2014. In the future, NPD synthetics could pose an identification challenge to the gem and jewelry industry. Careful gemological observations and advanced testing techniques were required to identify this undisclosed synthetic diamond.

Paul Johnson and Kyaw Soe Moe

Figure 26. These photomicrographs, magnified 35× (left) and 40× (right), show abundant inclusions of graphite inclusions. Note the yellow color of the host material.

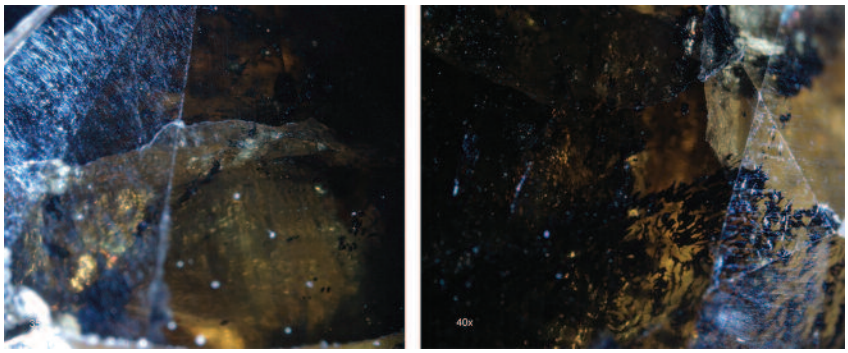

PHOTO CREDITS:
Johnny Leung—1; Sood Oil (Judy) Chia—3, 5, 7, 19; Martha Altobelli and Caitlin Dieck—4; Yixin (Jessie) Zhou—8; Jian Xin (Jae) Liao—9, 24; C.D. Mengason—10; Nathan Renfro—11–13; Robison McMurtry—14; Ziyin Sun—15, 16; Troy Ardon—21, 23; Paul Johnson—26.

G&G

Gem News International

Contributing Editors
Emmanuel Fritsch, *CNRS, Team 6502, Institut des Matériaux Jean Rouxel (IMN), University of Nantes, France* (fritsch@cnrs-imn.fr)
Kenneth Scarratt, *GIA, Bangkok* (ken.scarratt@gia.edu)

COLORED STONES AND ORGANIC MATERIALS

Demantoid from Baluchistan province in Pakistan. Demantoid garnet can be broadly divided into two petrogenetic groups, namely skarn-hosted and serpentinite-hosted demantoid. Those in the latter group represent the classic localities in the Russian Urals and at Val Malenco, Italy, in addition to sources such as Iran's Kerman province and the Kaghan Valley area in the Hazara district of Pakistan. The serpentinite formations hosting these demantoids are the result of relatively low-grade hydrothermal/metamorphic alteration of ultramafic parent rocks.

Nine demantoids reportedly from a new deposit in the Khuzdar area in Pakistan's Baluchistan province were recently examined in GIA's Carlsbad lab (figure 1). The material was bought by one of these contributors (VP) from a gem merchant based in Peshawar, Pakistan.

Figure 1. These nine Pakistani demantoids showed dodecahedral form, magnetite inclusions, and asbestiform chrysotile masses on some crystal faces. The smallest stone (bottom left) is 5.2 mm wide, and the largest (top left) is 9.9 mm wide. Photo by Don Mengason.

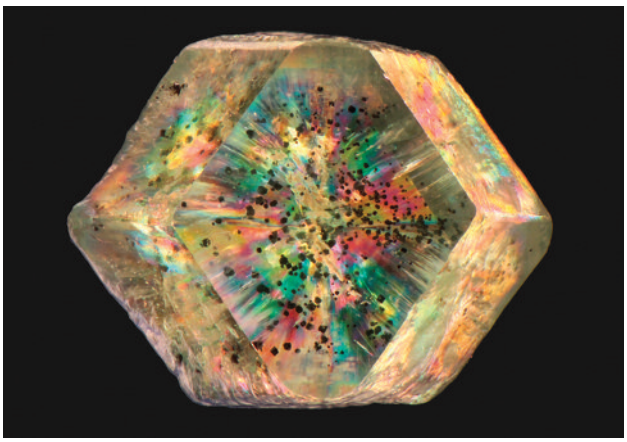

Figure 2. This demantoid is viewed through a polished window that is roughly parallel to the (110) crystal face. The sample was photographed with cross-polarized lighting and immersed in methylene iodide to highlight the anomalous birefringence. The sample measures 8.8 mm across. Photomicrograph by Aaron Palke.

The nine rough samples described here (1.74–3.73 ct) all exhibited well-developed crystal faces with typical dodecahedral form. Their color ranged from yellowish green to green, with yellow cores in a few samples. Each showed anomalous birefringence, often with a well-defined "octahedral" pattern (figure 2).

Editors' note: Interested contributors should send information and illustrations to Justin Hunter at justin.hunter@gia.edu or GIA, The Robert Mouawad Campus, 5345 Armada Drive, Carlsbad, CA 92008.

Gems & Gemology, Vol. 50, No. 4, pp. 302–315.

Several of the garnets had fibrous (asbestiform) masses of chrysotile adhering to one or more crystal faces, confirming their origin in a serpentinite deposit. Windows were polished into several of these samples for microscopic examination of their internal features. Inclusions of chrysotile fibers (i.e., horsetail inclusions) are concentrated around the rim and radiate out toward the crystal faces (again, see figure 2). The cores of many samples were marked by a field of opaque, equant black inclusions initially presumed to be chromite (figure 3), a commonly observed inclusion in serpentinite-hosted demantoid.

However, laser ablation–inductively coupled plasma–mass spectrometry (LA-ICP-MS) analysis of one of these grains that had breached a polished surface showed Cr below the detection limit (<2 ppm Cr). The analysis showed the almost exclusive presence of Fe, with minor Mg and Mn and trace amounts of other elements. This indicates that the opaque black inclusions in these demantoids are actually magnetite. This assignment was further confirmed by Raman analysis on another grain and the attraction of several of the garnets to a handheld magnet. LA-ICP-MS analysis of the host demantoid also revealed very low Cr concentrations from below the detection limit to approximately 10 ppm. This was in stark contrast to the typically Cr-rich serpentinite-hosted demantoid from other deposits. Along with the presence of magnetite instead of chromite, this probably indicated the absence of significant Cr in the ultramafic protolith. While the internal features were very similar to those in other serpentinite-hosted demantoid, the presence of magnetite instead of commonly reported chromite was a surprising feature of this newly described material.

Aaron C. Palke and Vincent Pardieu
GIA, Carlsbad and Bangkok

Figure 3. These magnetite and fibrous chrysotile inclusions are typical of the demantoids from this study. Field of view is 2.0 mm. Photomicrograph by Nathan Renfro.

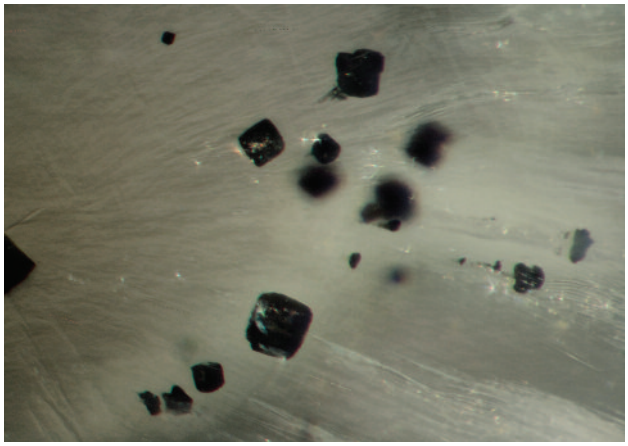

Figure 4. The Stayish black opal mine, active since 2013, is located in the Wollo province of northern Ethiopia.

New deposit of black opal from Ethiopia. Opal was first discovered in Ethiopia in the early 1990s. Specimens from Mezezo in the historical Shewa province consist of nodules of a reddish brown volcanic rock with orange, reddish brown, or "chocolate" brown precious opal inside. The next major discovery occurred in 2008, when white precious opal was found in the province of Wollo near Wegel Tena, about 550 km north of Addis Ababa (F. Mazzero et al., "Nouveau gisement d'opales d'Ethiopie dans la Province du Welo: Premières informations," *Revue de Gemmologie a.f.g.*, No. 167, pp. 4–5). This deposit still produces large amounts of white and crystal precious opal and occasionally some black material (Winter 2011 Lab Notes, pp. 312–313).

In 2013, yet another source was discovered in Wollo, at the Stayish mine near the town of Gashena (figure 4). This discovery has yielded mostly dark and black opal, along with some white and crystal opal. Although it is only now being reported, the deposit has been actively producing since 2013. It is set in a distinct opal-bearing layer in a

Figure 5. While acidic ash layers occur repeatedly within the stratigraphic sequence at Stayish, precious black opal occurs only in this stratum. Photo by Pierre Hardy.

mountainous area at an altitude of around 3,000 meters. It lies approximately 700 km northeast of Addis Ababa, more than 100 km from the historic town of Lalibela by road, and about 30 km north of the white opal deposit.

Like the white opal, the black opal is found at the contact zone between the volcanic rock series and the underlying clay-rich layer (figure 5). The layer is one in a sequence of repeating volcanic ash and ignimbrite layers. Field observations at different locations show that the opal-bearing layer is contained in a single stratum extending for tens and even hundreds of kilometers along the mountain belt. The opal-bearing clay layer is about 60 cm thick and contains opal of various quality and color. The black opal is retrieved from flat tunnels up to 15–20 meters long that are dug horizontally into the mountain slope by local villagers. The material generally comes in nodules and chunks 2–5 cm long, but 10 cm pieces have also been retrieved from this deposit (figure 6).

The specimens are usually very dark, reminiscent of dyed or smoke-treated opal except that the surface does not show any staining in surface pits or fissures (figure 7). The stones also display a dark, even color all the way through and are sometimes layered with dark gray common opal. This separates it from sugar-acid treated opal (Winter 2011 GNI, pp. 333–334), where the darker color is confined to a more or less thick surface layer.

Initial X-ray fluorescence analyses showed barium (Ba) values ranging from below detection limit for one deposit with more crystal-like opal to 1000 ppmw for another deposit with more dense and grayish material. The two deposits are on adjacent sides of the same mountain. The wide

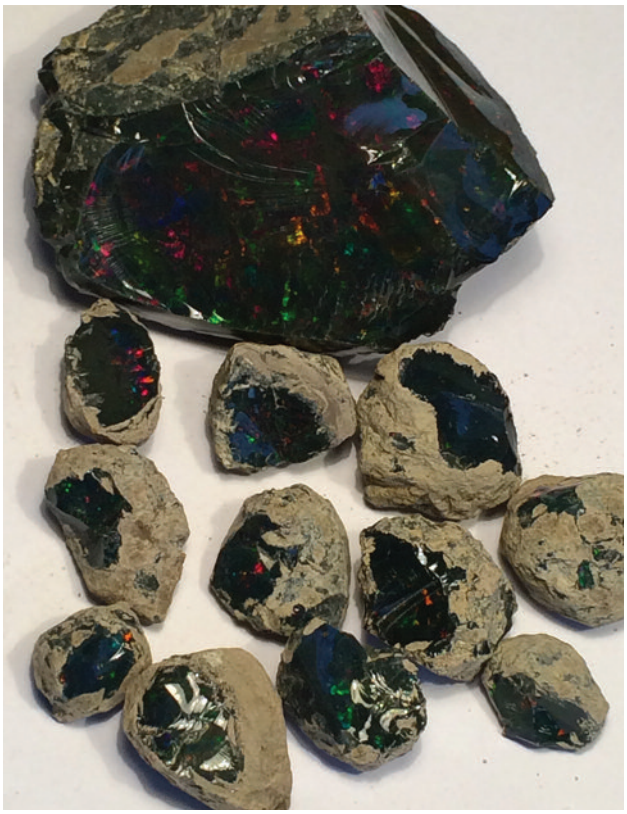

Figure 6. Pieces of black opal from the Stayish mine are usually 2–5 cm in diameter (bottom), though some may reach 10 cm in length (top). Photo by Tewodros Sintayehu.

Figure 7. This microscopic image of an Ethiopian black opal with surface scratches shows none of the black staining seen in smoke-treated or dyed opal. Some grayish non-precious opal material can be observed between the color patches. Photo by Hpone-Phyo Kan-Nyunt.

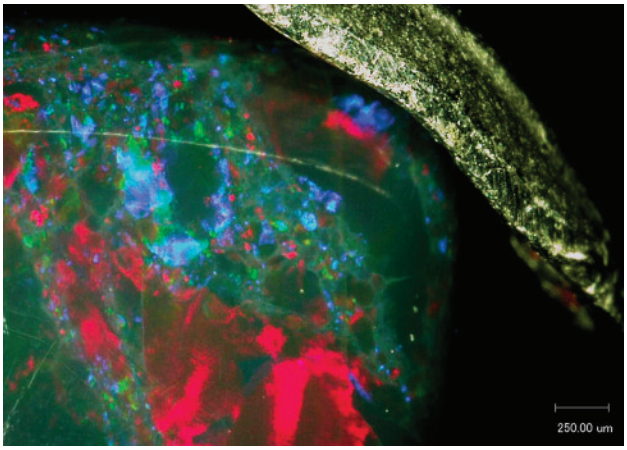

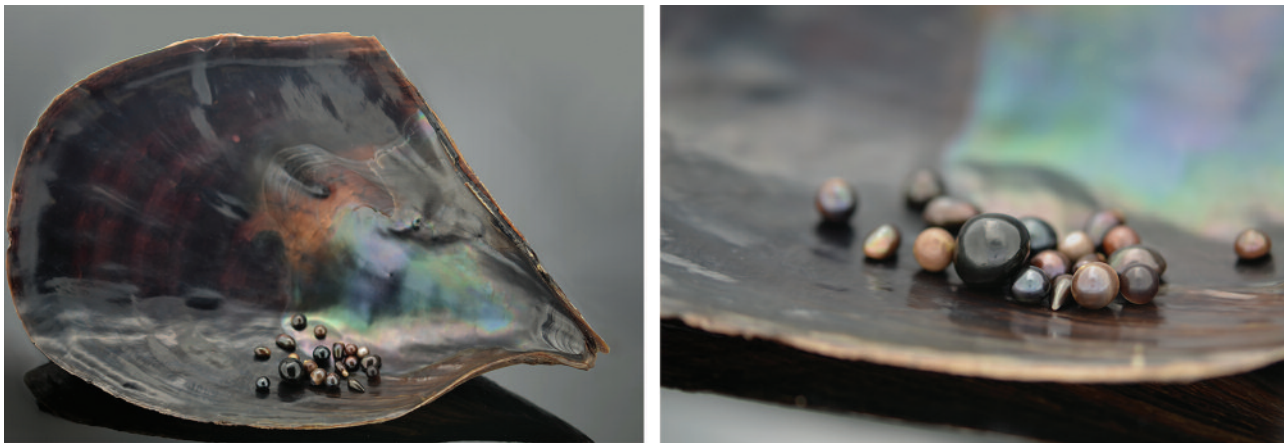

Figure 8. A parcel of natural pen pearls surrounds a 6.92 ct non-nacreous beaded cultured pearl. Photo by Olivier Segura.

range of Ba values confirmed the volcano-sedimentary character of the black opals, as previously described for white opals from Wegel Tena (B. Rondeau et al., "Play-of-color opal from Wegel Tena, Wollo Province, Ethiopia," Summer 2010 *G&G*, pp. 90–105).

Preliminary studies with Fourier-transform infrared (FTIR) spectrometry did not give conclusive results due to the relatively opaque character of our samples. Raman spectra showed very strong carbon peaks, though these alone do not allow a reliable distinction between treated opal from Wegel Tena and natural-color black opal from the Stayish mine. Careful microscopic observation should reveal the natural character of opal from this new deposit, and further studies are in progress.

Acknowledgments: The authors thank Mr. Bill Marcue from D.W. Enterprises for helping to finance this trip, as well as the Ministry of Mines of Ethiopia and the people of Wollo for their kindness and support.

Lore Kiefert and Pierre Hardy
Gübelin Gem Lab, Lucerne, Switzerland

Tewodros Sintayehu and Begosew Abate
Orbit Ethiopia PLC, Addis Ababa, Ethiopia

Girma Woldetinsae
Ministry of Mines, Addis Ababa, Ethiopia

The first identified non-nacreous beaded cultured pearl. The Laboratoire Français de Gemmologie (LFG) recently had the opportunity to examine a collection of non-nacreous pearls from the Pinnidae family (*Pinna* and *Atrina* species). Among these, one black pen pearl drew our attention for its relatively large size: a 10.6–10.6 × 9.6 mm round button weighing 6.92 ct.

Its dark black porcelaneous appearance was typical of pearls from the calcitic part of *Atrina vexillum*, the kind usually submitted for laboratory analysis (figure 8). Observation at 85× magnification (figure 9) revealed a distinctive pattern of convolution, with a few micro-cracks.

Our findings on these cultured pearls are similar to those of N. Sturman et al. ("Observations on pearls reportedly from the Pinnidae family [pen pearls]," Fall 2014 *G&G*, pp. 202–215) in terms of Raman spectra (confirming the calcitic nature), UV-Vis spectra, and chemical composition.

The most interesting findings came from X-radiography. Microradiography/tomography imaging clearly shows a bright white disk inside the pearl (figure 10). The continuous separation line around this feature leaves no doubt that there is a bead inside the cultured pearl. As the beads used to nucleate "nacreous" pearls typically come from large freshwater mussels, we know that they are of a slightly denser material than saltwater nacre. Thus, they appear whiter than the surrounding material (of saltwater origin). The bead's appearance was consis-

Figure 9. Surface magnification of the non-nacreous beaded cultured pearl revealed a typical calcitic pattern of pen pearls. Photo by Olivier Segura; magnified 85×.

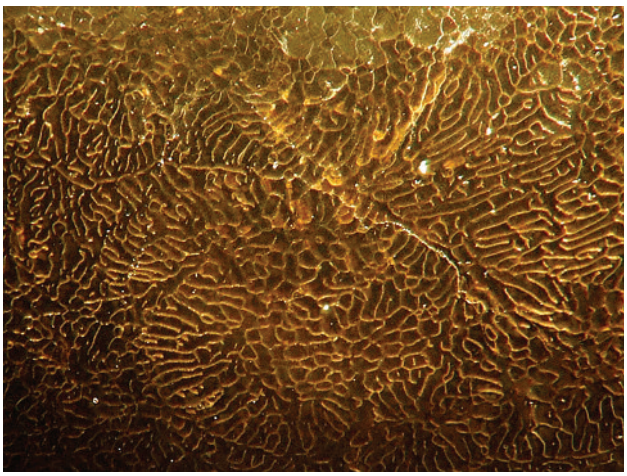

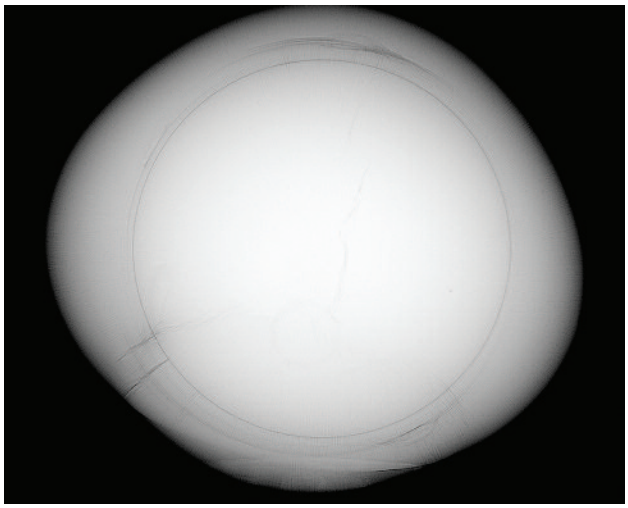

Figure 10. This microradiograph clearly identifies the pen pearl as a beaded cultured pearl. Image by Olivier Segura.

Figure 11. This green oval resembling an emerald proved to be a doublet with a beryl top and a topaz bottom. Photo by Olivier Segura.

tent with a classical nucleus of the kind used in bead-nucleated pearls. Measurement of the bead gave a 6.70 mm diameter.

Tomography confirmed the presence of a near-perfect spherical bead inside the cultured pearl. Even with the owner's consent, however, we decided not to cut the pearl, as the imaging techniques were sufficient to prove the bead-cultured origin.

We wonder if this gem represents a single specimen achieved by a curious experimenter, or if there is now an industrialized process for cultivating such pearls. The cultivation technique used, even if it is known to produce cultured pearls in farms, requires advanced knowledge of the process. The owner reports having handled a black round pen pearl "the size of a golf ball." From the size and symmetry and given this new discovery of a bead-cultured pen pearl, one can speculate that this too might be a bead cultured pearl.

This bead nucleation technique for unusual species could have easily been developed in the past. To our knowledge, though, this specimen represents the first nonnacreous beaded cultured pearl examined by a laboratory. Faced with the expansion of the bead culturing process and the possibility of successful trials in different mollusks, gemologists need to be very cautious in natural origin determinations, even when there is every reason to believe a pearl to be natural.

Olivier Segura (o.segura@bjop.fr)
Laboratoire Français de Gemmologie
Emmanuel Fritsch

SYNTHETICS AND SIMULANTS

An unusual doublet set in fine jewelry. The Laboratoire Français de Gemmologie (LFG) examined a finely made white gold ring set with a green oval faceted stone that measured approximately 20.2 × 14.7 × 8.6 mm and resembled an emerald (figure 11). The stone showed distinct parallel growth zones, visible to the eye, under the table and the crown. These slightly undulating features (figure 12) were strongly reminiscent of Russian hydrothermal synthetic emerald (see, e.g., K. Schmetzer, "Growth method and growth-related properties of a new type of Russian hydrothermal synthetic emerald," Spring 1996 *G&G*, pp. 40–43).

The pavilion showed fingerprint-like inclusions consisting of droplets that were easily visible with the loupe (figure 13). This feature might lead one to believe it was a

Figure 12. Slightly undulating growth zones under the table and crown were reminiscent of Russian hydrothermal synthetic emerald. Photomicrograph by Alexandre Droux; magnified 80×.

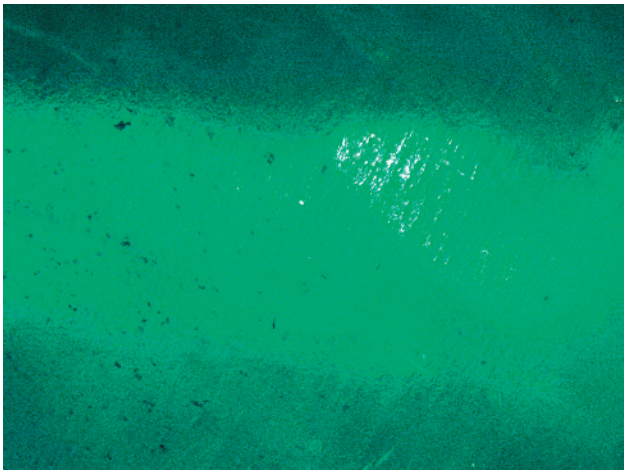

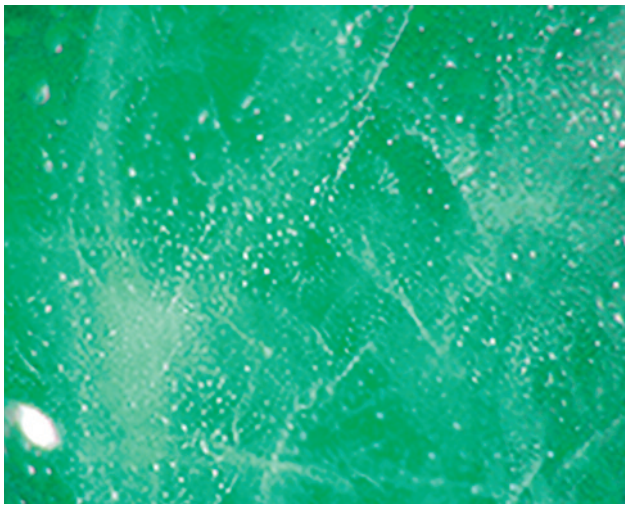

Figure 13. Fingerprint-like patterns reminiscent of flux synthetics are in fact very small two-phase liquid-gas inclusions. Photomicrograph by Alexandre Droux; magnified 80×.

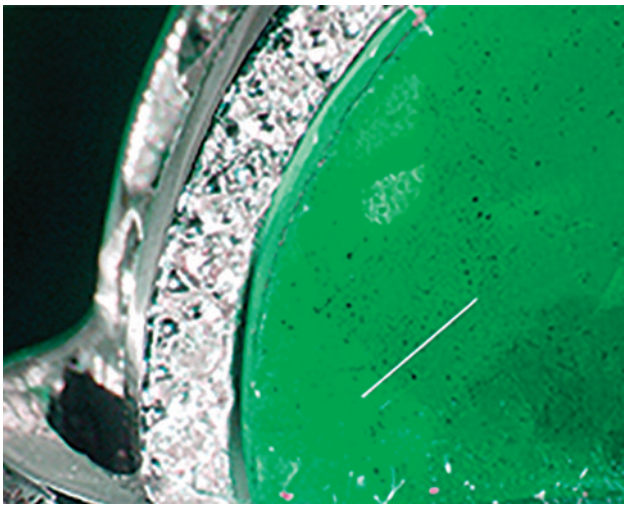

Figure 14. These small black spots are flat bubbles in cement along a separation plane. The line of separation was noticeable through the crown in only one area. Photomicrograph by Alexandre Droux; magnified 30×.

flux synthetic emerald, inconsistent with the observations on the crown. Magnification reveals, however, that the fingerprint-like inclusions are actually made up of very small cavities, with bubbles that are clearly visible in the larger cavities. Therefore, the pavilion is actually a natural gem.

At the level of the girdle, close examination revealed one area with a separation line, hidden elsewhere because of the closed setting (figure 14). Through the table, small but prominent black spots occurred on a single plane. These were flat bubbles in cement introduced at the separation plane.

Only the crown appeared a weak red under the Chelsea filter. Under short-wave ultraviolet radiation, the upper part was inert while the lower part showed a light blue, milky luminescence. Under long-wave UV, both were inert. Therefore, the green oval was clearly a doublet (R. Webster, *Gems: Their Sources, Descriptions and Identification*, 4th ed., rev. by B.W. Anderson, Butterworths, London, pp. 457–468). The refractive index was impossible to measure on either the table or the pavilion because the prongs extended into these two areas.

Raman spectroscopy with a 514 nm laser and 4 cm^{-1} resolution identified the crown as beryl and the pavilion as topaz. Hence the central stone of the ring is a doublet with a hydrothermal synthetic emerald top and a topaz bottom, which is quite unusual.

This case is consistent with an earlier report (J. Hyršl and U. Henn, "Synthetische smaragd-topas-dublette," *Zeitschrift der Deutschen Gemmologischen Gesellschaft*, Vol. 60, No. 3–4, pp. 111–112), which noted that the doublets were of Indian origin. The luminescence of the topaz bottom is slightly different in the present doublet, though still within the known variations of topaz luminescence.

Today far fewer doublets are being submitted to gemological laboratories. This specimen's unusual setting, closed at the girdle and with large prongs preventing access to the table and pavilion for refractometer measurement, suggests an intent to disguise the composite (and partially synthetic) nature of the central gem. Even fine jewelry can be set with gems that are not natural, and gemologists should remain wary of doublets.

Alexandre Droux and Sophie Leblan
Laboratoire Français de Gemmologie (LFG), Paris
Emmanuel Fritsch
Jaroslav Hyršl
Prague

Coated lawsonite pseudomorphs presented as chromian lawsonite. Green (chromium-bearing) lawsonite first appeared on the mineral market in 2011–2012. It came from an undisclosed locality on the Greek island of Syros. The only large chromian lawsonite crystals previously documented are from Turkey (S.C. Sherlock and A.I. Okay, "Oscillatory zoned chrome lawsonite in the Tavsanli Zone, northwest Turkey," *Mineralogical Magazine*, Vol. 63, No. 5, 1999, pp. 687–692) and the western Alps (C. Mevel and J.R. Kienast, "Chromian jadeite, phengite, pumpellyite, and lawsonite in a high-pressure metamorphosed gabbro from the French Alps," *Mineralogical Magazine*, Vol. 43, No. 332, 1980, pp. 979–984). The maximum crystal size observed by Sherlock and Okay was approximately 500 microns, while Mevel's and Kienast's largest grains were only 200 microns in length. Interestingly, these grains were reported to be pink. Samples available online ranged from US$50 to more than US$350, and all were reported to be from Syros. To the best of our knowledge, chromian lawsonite is not available from other localities.

We purchased a chromian lawsonite sample purport-

Figure 15. These large green crystals were reported as chromian lawsonite. Ankerite (orange) and actinolite (light green) are the major matrix minerals between the large green crystals (verified by Raman spectroscopy). The specimen is 4.8 cm long. Photo by Earl O'Bannon.

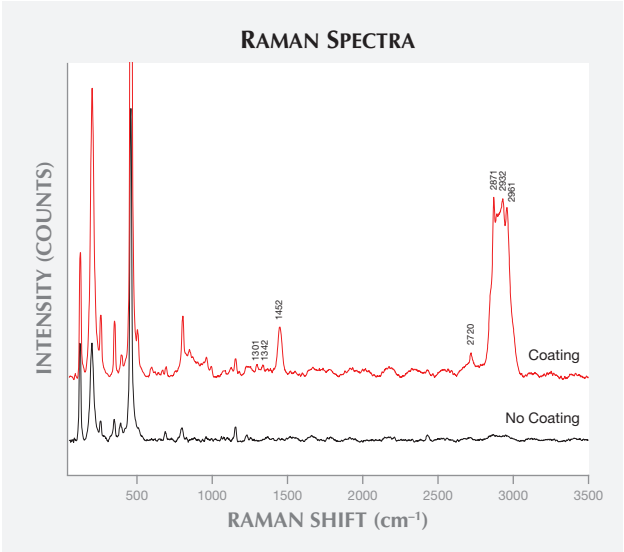

Figure 17. Raman spectra of the coating before and after cleaning the surface with acetone. Spectra were taken in the same location, with an approximately 2 micron spot size. The typical Raman spectrum of quartz, with clinochlore contamination, is observed in the low-frequency region. Spectra are offset for clarity.

edly from Syros for mineralogical analysis (figure 15). The sample measured 4.8 × 2.8 × 2 cm, and its largest crystal was about 1.5 cm in length. The crystals were deep green and present in a matrix dominated by ankerite and actinolite. Our sample appeared similar to most other chromian lawsonite samples available for purchase online.

Initial microscopic observations of the large green crystals revealed a smooth wavy surface (figure 16). Raman analysis of this surface showed peaks at 1301, 1342, 1451, and 2720 cm^{-1} and a broad peak at 2800–3000 cm^{-1} with secondary peaks at 2871, 2932, and 2961 cm^{-1} (figure 17). These peaks are typical of Group B fillers (strong aliphatic peaks), which have been used to enhance the appearance of emeralds (M.L. Johnson et al., "On the identification of various emerald filling substances," Summer 1999 *G&G*, pp. 82–107). The absence of Raman peaks in the approximately 1600 cm^{-1} region indicates that this coating is not likely a Group A, C, D, or E filler (Johnson et al., 1999; L. Kiefert et al., "Raman spectroscopic applications to gemmology," *Handbook of Raman Spectroscopy*, Vol. 28, 2001, pp. 469–490). This smooth surface was waxy to the touch and easily scratched with a fingernail, and wiping it off with acetone revealed a light green to white surface. All peaks associated with this coating disappeared after cleaning with acetone (again, see figure 17).

After the coating was removed, Raman analysis of the formerly dark green crystals revealed spectra corresponding to the minerals muscovite/phengite, clinochlore, and quartz (figure 18). About a hundred measurements were taken of all the large green crystals in the sample at the 2 micron scale-length, and no evidence of lawsonite was found. This assemblage of minerals is common in lawsonite pseudomorphs from Syros; prograde pseudomorphs, also containing zoisite and 0.5–3.0 cm in size, are reported

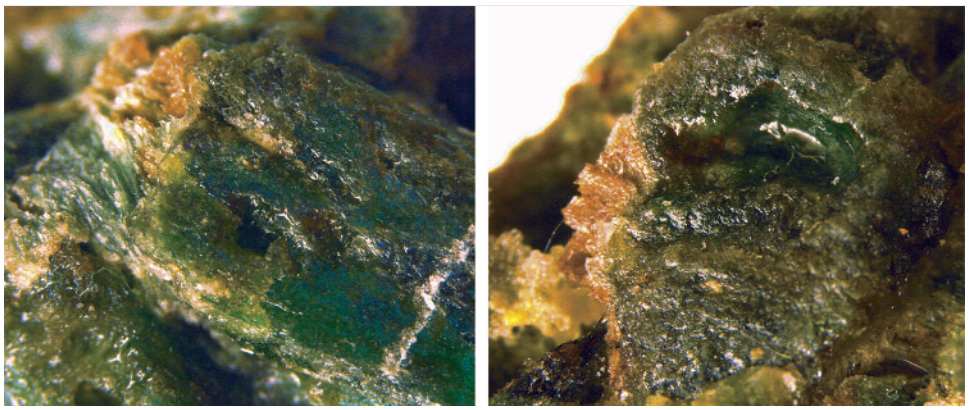

Figure 16. The photo on the left (magnified 1.25×) shows a fingernail scratch on the surface. The photo on the right (magnified 1.6×) shows pooling of the coating in a depression in the grain. Photos by Earl O'Bannon.

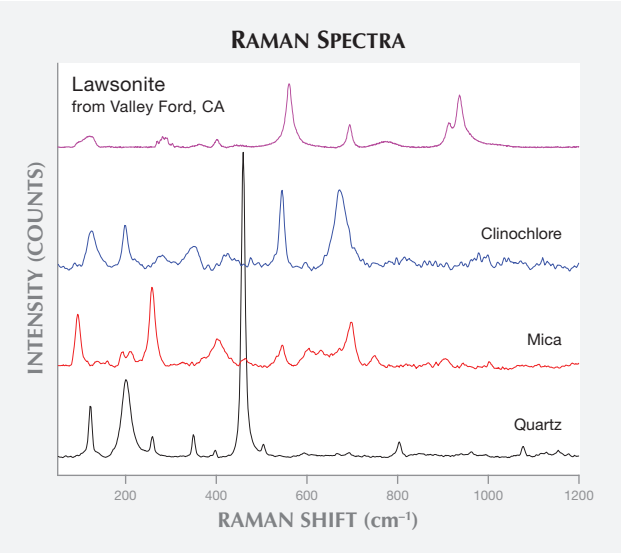

Figure 18. Raman spectra of acetone-cleaned large green crystals (bottom three spectra). Mica and clinochlore are the most abundant minerals in the large green crystals. The reference lawsonite spectrum is for a sample from the UCSC mineral collection (sample no. 6481), from Valley Ford in Sonoma County, California. Spectra offset for clarity.

to be abundant in this locale (J.B. Brady et al., "Prograde lawsonite pseudomorphs in blueschists from Syros, Greece," *GSA Annual Meeting*, 2001, paper 105-0).

We conclude that this sample is composed of lawsonite pseudomorphs, which were coated to make them appear deep green and imitate chromian lawsonite crystals. The euhedral crystals consisted of a fine-grained mixture of muscovite, clinochlore, and quartz. It is not known whether this sample was coated with the recognition that these were lawsonite pseudomorphs.

All samples of chromian lawsonite that we have found for purchase are from Syros. Thus, buyers should be aware that these could potentially be artificially coated lawsonite pseudomorphs. Further analysis of other "chromian lawsonite" samples is required to document whether any true chromian lawsonites from this locality actually exist.

Acknowledgments: Drs. Hilde Schwartz and Elise Knittle provided helpful discussions about pseudomorphs, and Chelsea Gustafson (UCSC Chemistry Department, Partch Lab) assisted with the microscope used to take images of the coating. The UCSC Mineral Physics Lab is supported by the NSF.

Earl O'Bannon and Quentin Williams
University of California, Santa Cruz

Unusual composite ruby rough. The Indian Gemological Institute – Gem Testing Laboratory recently examined an unusual 14.77 ct specimen that resembled ruby rough. Initial gemological testing (RI, hydrostatic SG, optical properties, visible spectrum, and infrared spectroscopic analysis) was consistent with ruby.

The rough was partially polished on two opposite sides, where hexagonal growth zoning was easily visible with the unaided eye (figure 19). Several striations and grooves were visible on the side of the rough.

The pattern and nature of these grooves raised suspicion about the rough's origin. Closer examination under magnification revealed that hexagonal zoning and fine silk on the partially polished surfaces were confined to a depth of approximately 1.5 mm. Two thin slabs of about 1.5 mm each appeared to be attached to the two opposite ends of the rough. No other inclusions were found under magnification. We did observe a slight difference in the color of the thin layer and the main body. The thin slabs were purplish red, while the main body was pinkish red. Since the hexagonal zoning was within the thin slabs and the physical properties were consistent with ruby, we concluded that they were natural ruby slabs. The natural ruby slabs were pasted with a glue that made them appear orangy in transmitted light, and trapped gas bubbles were also observed in the junction plane (figure 20). The two natural slabs were polished to show the hexagonal zoning, while the rest of the rough was kept coarse to restrict views of the interior. Fine triangular grooves were engraved on the rough's surface to imitate the natural growth markings of ruby.

Under magnification, a small cluster of gas bubbles was visible through one of the smooth grooves on the specimen's main body, evidence of synthetic origin. Several fractures were also present in the rough, probably an attempt to imitate fingerprint inclusions. Under short-wave UV, the natural slabs fluoresced red while the synthetic ruby

Figure 19. The 14.77 ct composite ruby rough was partially polished on opposite sides where natural ruby slabs were pasted to a synthetic ruby crystal. Notice the hexagonal zoning on the polished surface. Photo by Meenakshi Chauhan; magnified 15×.

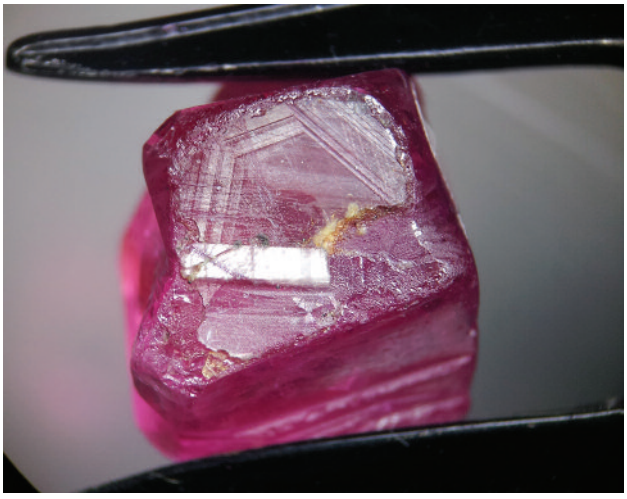

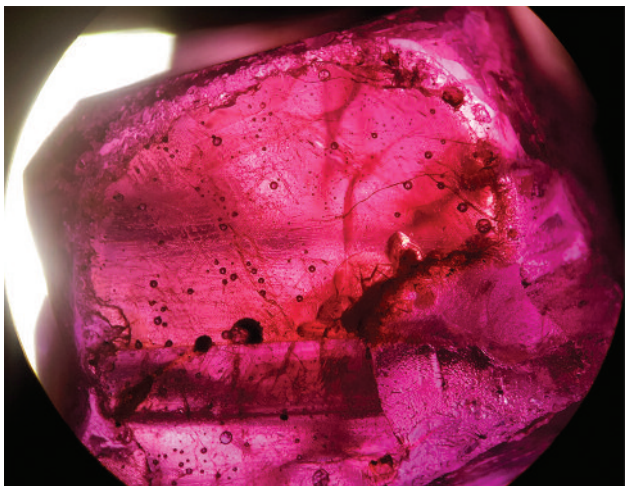

Figure 20. In transmitted light, the natural ruby slab appeared orangy due to the adhesive. Trapped gas bubbles are seen in the junction plane. Photo by Meenakshi Chauhan; magnified 30×.

Figure 21. Under short-wave UV light, the synthetic ruby portion of composite rough fluoresced chalky while the natural ruby slabs fluoresced red. Photo by Meenakshi Chauhan.

rough showed a strong chalky fluorescence (figure 21). Chalky fluorescence was further evidence of the rough's synthetic origin.

Cut and polished composites are regularly encountered, but a composite where synthetic rough is fashioned to imitate natural gem material poses a more significant challenge.

Meenakshi Chauhan (meenakshi@gjepcindia.com)
Indian Gemological Institute – Gem Testing Laboratory, Delhi

Dyed green marble imitating jadeite. A client of the Lai-Tai An Gem Lab in Taipei recently submitted for identification what was claimed to be a piece of fine jadeite mounted in a yellow metal pendant (figure 22). The oval cabochon measured 39.8 × 29.8 mm and exhibited a homogenous green color. At first glance, it bore a strong resemblance to jadeite. While dyes, polymer treatments, or a combination of the two are commonly applied to jadeite—and dyed green quartzite is sometimes used to imitate green jadeite and other materials such as glass and plastic—this piece proved to be dyed green marble with calcite as the main mineral. This was the first time dyed marble had been represented to us as jadeite.

Although marble is fairly abundant, calcite's low hardness and easily visible cleavages do not make it a viable substitute for jadeite. Yet it does lend itself well to carving. Chinese merchants often sell untreated carved marble by the trade names "Hanbai jade" or "Afghanistan jade," or even offer such material as "antique jade." Jade, pronounced "yu" in Chinese, is a general term that typically applies to aggregates of minerals. Marble in the Chinese jewelry market is frequently fashioned into bangles and carved pendants, and some may subsequently be dyed or partially dyed to imitate jadeite jade. Although it was impossible to calculate the SG of this mounted specimen, calcite's RI of 1.65 overlaps with jadeite jade's, leading to the possible misidentification of such material (J.M. Hobbs, "The jade enigma," Spring 1982 *G&G*, pp. 3–19).

The identification was determined using Raman and FTIR spectroscopy. The sample showed Raman peaks at around 1084, 712, 275, and 145 cm^{-1} (figure 23), with IR

Figure 22. This was claimed to be a high-quality piece of jadeite jade mounted in a yellow metal pendant. The oval cabochon measured 39.8 × 29.8 mm, exhibited a homogenous green color, and on first impression appeared to resemble jadeite. Photo by Lai Tai-An Gem Lab.

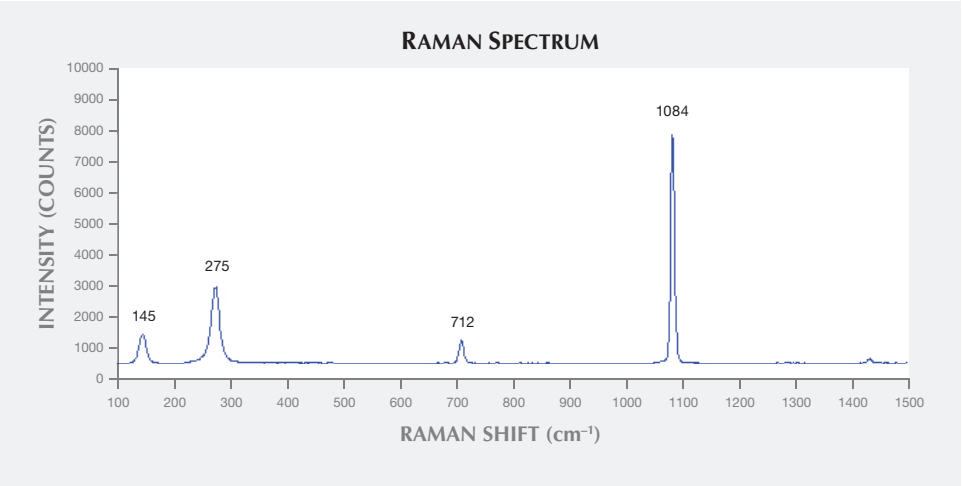

Figure 23. Raman peaks at around 1084, 712, 275, and 145 cm^{-1} were consistent with calcite.

peaks at around 1445 and 878 cm^{-1}. Microscopic observation revealed a network of dyed grain boundaries (figure 24). The dye treatment was confirmed with the spectroscope, where a single broad band typical of some green dyes was clearly evident in the red-orange region. Long-wave UV did not offer any distinction. Although destructive tests are always avoided, the client allowed us to gently scratch the surface with a metal pointer, which confirmed the material's low hardness. This submission reinforces the need to consider all types of material when dealing with items resembling jadeite.

Larry Tai-An Lai (service@laitaian.com.tw)
Lai Tai-An Gem Laboratory, Taipei

Dyed marble as a purple sugilite imitation. In the past two years, many sugilite products with a dark purple color and an obvious granular texture have appeared in the Chinese market. Sugilite pendants and bangles are very popular. Their internal texture and color distribution are inconsistent with previously documented natural specimens and suggest dyed artifacts. With that in mind, we obtained a "sugilite" bangle to investigate its gemological characteristics.

The bangle weighed about 71 grams and had a dark purple color that was distributed along the mineral grain boundaries (figure 25). Spot RIs of 1.48, 1.53, 1.57, and 1.63 were obtained from different areas of the bangle. Its hydrostatic SG was about 2.65, significantly lower than that of natural sugilite. The sample fluoresced strong purple and medium red under long- and short-wave UV radiation, respectively, which indicated treatment with organic dye(s). Five main peaks were observed in the 1600–700 cm^{-1} region of the FTIR spectrum (figure 26). The three peaks at 1427, 881, and 710 cm^{-1} are typical for calcite. The remaining two peaks at 1530 and 1505 cm^{-1} were believed to result from an organic dye.

Figure 24. Microscopic observation revealed a network of dyed grain boundaries. Photo by Lai Tai-An Gem Lab; magnified 50×.

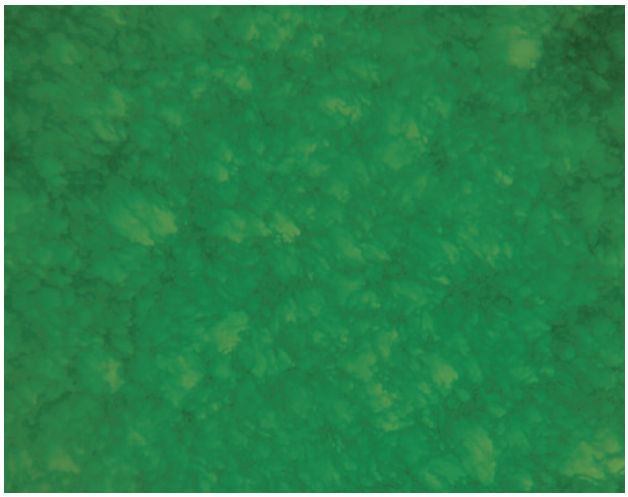

Figure 25. Testing of this bangle identified it as a dyed marble imitation of purple sugilite. Photo by Shanshan Du.

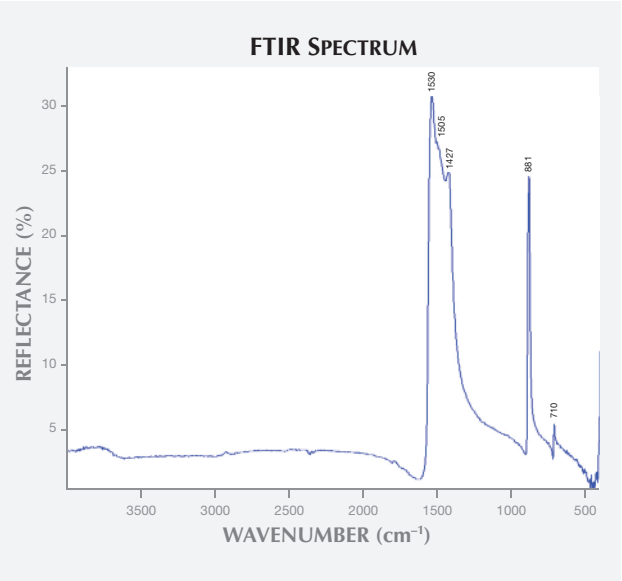

Figure 26. The FTIR spectrum of the purple bangle contained characteristic peaks at 1427, 881, and 710 cm^{-1} that are typical for calcite.

Figure 27. This 1.44 ct synthetic spinel was grown by the Verneuil process but displayed the short-wave UV reaction of a flux-grown sample. Photo by Pragati Verma.

Although the imitation resembles sugilite, its internal texture, RI, SG, fluorescence, and FTIR spectrum identify it as marble. Since marble usually occurs as a mineral aggregate with a loose texture, it is easily dyed to imitate other precious gemstones. We can therefore expect to see a steady influx of marble imitations in the market, and rigorous testing will be needed to protect consumers.

Ke Yin and Shan-shan Du
China University of Geosciences, Wuhan, China

Unusual short-wave UV reaction in synthetic blue spinel. The Indian Gemmological Institute – Gem Testing Laboratory recently examined a 1.44 ct blue oval mixed cut specimen (figure 27). Standard gemological testing revealed the following properties: RI—1.728; hydrostatic SG—3.64; strong anomalous double refraction under the polariscope; Chelsea filter reaction—strong red; and red transmission in fiber-optic light. The sample showed general absorption bands between 535–550, 560–590, and 615–635 nm in the handheld spectroscope. Microscopic examination with a fiber-optic light source revealed shiny dotted inclusions that were scattered and created a wavy pattern; in some areas, the dotted inclusions were arranged in a series (figure 28). This wavy pattern has not been reported in natural spinel. The author has seen this pattern in some Verneuil synthetic spinel. There is a possibility that these inclusions might be very minute gas bubbles or unmelted feed powder.

These properties—higher RI, higher SG, red Chelsea filter reaction, anomalous double refraction, and absorption spectrum features—are diagnostic features of cobalt-doped synthetic blue spinel grown by the Verneuil (flame-fusion) process (M. O' Donoghue, *Synthetic, Imitation & Treated Gemstones*, Butterworth-Heinemann, Oxford, UK, 1997, p. 153).

When tested with UV, this synthetic spinel had an unusual reaction. Under both long- and short-wave UV, the

Figure 28. Series of dotted inclusions were seen in some areas of the synthetic spinel. The dots were so concentrated that it was difficult to distinguish them individually. Photomicrograph by Pragati Verma; magnified 25×.

Figure 29. The synthetic spinel displayed red fluorescence under short-wave UV. Photo by Pragati Verma.

sample showed red fluorescence (figure 29). This was an unexpected short-wave UV reaction for Verneuil-grown blue synthetic spinel, which generally shows a mottled blue to bluish white reaction. This kind of fluorescence was observed in synthetic blue spinel grown by a flux method (S. Muhlmeister et al., "Flux-grown synthetic red and blue spinels from Russia," Summer 1993 *G&G*, pp. 81–98).

Pragati Verma
Indian Gemological Institute – Gem Testing Laboratory, Delhi

MARKET REPORT

Online diamond sales 17% of U.S. market. A recent De Beers study reported that worldwide retail sales of diamond jewelry totaled $79 billion in 2013, up $5 billion on a 7% increase in U.S. demand and a 12% increase in China.

Online sales of diamond jewelry comprise about 17% of the market in the U.S., according to the study. These sales include both strictly online companies such as Blue Nile and traditional retailers who also sell over the Internet.

The De Beers report also noted that 25% of Chinese consumers now research prospective diamond purchases online before making an actual purchase and that the number of retail stores selling diamond jewelry increased 30% from 2010 to 2013. There are, however, strong signs that the heady growth is beginning to slow, according to De Beers. Retailers in Guangdong Province reported that sales declined 5.1% for the first eight months of 2014, while sales of gold pieces nationwide fell 9.1% during that period, according to a government report.

In the U.S., the Department of Commerce reported that jewelry and watch sales from all sales channels increased 4.9% in August, compared to the same month in 2013. This rise reflects even greater sales volume because prices for gold and diamonds declined several percentage points in 2014.

De Beers noted that diamond production increased 7% to 145 million carats, still well under the 2005 peak of 175 million carats. It also predicted that production would decline, despite new sources coming on stream, because older mine deposits are becoming more costly to work as operations go deeper and ore grade declines.

Russell Shor
GIA, Carlsbad, California

Record prices at gem auctions. Auction records kept breaking in late 2014 as the world's ultra-wealthy buyers vied for rare, important gemstones. At Sotheby's October 7 Hong Kong auction, an 8.41 ct GIA-graded Fancy Vivid purple-pink, Internally Flawless diamond (figure 30) drew a winning bid of $17,768,041 from a private buyer from Asia. It was the highest price ever paid for a Vivid pink diamond at auction. And at $2.1 million per carat, it came close to besting the all-time per-carat price achieved by a gemstone.

On November 21 at Sotheby's New York, a 9.75 ct Fancy Vivid blue diamond (figure 31) sold for $32,645,000, a new auction record total price for any blue diamond. At $3,348,205 per carat, it was also a new record price per carat for any diamond. The pear-shaped diamond went to a private collector in Hong Kong who named it the Zoe diamond.

Russell Shor

ANNOUNCEMENTS

Pearl newsletter: *Margaritologia*. The Greek word for pearl, *margaritēs*, was used by Theophrastus in the fourth century BC in the first known effort to explain the scientific origin

Figure 30. This 8.41 ct pear-shaped Fancy Vivid purple-pink diamond sold for more than $17.7 million at Sotheby's Oct. 7 auction in Hong Kong. Photo courtesy of Sotheby's.

Figure 31. This 9.75 ct Fancy Vivid blue diamond sold at Sotheby's November 21 auction in New York for more than $32.6 million, a record total price for blue diamonds and a record per-carat price for any diamond. Photo courtesy of Sotheby's.

of the beloved organic gem. *Margaritologia*, or "the science of pearls," is a newsletter recently launched by Elisabeth Strack, founder and director of Gemmologisches Institut Hamburg and author of the comprehensive book *Pearls*. Ms. Strack is also a member of *G&G*'s editorial review board.

The newsletter, published four times a year in English and German, in print and electronic versions, offers a forum for pearl research findings and news. Topics range from science and history to pearl grading and testing, farming, and market conditions. The first issue, published in October, featured articles on Vietnamese cultured pearls, DNA fingerprinting of pearls, the International Gemmological Conference in Hanoi, *Spondylus* pearls, a Mikimoto necklace, and a museum exhibition in Mecklenburg, Germany.

A yearly subscription to *Margaritologia* is €70, with a discounted rate for CPAA or NAJA members. More information can be found at www.gemmologisches-institut-hamburg.de.

Erin Hogarth
San Diego, California

CONFERENCE REPORT

Gem session at 2014 GSA meeting. A full-day session on gem materials was held Oct. 20, 2014, in conjunction with the annual meeting of the Geological Society of America (GSA) in Vancouver.

The morning presentations focused mainly on diamonds. **Thomas Stachel** (University of Alberta) summarized work to constrain the geological conditions of diamond formation. It is thought to have formed in the mantle from an oxidized carbonate-bearing fluid with high carbon and low nitrogen concentrations. **Eloïse Gaillou** (Natural History Museum of Los Angeles County) discussed pink diamonds whose color originates from narrow lamellae created by plastic deformation parallel to the octahedral growth planes. These lamellae contain a high density of luminescent defects along with localized strain. As a result of plastic deformation in the mantle, these diamonds accommodate stress along the lamellae by mechanical twinning. The unidentified optical defects responsible for the pink coloration are also created by this deformation. **Richard Wirth** (GeoForschungsZentrum) described the use of a transmission electron microscope with a focused ion beam to characterize microstructures in materials. Blue color in quartz is caused by Rayleigh scattering from submicron- and nanometer-sized inclusions of mica, ilmenite, and rutile. The black color of carbonado diamond results from its polycrystalline nature and partially open grain boundaries that cause internal total reflection of light. Cloud-like inclusions in Madagascar sapphires are due to nanocrystalline titanium-rich oxide inclusions. **Wuyi Wang** (GIA) discussed the use of carbon isotope analysis to help distinguish natural diamonds from CVD-grown synthetic diamonds. He found no overlap in isotope composition between them, but within the synthetic diamonds there was variation between manufacturers and even from the same manufacturer. **Karen Smit** (GIA) described interesting features of diamond crystals from Marange, Zimbabwe, which display both cuboid and octahedral growth sectors and distinctive center-cross patterns (often highlighted by graphite-particle clouds). **Mike Breeding** (GIA) reviewed the properties of certain treated-color diamonds. Electron irradiation yields green colors in diamonds with higher nitrogen content, and blue colors in diamonds with lower amounts of nitrogen. Characterization of their optical defects provides a means of distinguishing them from natural-color diamonds. **Troy Ardon** (GIA) characterized some optical defects in hydrogen-rich diamonds from Zimbabwe. Spectral features associated with certain defects could be correlated with noticeable clouds in these diamonds. **Robert Luth** (University of Alberta) discussed a model of diamond formation in the mantle. He suggested that it takes place as carbon-hydrogen-oxygen (CHO) fluids rise in the lithosphere during isobaric cooling, or combined cooling and decomposition. This model helps explain a number of observations regarding the geologic occurrence of diamonds. **Mandy Krebs** (University of Alberta) discussed

size frequency distribution as a predictive tool for macro-diamond grade at Canada's Ekati mine. She found that Ekati diamonds of different size fractions display broadly similar nitrogen and carbon-13 isotope compositions. **Mederic Palot** (University of Alberta) studied diamonds from the Kankan deposit in Guinea that are believed to have formed at great depths (>300 km in the mantle). Characterization of nitrogen and carbon isotopes indicates rapid ascent from the mantle to shallower depths. **Charles Kosman** (University of British Columbia) studied the chemical composition of mineral inclusions in alluvial diamonds from the Kasai area of Congo. These diamonds originated from the kimberlites around Lucapa in neighboring Angola, which contain a significant proportion (~ 20%) of eclogitic diamonds.

The afternoon session covered a range of topics. **Lee Groat** (University of British Columbia) reviewed Canadian gem minerals. In addition to diamond, the country is an important source of nephrite jade, ammolite, and amethyst. Recent discoveries of ruby, sapphire, spinel, and emerald also show promise. **David Newton** (University of British Columbia) analyzed peridotite and pyroxenite xenoliths from the Muskox kimberlite in northern Canada to better understand the rock types in the underlying mantle. **Howard Coopersmith** (Fort Collins, Colorado) described a placer deposit at Mount Carmel in Israel that has yielded diamond, ruby, sapphire, and natural moissanite crystals and fragments that appear to have originated from different igneous and metamorphic source rocks. **Aaron Palke** (GIA) presented a trace-element study of demantoid garnet as the basis for distinguishing this important gem material from different geologic and geographic sources. **Cigdem Lule** (Glenview, Illinois) discussed the need for a more systematic approach to gem nomenclature, which is often determined by jewelry trade practices, as opposed to the more rigorous procedure used for assigning new mineral names. **Nancy McMillan** (New Mexico State University) presented a multivariate chemical analysis of tourmaline, a mineral that can be an exceptional provenance indicator in detrital sediments. This analysis has proven successful in assigning tourmaline samples to different geologic environments. **David Turner** (University of British Columbia) conducted a study of sapphires and associated minerals from the marble-hosted Beluga occurrence in northern Canada by hyperspectral imaging over the 550–2500 nm range. This technique could be useful in the field for analyzing rock samples and in airborne surveys over terrain with good rock exposures. **Philippe Belley** (University of British Columbia) studied blue calcite skarn deposits in Ontario and Quebec. Their geologic setting and low iron content make them potential sources of grossular garnet and other gem minerals. **J.N. Das** (Geological Survey of India) reviewed the exploration and mining of diamonds and colored gemstones throughout India. **Andrew Fagan** (University of British Columbia) described the Aappaluttoq ruby and pink sapphire deposit in Greenland. Based on field studies, it appears to be the world's largest geologically defined gem corundum deposit, with an estimated 400 million carats of material within 65 meters of the surface. Commercial mining is expected to begin in 2015. **Sytle Antao** (University of Calgary) studied optical anisotropy in cubic garnets, which has been recognized for more than a century but remains incompletely understood. X-ray diffraction study of several anisotropic samples revealed they contain two or three cubic phases with slightly different structural parameters. The intergrowth of these phases on a nano-domain scale produces the strain-induced optical anisotropy. **Barbara Dutrow** (Louisiana State University) discussed how tourmaline, an important accessory mineral in many geologic environments, can be used to help locate gem deposits.

In the separate poster session, **Ellen Svadlenak** (Oregon State University) and co-authors used electron microprobe analysis to study variations in the trace elements in emeralds from Muzo, Colombia. **Lauren Forbes** (Western Washington University) and co-authors analyzed emeralds from four different Muzo mines using SEM-CL (cathodoluminescence) along with LA-ICP-MS to better understand the chemical and physical conditions for their growth. All emeralds tested showed a strong red luminescence. The researchers concluded that Muzo emeralds are compositionally unique. **Gena Philibert-Ortega** (Murrieta, California) and co-authors described the scientific influence of James Sowerby's rare five-volume *British Mineralogy* in the early 19th century. **Elise Skalwold** (Cornell University) and coauthors reviewed their research on a highly unusual blue inclusion in a diamond. While it was identified as olivine, the reason for the blue color remains a mystery.

An overview of the gem research session from the 2014 GSA meeting is available at https://gsa.confex.com/gsa/2014AM/webprogram/Session35272.html.

James E. Shigley and Dona M. Dirlam
GIA, Carlsbad

ERRATA

1. The cover of the Fall 2014 issue listed the volume number as 49 rather than 50.

2. In the Fall 2014 lead article on the Sri Lankan gem and jewelry industry, the figure 4 caption (p. 176) should have acknowledged that the two sapphire crystals in the photo are courtesy of Bill Larson (Pala International, Fallbrook, California).

3. Also in the Fall 2014 issue, table 2 of the pen pearls article (p. 211) listed an incorrect value. For pearl sample 3, the ^{88}Sr composition was 806 ppmw, not 8067 ppmw.

4. In the Summer 2014 article on three-phase inclusions in emerald, the log-log plots in figures 24 and 25 (pp. 129 and 131) contained labeling errors on the x-axis scales. For figure 24, the Fe concentration scale should have extended from 100 to 10,000 ppmw rather than 10 to 1,000 ppmw. In figure 25, the Fe concentration scale should have extended from 100 to 100,000 ppmw rather than 100 to 1,000 ppmw.

LETTERS

ANALYSIS OF THREE-PHASE INCLUSIONS IN EMERALD

In the Summer 2014 issue of *Gems & Gemology* (pp. 114–132), Sudarat Saeseaw and her colleagues from GIA's Bangkok laboratory presented a study dealing with three-phase inclusions, absorption spectra, and trace-element analyses for origin determination of emeralds. Examples of three-phase inclusions were presented for samples from Zambia (the Musakashi and Kafubu deposits), the Panjshir Valley in Afghanistan, Davdar in China, and several Colombian localities (Coscuez, Muzo, Peñas Blancas, La Pita, and Chivor).

Unfortunately, the authors did not mention in their literature overview or in their discussion the various other emerald deposits which have supplied samples with three-phase inclusions. These include Nigeria (Henn and Bank, 1991); Capoeirana in Minas Gerais, Brazil (Epstein, 1989); Eastern Himalaya (Niedermayr et al., 2002); the Maria deposit in Mozambique (Vapnik and Moroz, 2002); the Lened emerald prospect in the Northwest Territories of Canada (Marshall et al., 2004); Malipo County in the Yunnan province of China (Huong, 2008); and Eidsvoll in Norway (Rondeau et al., 2008). While some of these occurrences might be of academic interest only, others such as Nigeria, Brazil, and Mozambique have supplied emeralds of gem quality to the market. These localities cannot be ignored in a research paper on origin determination and three-phase inclusions.

Although the chemical data presented in Saeseaw et al.'s table 2 were calibrated using the theoretical Si content of beryl as an internal standard, the laser ablation data show such a wide variation for the main elements that it is impossible to calculate a formula for the samples (compare, for example, the overview of chemical data for emeralds from various sources by Groat et al., 2008). Nevertheless, the authors were able to group their samples into five different categories and to present representative absorption spectra in the UV-Vis-NIR range for one sample from each group. Confusingly, four of the five spectra are labeled "E || c", but polarized spectra are given for the ordinary ray (ω, equivalent to E ⊥ c) and the extraordinary ray (ε, equivalent to E || c), which is impossible for a primary beam with E || c.

In the spectra of several samples with low iron contents, Saeseaw et al. measured some weak to moderate absorption bands in the near infrared at 810 nm, which were assigned to bivalent iron. In the spectra of samples from Kafubu, Zambia, with higher iron contents, an additional strong absorption band at 620 nm was also assigned to Fe^{2+}. These assignments fail to acknowledge numerous research papers dealing with the role of iron in the beryl structure, which has been established for decades. With regard to the bands mentioned at 810 nm, it has been shown that the intensities of the different iron bands in the near infrared with polarization || or ⊥ c are not directly correlated. Consequently, these absorption bands have been assigned to two different types or coordination states of iron, most likely to Fe^{2+} in tetrahedral and octahedral sites of the beryl lattice. Concerning the band noted at 620 nm, it has likewise been demonstrated that the intensities of the iron-related absorption bands in the near infrared are not directly correlated with the intensity of this broad band, polarized || c in the visible region around 620 nm (figure 1). Thus the broad absorption from about 600 to 750 nm in the spectra of Kafubu emeralds has been assigned to Fe^{2+}/Fe^{3+} charge transfer (Schmetzer and Bank, 1981). This indicates that emeralds from Zambia's Miku-Kafubu mining range contain, in addition to chromium as the dominant color-causing trace element, a distinct aquamarine component (figure 2). The aquamarine component is responsible for a color shift and pleochroism, especially of the color || c from green or bluish green in "ordinary" emeralds to greenish blue or blue in samples with such an aquamarine component. Emeralds from multiple sources show this phenomenon and similar absorption spectra (e.g., Schmetzer, 1988; Henn and Bank, 1991; Henn, 1992; Hänni, 1992; Moroz et al., 1999).

Another frequently occurring trace element in natural emeralds from various localities is vanadium. According to Saeseaw et al., vanadium absorption bands are observed in natural vanadium-bearing emeralds in the ω spectrum (equivalent to E ⊥ c) at 400 nm and in the ε spectrum (equivalent to E || c) at 654 nm. Natural vanadium-bearing, chromium-free emeralds are rare but have been documented (from Salininha, Brazil, for instance). These also reveal distinct amounts of iron, and the various bands in the absorption spectrum of this type of beryl have been assigned to vanadium and iron (Wood and Nassau, 1968). Nearly iron- and chromium-free samples have been grown synthetically; they are commercially available from Biron in Perth, Australia (Schwarz and Schmetzer, 2001), and from Tairus in Novosibirsk, Russia (Schmetzer et al., 2006; see also the summary of references describing vanadium-related absorption spectra in that paper).

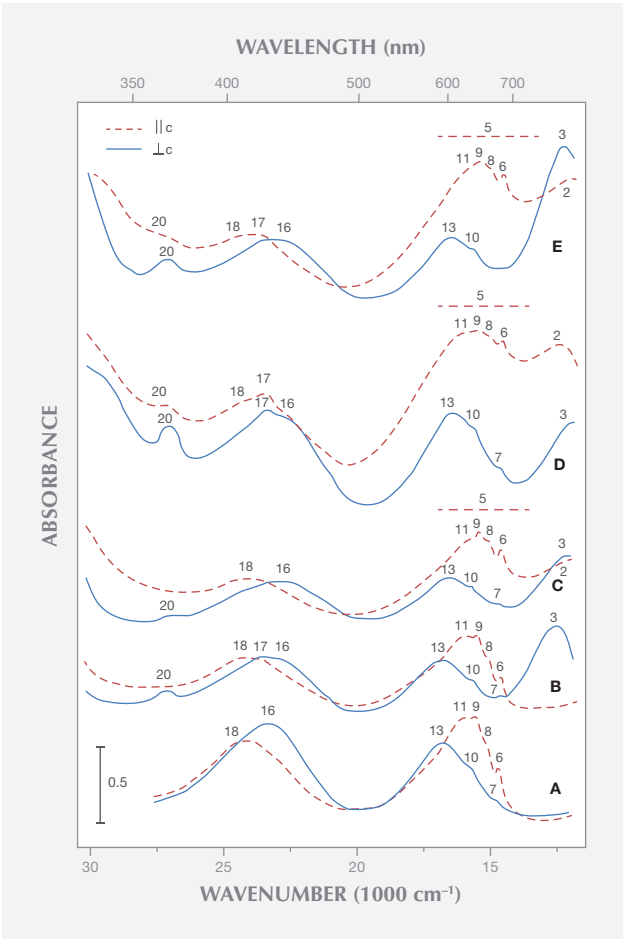

Figure 1. Polarized absorption spectra of emeralds from different sources. Sample A from Chivor, Colombia, represents a typical chromium-vanadium emerald spectrum without distinct iron absorption bands. Sample B from Jos, Nigeria, represents a typical chromium-vanadium emerald spectrum with an Fe^{2+}-related absorption band (3) in the near infrared and two Fe^{3+} bands in the bluish violet and ultraviolet range (17, 20). Samples C (Ankadilalana, Madagascar), D (Santa Terezinha de Goiás, Brazil), and E (Miku, Zambia) represent the superimposed spectra of chromium-vanadium emeralds with distinct aquamarine components of variable intensities, wherein the aquamarine spectrum consists of two absorption bands in the near infrared (2, 3), iron bands in the bluish violet and ultraviolet (17, 20) regions, and a broad polarized absorption in the red (5). After Schmetzer (1988).

Without going into the details of these spectra or discussing the possible presence of vanadium in valence states other than V^{3+} (see Hutton et al., 1991), it is evident that the spectrum of trivalent vanadium in beryl consists of two strong absorption bands in the visible range (figure 3). Parts of these absorption bands are split into different maxima or show various shoulders, but both absorption maxima are, in contrast to the spectroscopic characteristics noted by Saeseaw et al., present in both polarization directions, parallel and perpendicular to the c-axis.

Figure 2. Polarized absorption spectra of emeralds from two different sources and an aquamarine. Sample A, an emerald from Muzo, Colombia, displays a typical chromium-vanadium emerald spectrum without distinct iron absorption bands. Sample B, an emerald from Miku, Zambia, shows the superimposed spectra of chromium-vanadium emerald with a distinct aquamarine component. Sample C, an aquamarine from Tongafino, Madagascar, displays a typical aquamarine spectrum with two absorption bands in the near infrared (2, 3), iron bands in the bluish violet and ultraviolet regions (17, 20), and a broad polarized absorption in the red (5). After Schmetzer and Bank (1981).

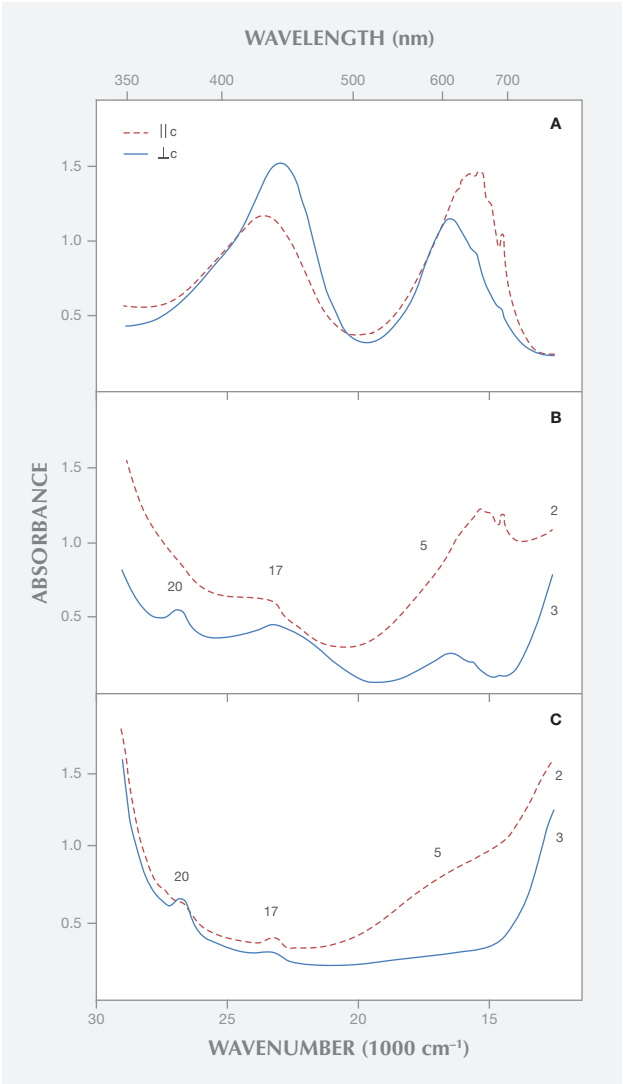

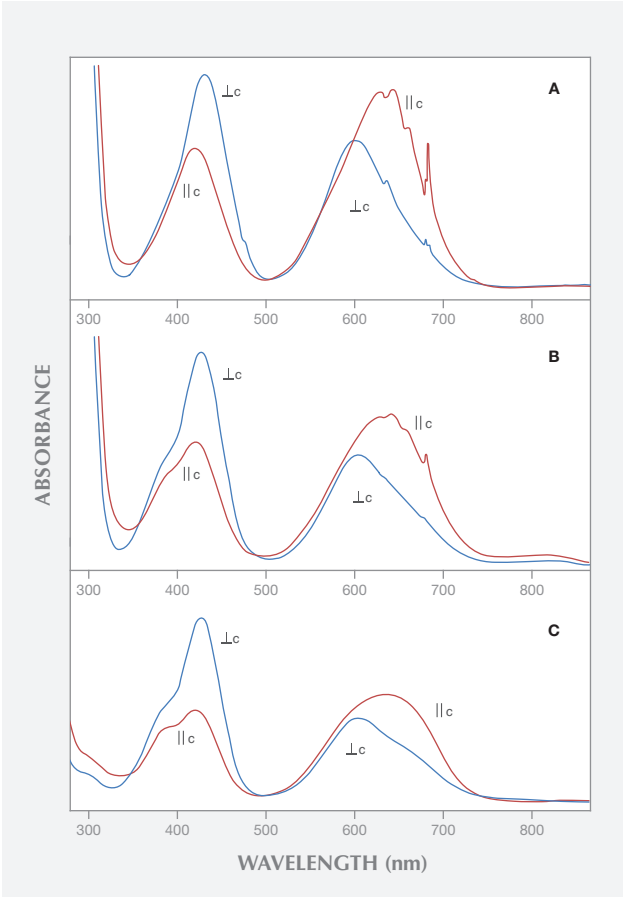

Figure 3. Polarized absorption spectra of two natural Colombian emeralds and a synthetic vanadium-bearing emerald. Sample A from Colombia shows distinctly higher chromium than vanadium contents, Cr >> V. Sample B shows almost equal amounts of vanadium and chromium, V ≈ Cr. Sample C, representing a Biron hydrothermally grown emerald, shows distinctly higher vanadium than chromium contents, V >> Cr. After Schwarz and Schmetzer (2001).

Natural beryl from most sources reveals some traces of both vanadium and chromium. The ratio of vanadium to chromium varies considerably, especially in samples from the Colombian emerald deposits (Schwarz, 1992). Because the absorption bands of these two trace elements are found in the same spectral range, vanadium- and chromium-related absorptions are superimposed in the spectra of emeralds containing both trace elements. As a result, the different vanadium and chromium maxima are not shown individually (figure 3).

The vanadium-chromium ratio in natural emeralds can be approximated from the intensity of the spin-forbidden sharp chromium bands in the 600–700 nm range of the vanadium-chromium spectra. These bands are stronger in samples with distinctly higher chromium than vanadium contents (figure 3A) and become weaker in samples with almost equal chromium and vanadium contents (figure 3B). Furthermore, in samples with distinct vanadium contents, the strong absorption band in the bluish violet range at about 430 nm displays a shoulder in the ultraviolet near 395 nm, observed in both polarization directions, || or ⊥ c (see figures 3B and 3C).

Emeralds from Davdar, China, reveal appreciable amounts of vanadium and chromium (Schwarz and Pardieu, 2009), and they can be distinctly zoned, with a wide variation of vanadium and chromium contents in various growth sectors of the same crystal (Marshall et al., 2012). In Saeseaw et al.'s spectrum for an emerald from Davdar, the sharp chromium lines are distinct and the shoulder in the UV is weak (in the spectrum ⊥ c) or almost invisible (in the spectrum || c), although a vanadium to chromium ratio of about 4:1 is reported for that sample. With such a high ratio, the sharp chromium lines should be noticeably weaker and the vanadium shoulder in the UV should be more intense. Therefore, it would seem desirable to control the chemical analyses obtained by laser ablation, especially for determining the concentration of vanadium and chromium, with other non-destructive methods such as X-ray fluorescence or electron microprobe.

Dr. Karl Schmetzer
Petershausen, Germany
September 3, 2014

REFERENCES

Epstein D.S. (1989) The Capoeirana emerald deposit near Nova Era, Minas Gerais, Brazil. *G&G*, Vol. 25, No. 3, pp. 150–158. http://dx.doi.org/10.5741/GEMS.25.3.150.

Groat L.A., Giuliani G., Marshall D.D., Turner D. (2008) Emerald deposits and occurrences: A review. *Ore Geology Reviews*, Vol. 34, No. 1–2, pp. 87–112, http://dx.doi.org/10.1016/j.oregeorev.2007.09.003.

Hänni H.A. (1992) Blue-green emerald from Nigeria (a consideration of terminology). *Australian Gemmologist*, Vol. 18, No. 1, pp. 16–18.

Henn U. (1992) Über die Farbe und Farbursachen grüner Berylle und ihre nomenklatorische Abgrenzung. *Zeitschrift der Deutschen Gemmologischen Gesellschaft*, Vol. 41, No. 4, pp. 156–158.

Henn U., Bank H. (1991) Außergewöhnliche Smaragde aus Nigeria. *Zeitschrift der Deutschen Gemmologischen Gesellschaft*, Vol. 40, No. 4, pp. 181–187.

Huong L.T.T. (2008) Microscopic, chemical and spectroscopic investigations on emeralds of various origins. Dissertation, University of Mainz, Germany, 113 pp. Available at http://ubm.opus.hbz-nrw.de/volltexte/2008/1673/pdf/diss.pdf.

Hutton D.R., Darmann F.A., Troup G.J. (1991) Electron spin resonance of V^{4+} (VO^{2+}) in beryl. *Australian Journal of Physics*, Vol. 44, No. 4, pp. 429–434, http://dx.doi.org/10.1071/PH910429.

Marshall D.D., Groat L.A., Falck H., Giuliani G., Neufeld H. (2004) The Lened emerald prospect, Northwest Territories, Canada: Insights from fluid inclusions and stable isotopes, with implications for Northern Cordilleran emerald. *Canadian Mineralogist*, Vol. 42, No. 5, pp. 1523–1539.
Marshall D., Pardieu V., Loughrey L., Jones P., Xue G. (2012) Conditions for emerald formation at Davdar, China: fluid inclusions, trace element and stable isotope studies. *Mineralogical Magazine*, Vol. 76, No. 1, pp. 213–226, http://dx.doi.org/10.1180/minmag.2012.076.1.213.
Moroz I.I., Roth M.I., Deich V.B. (1999) The visible absorption spectroscopy of emeralds from different deposits. *Australian Gemmologist*, Vol. 20, No. 8, pp. 315–320.
Niedermayr G., Brandstätter F., Ponahlo J., Schwarzer-Henhapl E. (2002) Vanadium-Berylle aus dem östlichen Himalaya. *Zeitschrift der Deutschen Gemmologischen Gesellschaft*, Vol. 51, No. 2–3, pp. 107–114.
Rondeau B., Fritsch E., Peucat J.-J., Nordrum F.S., Groat L. (2008) Characterization of emeralds from a historical deposit: Byrud (Eidsvoll), Norway. *G&G*, Vol. 44, No. 2, pp. 108–122, http://dx.doi.org/10.5741/GEMS.44.2.108.
Schmetzer K. (1982) Absorptionsspektroskope und Farbe von V^{3+}-haltigen natürlichen Oxiden und Silikaten – ein Beitrag zur Kristallchemie des Vanadiums. *Neues Jahrbuch für Mineralogie Abhandlungen*, Vol. 144, No. 1, pp. 73–106.
Schmetzer K. (1988) Characterization of Russian hydrothermally-grown synthetic emeralds. *Journal of Gemmology*, Vol. 21, No. 3, pp. 145–164.
Schmetzer K., Bank H. (1981) An unusual pleochroism in Zambian emeralds. *Journal of Gemmology*, Vol. 17, No. 7, pp. 443–446.
Schmetzer K., Schwarz D., Bernhardt H.-J., Häger T. (2006) A new type of Tairus hydrothermally-grown synthetic emerald, coloured by vanadium and copper. *Journal of Gemmology*, Vol. 30, No. 1/2, pp. 59–74.
Schwarz D. (1992) The chemical properties of Colombian emeralds. *Journal of Gemmology*, Vol. 23, No. 4, pp. 225–233.
Schwarz D., Pardieu V. (2009) Emeralds from the Silk Road countries – a comparison with emeralds from Colombia. *InColor*, No. 12, Fall/Winter, pp. 38–43.
Schwarz D., Schmetzer K. (2001) Grün ist nicht gleich grün. Oder doch? In: Smaragde der Welt. *extraLapis*, No. 21, Christian Weise Verlag, Munich, Germany, pp. 74–78.
Thoreux E. (2011) Le vanadium trivalent (V^{3+}) en tant que colorant dans les gemmes. Diplôme d'Université de Gemmologie, Nantes, 46 pp.
Vapnik Ye., Moroz I. (2002) Compositions and formation conditions of fluid inclusions in emerald from Maria deposit (Mozambique). *Mineralogical Magazine*, Vol. 66, No. 1, pp. 201–213, http://dx.doi.org/10.1180/0026461026610023.
Wood D.L., Nassau K. (1968) The characterization of beryl and emerald by visible and infrared absorption spectroscopy. *American Mineralogist*, Vol. 53, No. 5–6, pp. 777–800.

REPLY

We appreciate the opportunity to answer Dr. Schmetzer's interesting and informed response to our article. First of all, he has provided several helpful bibliographic references about multiphase inclusions in emeralds from a variety of geographic sources. Nevertheless, the stated purpose of our study was to compare the inclusions in emeralds from the new deposit in Musakashi (Zambia) with those from different sources in our Bangkok reference collection using standard laboratory equipment. In that regard, our article can be considered a preliminary study rather than the final word on the subject.

Dr. Schmetzer goes on to ask about our system of labeling wafers for spectroscopy. In our article, "E || c" means that the wafer plane is parallel to the c-axis, which enables us to collect both ω and ε rays.

Regarding Dr. Schmetzer's concerns about UV-Vis spectra, we focused our study on inclusions. Nevertheless, we provided some significant spectroscopic and chemical data, as these techniques are very important in emerald origin determination. Dr. Schmetzer's specific inquiries about UV-Vis spectra and iron and vanadium contributions are beyond the scope of our article. To understand clearly how impurity affects color in beryl, we would have needed to test known samples of beryl doped with different elements. This would have taken our study in an altogether different direction.

Lastly, Dr. Schmetzer points out our inability to correlate the LA-ICP-MS chemical data with the UV-Vis spectra for one emerald from the Davdar deposit. He suggests controlling our LA-ICP-MS data with other techniques. In our opinion, the lack of correlation has more to do with the fact that these different techniques are not analyzing the same thing: UV-Vis spectroscopy is a bulk analysis, while LA-ICP-MS is a spot analysis (40 microns in diameter in this study). As a result, UV-Vis spectroscopy and LA-ICP-MS usually do not provide a perfect correlation when it comes to inhomogeneous natural emeralds with color zoning and inclusions, such as the emerald from Davdar.

Again, we thank Dr. Schmetzer for his comments and assure him that GIA plans to obtain and study more emeralds from different mining areas, to further our lab's capacity to provide accurate origin determination reports.

Sudarat Saeseaw, Vincent Pardieu, and
Supharat Sangsawong
GIA, Bangkok